

**İZMİR KATİP ÇELEBİ UNIVERSITY ★ GRADUATE SCHOOL OF NATURAL AND
APPLIED SCIENCES**

**NONLINEAR ANALYSIS OF STEEL FRAMES CONSIDERING LATERAL
TORSIONAL BUCKLING EFFECT**



M.Sc. THESIS

Ertuğrul Türker UZUN

Department of Civil Engineering

Thesis Advisor: Asst. Prof. Dr. Mutlu SEÇER

JULY 2017

**İZMİR KATİP ÇELEBİ UNIVERSITY ★ GRADUATE SCHOOL OF NATURAL AND
APPLIED SCIENCES**

**NONLINEAR ANALYSIS OF STEEL FRAMES CONSIDERING LATERAL
TORSIONAL BUCKLING EFFECT**

M.Sc. THESIS

**Ertuğrul Türker UZUN
(Y140104009)**

Department of Civil Engineering

Thesis Advisor: Asst. Prof. Dr. Mutlu SEÇER

JULY 2017

İZMİR KÂTİP ÇELEBİ ÜNİVERSİTESİ ★ FEN BİLİMLERİ ENSTİTÜSÜ

**ÇELİK ÇERÇEVELERİN YANAL BURULMALI BURKULMA ETKİSİ
DİKKATE ALINARAK DOĞRUSAL OLMAYAN ANALİZİ**

YÜKSEK LİSANS TEZİ

**Ertuğrul Türker UZUN
(Y140104009)**

İnşaat Mühendisliği Ana Bilim Dalı

Tez Danışmanı: Yrd. Doç. Dr. Mutlu SEÇER

TEMMUZ 2017

Ertuğrul Türker UZUN, a M.Sc. student of **IKCU Graduate School of Natural and Applied Sciences**, successfully defended the thesis entitled “**NONLINEAR ANALYSIS OF STEEL FRAMES CONSIDERING LATERAL TORSIONAL BUCKLING EFFECT**”, which he prepared after fulfilling the requirements specified in the associated legislations, before the jury whose signatures are below.

Thesis Advisor : **Asst. Prof. Dr. Mutlu SEÇER**
İzmir Katip Çelebi University

Jury Members : **Prof. Dr. Lütfullah GÜNDÜZ**
İzmir Katip Çelebi University

Assoc. Prof. Dr. Erkan DOĞAN
Manisa Celal Bayar University

Date of Submission : 11 July 2017

Date of Defense : 27 July 2017



FOREWORD

I would like to thank my supervisor Asst. Prof. Dr. Mutlu SEÇER, who endlessly helped me with his extensive knowledge and experience.

I would like to thank my mother, Aysun UZUN, my father, Hakan UZUN, my sister, Şebnem UZUN, and of course other family members, especially my grandfather and grandmother for their continuous support and trust in every area of my life. Thanks for always being there for me, believing in me, and motivating me to set out on my own path.

I am very thankful to Zahide ÇETİN, who helped me with endless support at every stage of my work.

Lastly, I would like to thank my great friends in our departments for motivational contributions for this thesis project.

July 2017

Ertuğrul Türker UZUN
(Civil Engineer)



TABLE OF CONTENTS

	<u>Page</u>
FOREWORD	vii
TABLE OF CONTENTS	xi
ABBREVIATIONS	xiii
LIST OF SYMBOLS	xv
LIST OF TABLES	xvii
LIST OF FIGURES	xix
SUMMARY	xxii
ÖZET	xxiii
1. INTRODUCTION	25
1.1. Topic	25
1.2. Aim	25
1.3. Scope	26
2. LITERATURE REVIEW	26
2.1. Researches about Nonlinear Analyses and Lateral Torsional Buckling.....	27
2.2. Literature Evaluation	34
3. ANALYSIS METHODS	35
3.1. Nonlinear Analysis of Steel Frames	35
3.1.1. First-order elastic-plastic analysis	36
3.1.2. Second-order elastic-plastic analysis	38
4. LATERAL TORSIONAL BUCKLING	40
4.1. Methods of Stability Analysis	40
4.2. Uniform Torsion of Thin-Walled Open Sections.....	41
4.3. Non-Uniform Torsion of Thin-Walled Open Sections.....	42
4.4. Lateral Buckling of Beams	44
4.4.1. Simply supported beam under pure bending.....	44
4.5. Design of Members Subjected to Lateral Torsional Buckling Effect	46
4.5.1. Australian Standard – (AS 4100)	46
4.5.2. American Design Specification – (AISC 360-10 / LRFD)	47
4.5.3. British Standard – (BS 5950-1: 2000)	49
4.5.4. European Standard – European Code 3 (EN 1993-1-1)	50
4.5.5. Turkish Steel Design Code – (TSDC-2016)	51
4.5.6. Turkish Standard according to plastic theory – (TS 4561)	52
4.6. Considering Lateral Torsional Buckling Effects in Nonlinear Analysis Steps 53	
5. NUMERICAL EXAMPLES	55
5.1. Comparison of Lateral Torsional Buckling Effect According to Design Specifications	55
5.2. Nonlinear Analysis of Fix Supported Beam under Uniformly Distributed Load 61	
5.3. First-Order Elastic-Plastic Analysis of One Story Side-Sway Prevented Frames	63
5.4. First-Order Elastic-Plastic Analysis of Ziemann Frame.....	65

5.5. Second-Order Elastic-Plastic Analysis of Two Stories and Two Spans Frame	67
5.6. Second-Order Elastic-Plastic Analysis of Three Stories and Two Spans Frame	69
5.7. Analysis of Simply Supported Beam with Different Unbraced Length	
Conditions	71
5.8. First-Order Elastic-Plastic Analysis of Multi-Story Frame.....	73
5.9. Solution Details for Second-Order Elastic-Plastic Analysis of One Story and	
One Span Frame	75
5.9.1. Nonlinear analysis of one story and one span frame ignoring lateral	
torsional buckling effect.....	78
5.9.2. Nonlinear analysis of one story and one span frame considering lateral	
torsional buckling effect.....	82
5.9.3. Second-Order Elastic-Plastic Analysis of One Story and One Span	
Frame Considering Braces in Out-of-Plane Directions	86
5.10. Second-Order Elastic-Plastic Analysis of Two Stories and One Span Frame	88
5.11. Second-Order Elastic-Plastic Analysis of Three Stories and One Span Frame	
	90
6. CONCLUSION	94
REFERENCE	97
CURRICULUM VITAE.....	101

ABBREVIATIONS

AISC	: American Institute of Steel Construction
AS	: Australian Standard for the Design of Steel Structures
BS	: British Standards Institution
EC	: Eurocode
FEM	: Finite Element Method
LRFD	: Load Resistance Factor Design
LTB	: Lateral Torsional Buckling
TS	: Turkish Standard
TSDC	: Turkish Steel Design Code





LIST OF SYMBOLS

B_1 :	multiplier to account for P- δ effects, determined for each member subject to compression and flexure, and each direction of bending of the member
B_2 :	multiplier to account for P- Δ effects, determined for each story of the structure and each direction of lateral translation of the story
b_f :	width of the flange
C_b :	lateral torsional buckling moment modification factor
C_m :	coefficient assuming no lateral translation of the frame
C_w :	warping constant
E :	modulus of elasticity of steel
F_y :	specified yield stress of the steel
f_y :	yield strength
G :	shear modulus
GK_T :	section torsional stiffness (TS 4561)
h :	section height
h_o :	distance between the flange centroids
I_t :	torsional constant (EN 1993-1-1)
I_y :	moment of inertia taken about weak axis
i_y :	radius of gyration about weak axis
I_z :	second moment of area about the minor axis (EN 1993-1-1)
I_w :	warping constant (EN 1993-1-1)
J :	torsional constant
L_b :	length of the unbraced segment of the member
L_p :	length limits
L_r :	length limits
L_{Kr} :	length of the part that the element can freely twist laterally (TS 4561)
M :	bending moment
M_x :	maximum major axis moment (BS 5950)
M_b :	buckling resistance moment (BS 5950)
M_{lf} :	first-order moment due to lateral translation of the structure only, (Nmm).
M_n :	bending moment strength taken into account for lateral torsional buckling
M_{nt} :	first-order moment with the structure restrained against lateral translation, (Nmm)
M_p :	plastic moment capacity
M_r :	required second-order flexural strength, (Nmm)
M_L :	larger end moment
M_S :	smaller end moment
M_{max} :	maximum moment for the unbraced length of the member
M_A :	moment at 0.25 of the unbraced length of the member
M_B :	moment at 0.5 of the unbraced length of the member
M_C :	moment at 0.75 of the unbraced length of the member
M_D :	critical elastic moment for lateral torsional buckling (TS 4561)
M_{kr} :	maximum bending moment (TS 4561)
M_x :	bending moment in the laterally connected section adjacent to the plasticized section (TS 4561)

M: bending moment in section (TS 4561)
M_p: plastic moment
M_b: nominal member moment capacity (AS 4100)
M_s: nominal section moment capacity (AS 4100)
M_{oa}: reference buckling moment (AS 4100)
N: axial force (TS 4561)
N_e: Euler buckling load (TS 4561)
N_{Kr}: maximum axial force (TS 4561)
η: ratio of the distance between the load impact point and the center of gravity to the half-height of the section (TS 4561)
L: length of the beam between points which have lateral restraint (EN 1993-1-1)
L_E: effective length between points of restraint (BS 5950)
P: axial force
P_{el}: Euler buckling load = $\pi^2 EI / (KL)^2$
P_{lt}: first-order axial force due to lateral translation of the structure only, (N)
P_{nt}: first-order axial force with structure restrained against lateral translation, (N)
P_{story}: total vertical load supported by the story, (N)
P_{e,story}: elastic critical buckling strength for the story in the direction of translation being considered, (N), determined by sides-way buckling analysis.
P_y: squash load
r: radius of the section
r_y: radius of gyration about weak axis
S_x: elastic section modulus about the strong axis
t_b: section flange thickness
t_f: thickness of the flange
t_w: thickness of the web
Z_x: plastic section modulus about the strong axis
W_{ex}: elastic section modulus about strong axis
W_y: section modulus (EN 1993-1-1)
α_{LT}: imperfection factor (EN 1993-1-1)
α_m: moment modification factor (AS 4100)
α_s: a slenderness reduction factor (AS 4100)
ψ: end moment ratio
β: end moment ratio
β_w: a constant, changed according to section type as plastic, compact, semi-compact or slender section type (BS 5950)
m_{LT}: equivalent uniform moment factor (BS 5950)
σ_a: yield limit of steel material (TS 4561)
χ_{LT}: reduction factor (EN 1993-1-1)
γ_{MI}: partial safety factor (EN 1993-1-1)
v: a slenderness factor (BS 5950)
x: torsional index, obtained from section property tables (BS 5950)

LIST OF TABLES

	<u>Page</u>
Table 5.1 : Ultimate load parameter and decreasing in load carrying capacity for two stories and two spans frame.....	68
Table 5.2 : Ultimate load parameter and decreasing in load carrying capacity for three stories and three spans frame.	71
Table 5.3 : Load carrying capacity of simply supported beam.	72
Table 5.4 : Ultimate load parameter and decreasing in load carrying capacity for three stories and three spans frame.	75
Table 5.5 : W12x30 section properties.	76
Table 5.6 : First load parameter and control values.....	79
Table 5.7 : Second load parameter and control values.....	81
Table 5.8 : Third load parameter and control values.	81
Table 5.9 : Fourth load parameter and control values.....	82
Table 5.10 : First load parameter and control values.....	83
Table 5.11 : Second load parameter and control values.....	83
Table 5.12 : Third load parameter and control values.	84
Table 5.13 : Fourth load parameter and control values.....	85
Table 5.14 : Ultimate load parameter and decreasing in load carrying capacity for one story and one span frame.	87
Table 5.15 : Ultimate load parameter and decreasing in load carrying capacity for two stories and one span frame.....	90
Table 5.16 : Ultimate load parameter and decreasing in load carrying capacity for three stories and one span frame.....	93



LIST OF FIGURES

	<u>Page</u>
Figure 3.1 : General analysis types of framed structures [12].	36
Figure 3.2 : Bilinear interaction curve.	37
Figure 3.3 : Procedure for second-order analysis using B ₁ -B ₂ method [44].	39
Figure 4.1 : Lateral displacement and twisting of the simply supported I-beam subjected to bending moments [45].	40
Figure 4.2 : Simply supported I-beam (a) subjected to twisting moment (b) warping of I-section under uniform twisting moment.	41
Figure 4.3 : St. Venant shear stress distribution due to uniform torsions in an I-section.	42
Figure 4.4 : A cantilever beam subjected to a twisting moment at the free end.	43
Figure 4.5 : Moment and shear developed at the fixed-end cross section of an I-section due to non-uniform torsion	43
Figure 4.6 : Nominal flexural strength and unbraced length graphic under lateral torsional buckling for I-shaped members.	47
Figure 5.1 : Simply supported I-shaped member under linear moment gradient.	56
Figure 5.2 : Lateral torsional buckling with LTBeam [54].	56
Figure 5.3 : Lateral torsional buckling with FE Analysis [55].	56
Figure 5.4 : End moment ratio (β) and M_{cr} for doubly symmetric I-beam with $L_b = 8$ m.	57
Figure 5.5 : End moment ratio (β) and M_{cr} for doubly symmetric I-beam with $L_b = 8$ m considering C_b factors.	58
Figure 5.6 : End moment ratio (β) and M_{cr} for doubly symmetric I-beam with $L_b = 10$ m.	58
Figure 5.7 : End moment ratio (β) and M_{cr} for doubly symmetric I-beam with $L_b = 10$ m considering C_b factors.	59
Figure 5.8 : End moment ratio (β) and M_{cr} for doubly symmetric I-beam with $L_b = 12$ m.	59
Figure 5.9 : End moment ratio (β) and M_{cr} for doubly symmetric I-beam with $L_b = 12$ m considering C_b factors.	60
Figure 5.10 : End moment ratio (β) and M_{cr} for doubly symmetric I-beam with $L_b = 16$ m.	60
Figure 5.11 : End moment ratio (β) and M_{cr} for doubly symmetric I-beam with $L_b = 16$ m considering C_b factors.	61
Figure 5.12 : Fixed end beam.	62
Figure 5.13 : Fixed end beam analysis results.	62
Figure 5.14 : Single-story frame with fix support and pin support.	63
Figure 5.15 : Load parameter – beam midpoint vertical displacement of single-story frame with fix supports.	64
Figure 5.16 : Order of plastic hinge formations (a) for fix support frame (b) for pin support frame.	64
Figure 5.17 : Ziemann Frame [59].	65

Figure 5.18 : Peak point lateral displacements and load parameters of Ziemann frame.	66
Figure 5.19 : Order of plastic hinge formations (a) lateral torsional buckling ignored (b) lateral torsional buckling considered.....	66
Figure 5.20 : Two story and two span frame.	67
Figure 5.21 : Peak point lateral displacements and load parameters of two stories and two spans frame.	68
Figure 5.22 : Order of plastic hinge formations (a) lateral torsional buckling ignored (b) lateral torsional buckling considered.....	68
Figure 5.23 : Three stories and two spans frame.	69
Figure 5.24 : Peak point lateral displacements and load parameters of three stories and two spans frame.	70
Figure 5.25 : Order of plastic hinge formations (a) lateral torsional buckling ignored (b) lateral torsional buckling considered.....	70
Figure 5.26 : Simply supported beams with different unbraced conditions.	72
Figure 5.27 : Multi-story frame (a) braced from joints (b) braced from joints and midpoints of the beams.	73
Figure 5.28 : Multi-story frame analysis results.	74
Figure 5.29 : Order of plastic hinge formations (a) lateral torsional buckling ignored (b) lateral torsional buckling considered.....	74
Figure 5.30 : One story and one span frame.	75
Figure 5.31 : Sections of one story and one span frame.....	76
Figure 5.32 : One story and one span frame analysis results.....	85
Figure 5.33 : Out of plane motion prevented from (a) only joints (b) mid-point of the beam (c) three points of the beam for one story frame.....	86
Figure 5.34 : Peak point lateral displacements and load parameters of one story and one span frame.....	87
Figure 5.35 : Out of plane motion prevented from (a) only joints (b) mid-point of the beam (c) three points of the beam for one story frame.....	88
Figure 5.36 : Peak point lateral displacements and load parameters of two stories and one span frame.	89
Figure 5.37 : Order of plastic hinge formations (a) lateral torsional buckling ignored (b) lateral torsional buckling considered.....	89
Figure 5.38 : Out of plane motion prevented from (a) only joints (b) mid-point of the beam (c) three points of the beam for one story frame.....	91
Figure 5.39 : Peak point lateral displacements and load parameters of three stories and one span frame.	92
Figure 5.40 : Order of plastic hinge formations (a) lateral torsional buckling ignored (b) lateral torsional buckling considered.....	92



NONLINEAR ANALYSIS OF STEEL FRAMES CONSIDERING LATERAL TORSIONAL BUCKLING EFFECT

SUMMARY

The use of nonlinear analysis methods is widely preferred to determine the realistic behavior of the structures through the computer technologies developed in recent years. However, the stability problems that significantly affect the structure behavior are often neglected in nonlinear analysis and in computer programs that are frequently used to the realization of these analyses. Lateral torsional buckling behavior, which is one of the stability problems, is considered to be neglected in many studies using nonlinear analysis methods in the literature. As a result, the realistic behavior of the structures cannot be achieved, the designs are carried out that the structures can carry much more load than the foreseen load carrying capacities.

Due to the necessity of achieving realistic behavior of the structures in this study, the steel frames are selected which are previously neglected in the literature for the calculation of lateral torsional buckling behavior and analyzed by nonlinear analysis methods. The steel frames are analyzed with and without considering lateral torsional buckling effect and their effect on the structure behavior are shown. Approaches presented in the regulations have been used in the analyses.

The analysis taking into account the lateral torsional buckling effect is first carried out on a single element and followed by the nonlinear analysis steps of the steel frames. The results of the analysis are given comparatively and significant effects of lateral torsional buckling on the load carrying capacity of the structure have been demonstrated. Besides, out-of-plane motions are prevented by lateral supports, the frames with different frame span lengths and floor heights are also examined. Also, TSDC and TS 4561 regulations are compared in the results of this study.

It has been observed that lateral torsional buckling reduces the load carrying capacity of the structures significantly in all the frames examined by the nonlinear analysis methods. Moreover, order of plastic hinge formations occurred in steel frames has changed and displacement capacities of frames have decreased because of the lateral torsional buckling effect. Horizontal displacements can be avoided with sufficient lateral support. Thus, the lateral torsional buckling effect can be eliminated. According to the obtained analysis results, it is concluded that lateral torsional buckling is very important in determining the actual behavior of the structures and that it should be taken into account in the analyses.

Keywords: Nonlinear analysis, lateral torsional buckling, steel frame, out-of-plane motion

ÇELİK ÇERÇEVELERİN YANAL BURULMALI BURKULMA ETKİSİ DİKKATE ALINARAK DOĞRUSAL OLMAYAN ANALİZİ

ÖZET

Yapı davranışının gerçeğe yakın şekilde belirlenmesinde doğrusal olmayan analiz yöntemlerinin kullanılması, son yıllarda gelişen bilgisayar teknolojileri doğrultusunda yaygın olarak tercih edilmektedir. Ancak, yapı davranışını önemli ölçüde etkileyen stabilite problemleri çoğu zaman doğrusal olmayan analizlerde ve bu analizlerin gerçekleştirilmesinde sıklıkla kullanılan bilgisayar programlarında ihmal edilmektedir. Stabilite problemlerinden biri olan yanal burulmalı burkulma davranışı da literatürde doğrusal olmayan analiz yöntemlerini kullanan birçok çalışmada bu stabilite probleminin ihmal edildiği kabulü yapılarak gerçekleştirilmiştir. Bunun sonucu olarak, yapıların davranışı gerçeğe yakın şekilde temsil edilememekte, yapıların öngörülen yük taşıma kapasitelerinden çok daha fazla yük taşıyabileceğine yönelik tasarımlar gerçekleştirilmektedir.

Yapıların gerçeğe yakın davranışına ulaşılması gerekliliğinden dolayı bu çalışmada daha önce literatürde yanal burulmalı burkulma davranışını hesaplarda ihmal edildiği ve doğrusal olmayan analiz yöntemleriyle incelenen çelik çerçeveler seçilmiştir. Çelik çerçeveler yanal burulmalı burkulma etkisi hesaplarda dikkate alınarak ve alınmaksızın analiz edilerek bunun yapı davranışı üzerine etkileri gösterilmiştir. Bu analizlerin gerçekleştirilmesinde yönetmeliklerde sunulan hesap yaklaşımları kullanılmıştır.

Yanal burulmalı burkulma etkisini dikkate alan analizler ilk olarak tek bir eleman üzerinde ardından çelik çerçevelerin doğrusal olmayan analiz adımlarında dikkate alınmıştır. Analiz sonuçları karşılaştırmalı olarak verilmiş ve yanal burulmalı burkulmanın yapının yük taşıma kapasitesine olan önemli etkileri gösterilmiştir. Bunun yanında, yanal burulmalı burkulmayı etkileyen farklı düzlem dışı hareketlerin önlendiği durumlar, farklı çerçeve açıklık uzunluğuna ve kat yüksekliğine sahip çelik çerçeveler incelenmiştir. Ayrıca, Çelik Yapıların Tasarım, Hesap ve Yapım Esasları ve TS 4561 standardı bu çalışmanın sonuçlarında karşılaştırılmıştır.

Doğrusal olmayan analiz yöntemleri ile incelenen tüm çerçevelerde yanal burulmalı burkulmanın yapının yük taşıma kapasitesinde önemli oranda azalmaya neden olduğu görülmüştür. Ayrıca, çelik çerçevelerde oluşan plastik mafsallık noktaları değişmiş ve çerçevelerin yer değiştirme kapasitelerinde yanal burulmalı burkulma etkisinden dolayı azalma olmuştur. Uygulanacak yeterli yanal desteklerle yer değiştirmelerin önlenildiği ve sonucunda yanal burulmalı burkulma etkisinin giderilebildiği sonucuna varılmıştır. Elde edilen analiz sonuçlarına göre yanal burulmalı burkulmanın yapıların gerçek davranışının belirlenmesinde oldukça önemli olduğu ve analizlerde dikkate alınması gerektiği sonucuna varılmıştır.

Anahtar Kelimeler: Doğrusal olmayan analiz, yanal burulmalı burkulma, çelik çerçeve, düzlem dışı hareket



1. INTRODUCTION

1.1. Topic

Determining the realistic behavior of structures is an important parameter for structural engineering problems. Nonlinear analyses play a significant role for design purpose since strength and stability of the whole structure can be represented in terms of applied load and monitored displacements. Nonlinear analysis methods have computational cost and require highly trained engineers unlike linear analysis. However, in recent years, nonlinear analysis of structural steel frames becomes popular among researchers and design engineers with parallel to the development in the computer technology [1]. After these developments process, it is seen that stability conditions of the structures are also important parameter for determining the realistic behavior of the structures. In order to get the realistic results, structural stability problems have to be considered in the nonlinear analysis steps. Lateral torsional buckling is also a one the most important stability problems for slender steel structures. Therefore, lateral torsional buckling behavior should be investigated from many perspectives accounting several conditions for determining the effects on the member behavior.

In this study, nonlinear analysis of steel frames is aimed to be investigated with and without considering lateral torsional buckling behavior. A methodology based on the regulation approaches is proposed for improving nonlinear analysis of steel frames considering lateral torsional buckling.

1.2. Aim

Contemporary design codes necessitate ways to determine realistic behavior of structures. Nonlinear analyses are used extensively for design purpose since strength and stability of the whole structure can be represented. In nonlinear analyses, some assumptions for stability issues are made to ensure the unrestricted plastic

redistribution of moments between the frame members. In this study, a methodology is presented for improving nonlinear analysis of steel frames considering lateral torsional buckling.

The aim of the research is determining the realistic behavior of the steel frame structures and showing the importance of stability conditions on steel structure behavior using nonlinear analysis methods considering the lateral torsional buckling effect.

1.3. Scope

Nonlinear analysis methods of steel structures gained importance parallel to the development of the computing technology. Researchers and design engineers aimed to use nonlinear analysis in structural steel frames and tried to contribute to the literature in order to model the realistic structural behavior. Studies focused more on improving the methods of nonlinear analysis and various analysis techniques are developed [2]. On the other hand, stability of the steel frames are limited by checking the single member behavior and this is investigated based on member local failures. Within this scope, selected steel frames from the literature are investigated considering lateral torsional buckling in nonlinear analysis steps. Moreover, out-of-plane motions have been prevented from different length of the beam members in the analyses. Likewise, different design code approaches on lateral torsional buckling calculations are examined and the results are compared.

2. LITERATURE REVIEW

Studies related with nonlinear analysis methods and lateral torsional buckling behavior are presented in the literature. Studies examined in the literature review are given in chronological order. During this review, nonlinear analysis methods and lateral torsional buckling behavior are generally investigated separately and their effects on each other are not frequently considered. Evaluation of these studies are presented.

2.1. Researches about Nonlinear Analyses and Lateral Torsional Buckling

Giberson [3] modeled nonlinear behavior of structural steel frames with using an end-spring model to establish the elasto-plastic stiffness equation of a beam element accounting yielding of the section.

El-Zanaty et al. [4] investigated inelastic behavior of multistory, planar steel frames. Different forms of formulation were used for stability and strength analysis. A method to compute elastic buckling loads for multistory frames were discussed. A general approach to the elastic and inelastic nonlinear analysis of multistory frames were presented and finite element formulation was developed. Also, the features of the elastic-plastic response of frames for first and second order analyses were presented.

Banarjee and Raveendra [5] defined a new incremental direct solutions of two-dimensional problems of elasto-plasticity. A new direct numerical solution scheme comparable to the variable stiffness method used in the finite element analyses has been developed and applied to a number of standard plasticity problems. Analysis results were similar to the variable stiffness formulation of the finite element method.

Shi and Atluri [6] studied on the elasto-plastic large deformation analysis of space frames. Complementary energy approach was the basis of work. In order to show accuracy and efficiency of the approaches, both quasi-static and dynamic loading were used when examined the numerous examples. A suppose stress approach and a plastic-hinge method were employed to get explicit expressions for the tangent stiffness matrix. For large deformations of practical interest it is essential to use a single element to model each member of the space-frame. According to the analysis results, this procedure was exact in analyzing large deformation inelastic response of frames.

Gharpuray and Aristizabal-Ochoa [7] introduced a simplified nonlinear computer algorithm. This algorithm consisted of a simplified second-order elastic-plastic analysis in which the effects of bowing and the incremental part of the stiffness matrix in each member were neglected. Because of these two simplifications and as expected, load-deflection curves predicted by the proposed algorithm were slightly stiffer than those obtained by the exact second-order elastic-plastic analysis, particularly near the collapse load. The predicted collapse loads were slightly overestimated and the corresponding deflections were slightly underestimated by the proposed algorithm. It is expected that in structures with very flexible members and connections (hinged) and

subjected to large axial loads, the effects of bowing and the incremental part of the element stiffness matrix could become substantial and, therefore, an exact second-order analysis might become necessary.

Haldar and Nee [8] proposed an efficient second-order finite element-based method. Geometric and material nonlinear behavior of steel frames with nonlinear flexible connections and local plasticity effects were considered in this method. An obvious form of the tangent stiffness matrix of the structure was obtained that makes the proposed method extremely efficient in nonlinear analysis. The unique feature of the proposed method is that since the tangent stiffness had an explicit form and could easily be modified to consider different factors, it was extremely efficient.

Clarke et al. [9] studied on the advanced analysis. Some aspects of the inclusion of residual stresses, geometrical imperfections and capacity factors in advanced analysis were examined. An advanced analysis based on the finite element method and utilizing a distributed plasticity formulation was developed and used to perform numerical studies of the behavior of simple structural elements and frames. It was concluded that it was no longer necessary to perform member or section capacity checks with advanced analysis, because the effects of the material and geometrical imperfections and of the material and geometrical nonlinearities have already been included in the analysis.

Kim and Chen [10] presented three practical advanced analysis procedures for a two-dimensional braced steel frame design. These procedures could be used to assess realistically both strength and behavior of a structural system and its individual members in a direct manner. Also, the procedures incorporated the refined plastic-hinge concept for spread of plasticity together with practical modeling for geometric imperfections. Although the current LRFD method does not consider the effect of the weak column leaning on the stronger column, but the proposed methods were done.

Liew et al. [11] concerned with second-order plastic hinge analysis of three-dimensional frame structures. They developed a computer program which used to predict accurately the elastic flexural buckling load of columns and frames by modelling each physical member as one element. It could also be used to predict the elastic buckling loads associated with axial torsional and lateral torsional instabilities, which were essential for predicting the nonlinear behavior of space frame structures.

Chan [12] was addressed to a review and summary of the work conducted on the non-linear analysis and design of steel frames in the past few decades from the vision of the current computer age.

Choi and Kim [13] developed optimal design of steel frame with using practical nonlinear inelastic analysis. To capture second-order effects associated with $P-\delta$ and $P-\Delta$ moment, stability functions were used to minimize modeling and solution time. The Column Research Council tangent modulus concept was used to account for gradual yielding due to residual stresses. A softening plastic hinge model was used to represent the degradation from elastic to zero stiffness associated with development of a hinge. A direct search method was used for minimum weight optimization. The practical nonlinear inelastic analysis overcame the difficulties due to incompatibility between the elastic analysis of the structural system and the limit state member design in the conventional LRFD method.

Zieman [14] described a modification to the second-order inelastic hinge method that could produce the accuracy of more sophisticated plastic zone methods in the analysis of in-plane behavior of compact doubly symmetric sections. To overcome the shortcomings of the elementary plastic hinge method, a modified tangent modulus approach was presented. It was demonstrated that a second-order inelastic hinge analysis could provide results in close agreement with those of a more sophisticated and computationally expensive plastic zone analysis.

Zhou and Chan [15] investigated the plastic hinge approach which can occur at the ends or any position along the element length. A member was divided into many elements in order to approximate the location of a plastic hinge. To describe the formation of a plastic hinge along an element in a member at the ultimate limit state, a single element capable of modeling the $P-\delta$ effect as well as the formation of the plastic hinge was needed. This work adopted a simple concept of superimposition of triangular deflected shapes due to the formation of plastic hinge to the fifth order deflection shape for elastic deflection to yield the final deflection of the element, the plastic point wise equilibrium polynomial element. After that, Chan and Zhou [16] extended previous study on geometrically nonlinear analysis of skeletal structures combined geometrically and material nonlinear analysis of slender frames using a single element per member. Three plastic hinges were allowed to form in an element with two at the two ends and one at the location of maximum combined stress due to

axial force and moment in the proposed element. The formulation was capable of conducting an elastoplastic buckling analysis of a beam column modeled by one element per member, which was not available in literature before.

Kim et al. [17] developed an automatic design method of steel frames using practical nonlinear analysis. The geometric nonlinearity was considered by the use of stability functions. A direct search method was used as an automatic design technique in the study. The member with the largest unit value was replaced one by one with an adjacent larger member selected in the database. The practical nonlinear analysis and the automatic design method were combined. This contribution provided much benefit to practicing engineering.

Yoo and Choi [18] proposed a new method of inelastic buckling analysis in order to determine the critical load of steel frames. This inelastic analysis was based on the concept of modified bifurcation stability using a tangent modulus approach and the column strength curve. The validity and applicability of the proposed inelastic buckling analysis were evaluated alongside elastic buckling analysis and refined plastic hinge analysis. The results revealed that the proposed inelastic buckling analysis suitably evaluated the critical load and failure modes of steel frames, and could be a good alternative for the evaluation of critical load in the design of steel frames.

Thai and Kim [19] developed a practical advanced analysis software which can be used for nonlinear inelastic analysis of space steel structures. The software employed the stability functions and the refined plastic hinge model to minimize modeling and computational time. The generalized displacement control method was adopted to solve the nonlinear equilibrium equations.

Saffari et al. [20] developed a new nonlinear method based on Homotopy Perturbation Method and was applied to elasto-plastic analysis of steel plane frames. The method developed here was applied to plane frames in which elastic perfectly plastic behavior was assumed for structural material while conventional plastic hinges of zero length were used to model plasticity effect. According to analysis results, it was showed that developed method was used for elasto-plastic analysis of structures, using various yield criteria for steel elements, less iteration was required to reach solution, and convergence was achieved very fast.

Doan-Ngoc et al. [21] presented a new beam-column element for nonlinear analysis of planar steel frames under static loads. The second-order effect between axial force and bending moment and the additional axial strain due to the element bending were incorporated in the stiffness matrix formulation by using the approximate seventh-order polynomial function for the deflection solution of the governing differential equations of a beam-column under end axial forces and bending moments in a correlational context. The analysis results of numerical examples proved that and the developed program from the proposed correlational element was capable of accurately predicting the nonlinear behavior of structural members and frames under the static loads.

On the other hand, previous studies considering lateral torsional buckling which is one of the stability problems has been investigated. In this part, progresses related with the lateral torsional buckling are presented with theoretical and experimental studies.

Dux and Kitipornchai [22] carried out a series of experiments on the buckling of simply supported laterally continuous I-beams to investigate the influence of major axis moment gradient on the capacity of inelastic beams in the inelastic range. Nine beams were tested in three groups, each group having a different predominant moment gradient. Points of load application were prevented from moving laterally and twisting. The results demonstrate that capacity is a function of moment gradient. Beams with the less severe gradients were able to sustain higher moments than could much stockier beams in uniform bending.

Pandey and Sherbourne [23] presented a more accurate solution for the elastic, lateral torsional buckling of I-beams under unequal end moments which incorporates accurately the effects of moment gradient, lateral end restraint, and beam slenderness. The proposed analytical model was used to derive new parametric expressions for moment modification and effective length factors as design aids. This research successfully demonstrated that the conditions of loading and support directly influence warping and torsional modes, which, in turn, control the critical moment of the combined mode. The effective length factor was also found to be very useful in the limit states design of beams.

Kemp [24] described a model in order to assess the maximum moment and available inelastic rotation prior to strain weakening due to the interactive local flange and web

buckling and lateral-torsional buckling. The results of 44 tests on I-shaped steel beams under pure flexure and 14 tests on similar specimens under combined bending and simulated axial force were executed. The rotation capacities measured in these tests were examined in terms of standard local and lateral buckling parameters as well as the proposed model.

Helwig et al. [25] conducted finite element buckling analyses of singly symmetric I-shaped girders subjected to transverse loading applied at different heights on the cross section. For single-curvature bending, the finite element results showed that traditional values of moment gradient factors can be used to estimate the buckling capacity of singly symmetric girders. Moreover, the finite element results demonstrated that the height of load application on the cross section has a significant effect on the buckling capacity.

Trahair and Pi [26] summarized a series of investigations into the behavior, analysis and design of members subjected to combined torsion and bending because of torsion was generally ignored by designers. Steel torsion members might be designed for local buckling or plastic collapse.

Papangelis et al. [27] presented a computer program for or the elastic flexural torsional buckling analysis of a wide range of beams, beam-columns, and plane frames. It was designed to assist designers to implement the method of design by buckling analysis which is permitted in modern structural steel design standards, either explicitly or implicitly. This computer program makes a first-order elastic analysis of the in-plane behavior of the frame, and then uses the results of this in a finite element analysis of the elastic flexural torsional buckling of the frame out of its plane. The program also uses the method of design by buckling analysis to design beams.

Suryoatmono and Ho [28] studied on the equations for evaluating the moment-modification factor (C_b) because the equations which presented in AISC 1994 [29] edition given incorrect results for some moment diagrams. From the results, it was shown that the equations for evaluating the C_b factor in both editions (1986 [30] and 1994 [29]) of the AISC Specifications were not accurate for some of the cases considered in this paper. Therefore, instead of using one single equation for any moment diagram, alternative equations for evaluating the C_b factor for each loading case was proposed.

Lim et al. [31] investigated the elastic lateral torsional buckling of I-beams under linear moment gradient that very precisely incorporates the effects of moment gradient and various end restraints. The elastic critical buckling moments were obtained independently by using the Bubnov–Galerkin method and the finite element method. According to analysis results, alternative equations were proposed in order to evaluate the moment gradient correction factor with considering end restraint conditions.

Serna et al. [32] focused on the equivalent uniform moment factor which is used to compute the elastic critical moment. Results obtained using both finite elements and finite differences. The new values refer to the equivalent uniform moment factor for linear moment distributions, uniform distributed loading and concentrated load with two and one end moments. All these cases have been solved considering all possible end support conditions: no prevention to lateral bending and warping; prevention to lateral bending and warping; and prevention to lateral bending or prevention to warping. The results show that warping prevention leads to a significant increase in the coefficient. The paper has presented a closed-form expression to obtain the equivalent uniform moment factor for any moment distribution.

Aydin [33] developed a stiffness matrix for the elements of framed systems which are under constant axial force and moment. The procedure presented here considers the second-order effects due to the axial forces on the bars which are used to calculate the critical buckling loads of the framed system. This approach provides more accurate and dependable results than the energy methods.

Taras and Grenier [34] proposed a new analytical description of buckling curves for lateral torsional buckling. The proposal made in this paper represented a clear improvement of the accuracy and consistency of the analytical description of lateral torsional buckling curves.

Bradford and Pi [35] investigated the lateral-torsional buckling of a pin-ended circular arch with a uniform thin-walled cross section that was subjected to a uniform radial load. It was demonstrated by comparisons with the FE results that the solution provided good predictions for the lateral torsional buckling loads of both shallow and deep arches.

Wu and Mohareb [36] developed a finite element formulation for the lateral torsional buckling analysis of plane frames with moment connections consisting of two pairs of

welded plate stiffeners. The study developed a joint finite element, which accurately quantifies the partial warping restraint provided by common moment connections to adjoining members framing at right angles. The new element provided a more accurate representation of the joint stiffness than the continuous warping deformation assumption.

Kucukler et al [37] presented a stiffness reduction approach utilizing linear buckling analysis with developed stiffness reduction functions for the lateral torsional buckling assessment of steel beams. The proposed method was verified against the results obtained through nonlinear finite element modelling. The proposed stiffness reduction method obviated the need for using lateral torsional buckling assessment equations and considers the influence of the development of plasticity on the response of steel beams, so offering a realistic and practical means of design.

Ozbasaran et al. [38] presented an alternative design procedure for lateral torsional buckling of cantilever I-beams which aims to simplify the calculation of critical loads and design moments. It was seen that the presented design curve was in good agreement with mentioned steel design codes.

2.2. Literature Evaluation

Having examined the literature about nonlinear analysis, nonlinear analysis is a key issue determining the realistic behavior of structures. Previously, nonlinear analysis methods were complex and time consuming for researchers. However, developments in the computer technology make it easy and help to use it widely in the structural analysis among the structural engineers. In this development process, it is observed that not only nonlinear analysis procedures but also structural stability behavior has significant influence on the design of structures.

In order to determine realistic behavior of structures, nonlinear analyses and structural stability conditions have to be considered together in the analyses. In which, lateral torsional buckling is one of the most important stability problems for especially slender steel structures. However, after examining the literature works, it is seen that this stability problem is not considered in nonlinear analysis steps. Consequently, lateral torsional buckling behavior is investigated from many perspectives accounting several conditions for determining the effects on the member behavior but this works are

generally performed on a single member scale. Moreover, effects of lateral restraints on torsional and flexural buckling of members are examined for elastic and inelastic ranges. Additionally, moment factors of beams, geometric imperfection effects and curved members are discussed and influences on the member behavior are focused. Also, approaches using finite elements and experimental studies are performed to evaluate lateral torsional buckling behavior.

As a conclusion, both subjects of nonlinear analyses and lateral torsional buckling have progressed separately and there were limited works linked to each other. Therefore, need to use lateral torsional buckling effect in the nonlinear analyses has been the basis of this study.

3. ANALYSIS METHODS

In this study, nonlinear analysis methods are used to determine behavior of steel frames considering lateral torsional buckling. For this purpose, various structural steel design standards are used to determine the design parameters.

3.1. Nonlinear Analysis of Steel Frames

Many of the nonlinear formulations of steel structures presented in the literature are based on the displacement method, for its relative ease in implementation [39]. Nonlinearities in structures exist in two forms, these are geometrical and material nonlinearities. Geometric nonlinearities gives P- Δ effects which is directly reflected in second-order analysis. Material nonlinearities emerge when material yield or stress-strain behavior shows nonlinear characteristics. In which, two models of material nonlinear frame analyses arise depending on the degree of the accuracy. These are concentrated plasticity (plastic hinge) model and distributed plasticity (plastic zone) model. Plastic hinge model ignores the progressive yielding that takes place in cross section, likewise, plastic zone method takes into consideration the spread of yield in the cross section. In plastic hinge method, yielding is also assumed to be concentrated in a small region of zero length, generally termed as the plastic hinge. Although the plastic zone approach yields results that are very close to the reality, it is limited to use

due to the difficulties that modeling systems have in modeling and the resolution time of these models is very long. Therefore, a popular approach for modelling nonlinear behavior of steel frames is concentrated plastic hinge method.

In nonlinear analysis of steel frames, the load parameter leading to the formation of the first plastic hinge is computed. After determining the location and load parameter of first plastic hinge, member is assumed to remain elastic except at places where zero length plastic hinges are allowed to form. Plasticity is formulated based on the members cross sectional constitutive model that represents the plastic interaction between the axial force and the bending moments. Plastic hinges are located when the section internal forces exceed the plasticity criterion. This is repeated in step by step manner until losing of mechanism of behavior or stability of the structure. Nonlinear analysis of steel frames aims to determine the global behavior of structures instead of isolated member checks that linear analysis methods uses. For steel structures, the plastic interaction curve representing full yielding of the cross section is expressed by the design codes. A graphical comparison of the load-deflection behavior of a plane frame with using previously mentioned conditions are given in Figure 3.1.

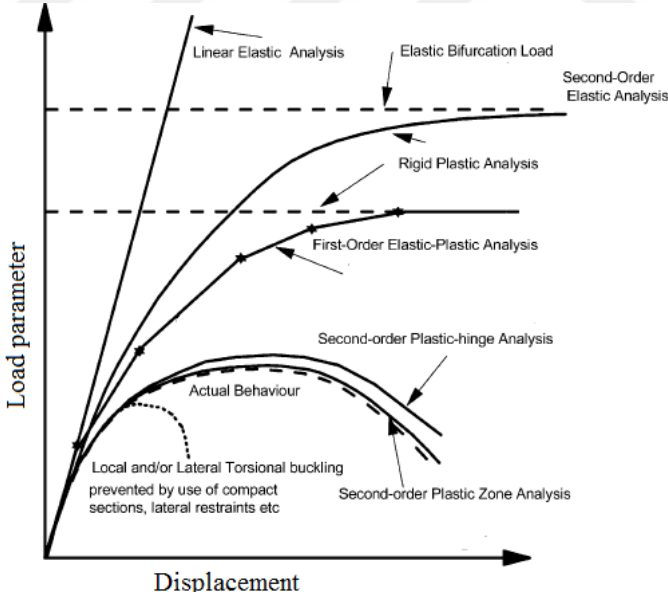


Figure 3.1 : General analysis types of framed structures [12].

3.1.1. First-order elastic-plastic analysis

First-order elastic-plastic analysis is one of the most basic type of nonlinear analyses and effects of the change of geometry are ignored in this analysis. This method models the effects of section yielding under incremental loading. Consequently, it does not

consider second-order stability effects [40]. The plastic limit load can be gained directly by a simple elastic-plastic analyses. An elastic-plastic hinge idealization of the cross section behavior is used in the formulation of first-order elastic-plastic analysis. Members in a structure are assumed to be fully elastic prior to the formation of the plastic hinges. Perfectly plastic hinges are used to account the inelastic behavior by inserting in the member where the full plastic strength is reached.

According to AISC 360-10 LRFD [41], cross section's plastic strength is defined using (3.1) and (3.2).

$$\frac{P}{P_y} + \frac{8M}{9M_p} = 1.0 \quad \text{for} \quad \frac{P}{P_y} \geq 0.2 \quad (3.1)$$

$$\frac{P}{2P_y} + \frac{M}{M_p} = 1.0 \quad \text{for} \quad \frac{P}{P_y} < 0.2 \quad (3.2)$$

Relation between (3.1) and (3.2) is given in Figure 3.2 and this curve is called as the bilinear interaction curve. The average I-shapes accounting AISC 360-10 LRFD [41] interaction equations is plotted.

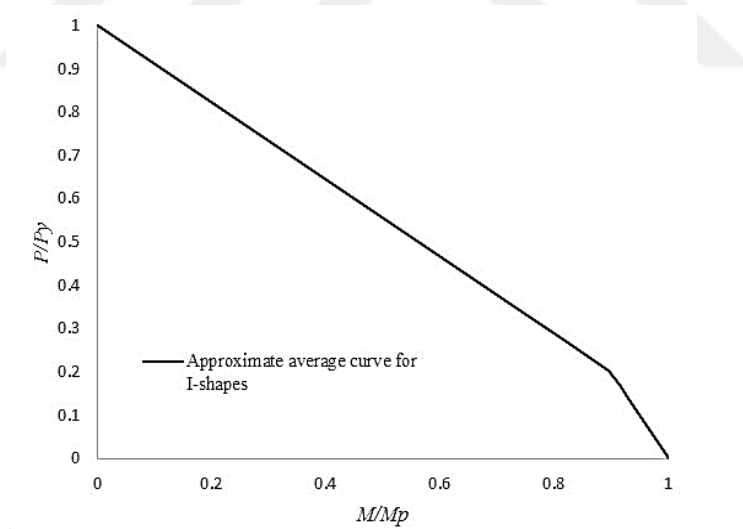


Figure 3.2 : Bilinear interaction curve.

Moment and normal force are written according to load parameter and (3.3) and (3.4) are used;

$$M_{i+1} = M_i + \Delta p \times \Delta M \quad (3.3)$$

$$P_{i+1} = P_i + \Delta p \times \Delta P \quad (3.4)$$

Obtained values from (3.3) and (3.4) are inserted in (3.1) or (3.2). There are two cases [42];

For 1.case $\frac{P}{P_y} \geq 0.2$, load parameter is decided using (3.5);

$$\Delta p = \frac{9 \times M_p \times P_p - 9 \times M_p \times P_i - 8 \times M_i \times P_p}{9 \times M_p \times \Delta P + 8 \times \Delta M \times P_p} \quad (3.5)$$

For 2.case $\frac{P}{P_y} < 0.2$, load parameter is decided using (3.6);

$$\Delta p = \frac{2 \times P_p \times M_p - M_p P_i - 2 \times P_p \times M_i}{\Delta P \times M_p + 2 \times P_p \times \Delta M} \quad (3.6)$$

After every hinge is formed, joint displacements and internal forces of members are calculated using (3.7), (3.8) and (3.9), respectively.

$$\delta = \Delta p_1 \times \delta_1 + \Delta p_2 \times \delta_2 + \dots + \Delta p_i \times \delta_i \quad (3.7)$$

$$M = \Delta p_1 \times M_1 + \Delta p_2 \times M_2 + \dots + \Delta p_i \times M_i \quad (3.8)$$

$$P = \Delta p_1 \times P_1 + \Delta p_2 \times P_2 + \dots + \Delta p_i \times P_i \quad (3.9)$$

Total load parameters are calculated until the structure reach ultimate load carrying capacity. (3.10) is used in order to calculate ultimate load parameter of the structure.

$$\Delta p_p = \Delta p_1 + \Delta p_2 + \Delta p_3 + \dots + \Delta p_n = \sum_{i=1}^n \Delta p_i \quad (3.10)$$

Plastic moment and normal force capacity are defined in (3.11) and (3.12). These are used in the nonlinear analysis steps.

$$M_n = M_p = F_y \times Z_x \quad (3.11)$$

$$P_p = F_y \times A \quad (3.12)$$

3.1.2. Second-order elastic-plastic analysis

Second-order elastic-plastic analysis takes account of geometry changes which are associated with the increase of P- Δ effects (sway deflection) [40]. Moreover, the effect of the geometric changes of the frame and frame elements on the equilibrium equations can be calculated by considering the second-order theory. For second-order analysis

of steel structures, stability functions, geometric stiffness matrices and iterative vertical loads and fictitious horizontal load practical calculation approaches can be used. In TSDC-2016 [43] and AISC 360-10 [41], the moment coefficients method, also known as the $B_1 - B_2$ method, is used for practical second-order analysis. In the moment coefficients method, the internal forces obtained from the analysis of the first-order analysis are increased indirectly with certain coefficients by the second-order effects. In this method, the effects of element shape changes ($P-\delta$) and system displacement effects ($P-\Delta$) are taken into consideration. In Figure 3.3, procedure for second-order analysis is given.

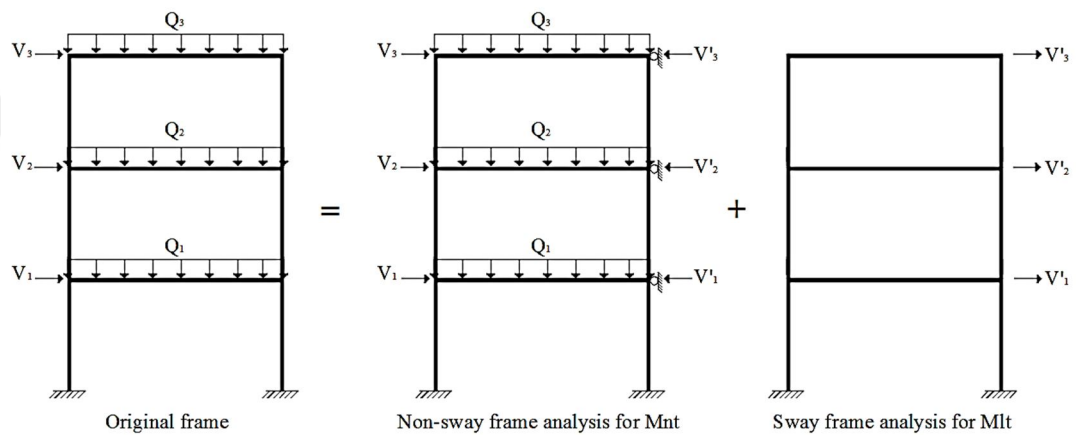


Figure 3.3 : Procedure for second-order analysis using B_1 - B_2 method [44].

The effect of the geometric changes of the frame and frame elements on the equilibrium equations can be calculated by considering the second-order theory. (3.13) (3.14), (3.15) and (3.16) are presented in AISC 360-10 [41];

$$M_r = B_1 M_{nt} + B_2 M_{lt} \quad (3.13)$$

$$P_r = P_{nt} + B_2 P_{lt} \quad (3.14)$$

$$B_1 = \frac{C_m}{1 - \frac{P_r}{P_{el}}} \geq 1 \quad (3.15)$$

$$B_2 = \frac{1}{1 - \frac{P_{story}}{P_{e,story}}} \geq 1 \quad (3.16)$$

4. LATERAL TORSIONAL BUCKLING

There are three major fields which are related with the stability designs of steel frame structures. These are global buckling, local buckling and structural instability due to the plastic hinge formation. Lateral torsional buckling is a form of global buckling and it is focused in this part. Lateral torsional buckling is a behavior which is one of the instability conditions induced by the compressed flange of unrestrained beam subjected to bending around the major axis. If a beam reaches the critical moment value under the applied load or moment, this beam may expose to lateral torsional buckling failure. The critical moment is a function of lateral and torsional stiffness. This is affected by the boundary conditions, unbraced length, material nonlinearities, load pattern and dimensions of the member cross section. If a beam is under the influence of lateral torsional buckling, it experiences simultaneous in-plane displacement, lateral displacement and twisting because of bending. Lateral displacement and twisting of the simply supported beam under the bending moment considering lateral torsional buckling behavior is shown in Figure 4.1.

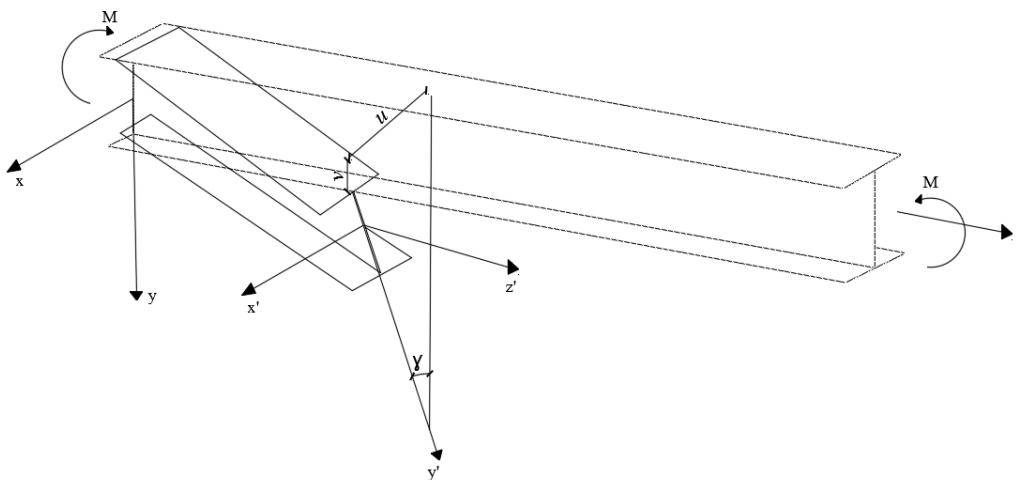


Figure 4.1 : Lateral displacement and twisting of the simply supported I-beam subjected to bending moments [45].

4.1. Methods of Stability Analysis

Understanding of structural stability conditions have not been achieved exactly and ignored mostly in the analysis of steel structures. Therefore, design engineers have encountered a number of failures because of the lack of understanding these stability

requirements. Beams are one of the main structural members and resist the applied load by bending and shearing actions. Open cross sections like I-shape beams have very low torsional rigidities and their resistance to torsional instability is very limited. As a result of this, they are mainly vulnerable against lateral torsional buckling effect. There are two types of torsional rigidity that might exist in a member with thin plate cross section. They are uniform torsion and non-uniform torsion [45].

4.2. Uniform Torsion of Thin-Walled Open Sections

A simply supported beam under an equal and opposite twisting moment is shown in Figure (4.2). Under this condition, the twisting moment along the length of the member is constant and a uniform torsion occur in the beam member, it is showed in Figure 4.2 (a). Also, warping of the cross section arise because of this torque. Figure 4.2 (b) illustrates warping of I section beam under uniform twisting moment.

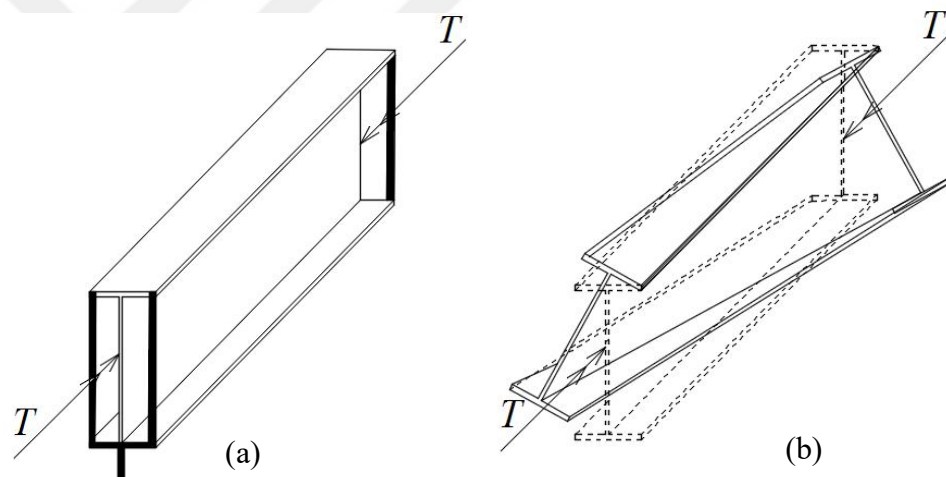


Figure 4.2 : Simply supported I-beam (a) subjected to twisting moment (b) warping of I-section under uniform twisting moment.

Warping of all the cross sections is unrestrained for simply supported beam and this is caused twisting moment by applied torque T . Torque is also attacked only by shear stresses developed in the cross section of beam member. These stresses act parallel to the edge of the component plates of the cross section, as shown in Figure 4.3.

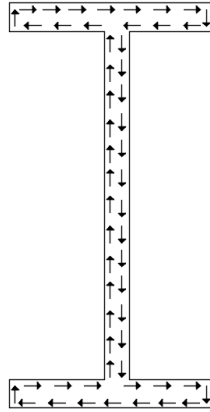


Figure 4.3 : St. Venant shear stress distribution due to uniform torsions in an I-section.

These shear stresses are called St. Venant shear stresses. The torsion is related with these shear stresses and is stated to as St. Venant torsion, T_{sv} . The St. Venant torsion expressed in (4.1) is also referred to as uniform or pure torsion. $d\gamma / dz$ is the rate of twist.

$$T_{sv} = GJ \frac{d\gamma}{dz} \quad (4.1)$$

4.3. Non-Uniform Torsion of Thin-Walled Open Sections

A cantilever beam subjected to a torque T is shown in Figure 4.4. This torque is applied at the free end of the beam. At the fixed end, warping is prevented but at the free end, warping is free. Therefore, the applied torque is resisted merely by St. Venant torsion at the free end. As a result of this, in addition to St. Venant torsion, there exists another type of torsion known as warping restraint torsion in the cross section. There are also axial stress in addition to shear stress because the cross section is prevented from warping. These axial stresses occur at the fixed end of the beam. Emerged these axial stresses in the two flanges creates a pair of equal moments. These moments are called as the bi-moment M_f which act oppositely in each of these two planes of the flanges.

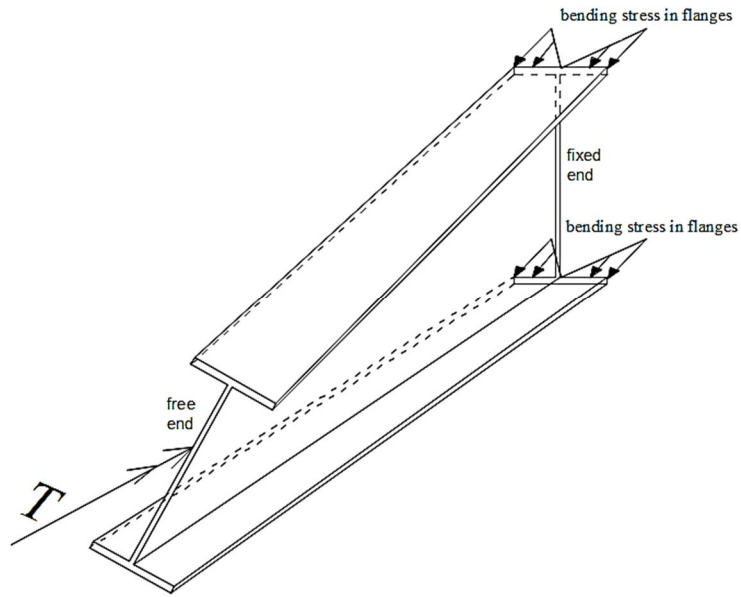


Figure 4.4 : A cantilever beam subjected to a twisting moment at the free end.

The bending moment M_f in either the top or the bottom flange is calculated as (4.2). There are also occurred the shear forces V in both flanges and opposite directions associated with the bending moment. (4.3) is used to calculate the shear forces. These arisen bending moments and shear forces are illustrated in Figure 4.5.

$$M_f = EI_f \frac{d^2 u_f}{dz^2} \quad (4.2)$$

$$V_f = -\frac{dM_f}{dz} = -EI_f \frac{d^3 u_f}{dz^3} \quad (4.3)$$

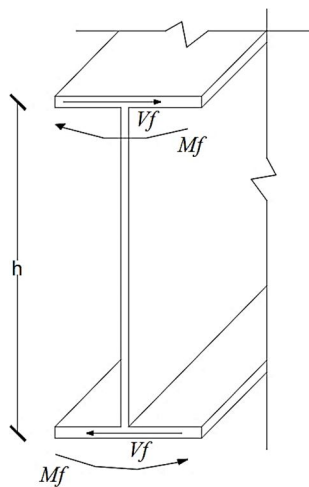


Figure 4.5 : Moment and shear developed at the fixed-end cross section of an I-section due to non-uniform torsion

This pair of shear forces create a couple acting on the cross section. The resulting torsion, which is referred to as non-uniform torsion T_w , is given by (4.4). h is the distance between the shear forces.

$$T_w = V_f h \quad (4.4)$$

Non-uniform torsion can also be written as (4.5)

$$T_w = -EI_f \frac{h^2}{2} \frac{d^3 \gamma}{dz^3} = -EC_w \frac{d^3 \gamma}{dz^3} \quad (4.5)$$

In which, warping constant of the I-section, C_w is decided to use (4.6). It is important that warping constant is different for each of the cross section.

$$C_w = \frac{I_f h^2}{2} \quad (4.6)$$

When the member is twisted and the applied twisting moment is resisted by St. Venant torsion and warping restraint torsion, the internal twisting moment T equals to (4.7).

$$T = T_{sv} + T_w \quad (4.7)$$

The internal twisting moment can be defined as (4.8) considering (4.1) and (4.5).

$$T = GJ \frac{d\gamma}{dz} - EC_w \frac{d^3 \gamma}{dz^3} \quad (4.8)$$

4.4. Lateral Buckling of Beams

If a beam is bent about its axis of greatest flexural rigidity, out-of-plane bending and twisting may occur when the applied load reaches its critical value, unless the beam is provided with a necessary lateral support. The following situations are mentioned and examined by Chen and Lui [45].

4.4.1. Simply supported beam under pure bending

When a simply supported I- section beam subjected to a couple of equal and opposite end moments, in addition to St. Venant torsion, there is also a warping restraint torsion. The external moments at any cross section are given in (4.9), (4.10) and (4.11) for each axis.

$$M_{x'(ext)} \approx M_{x(ext)} = M_0 \quad (4.9)$$

$$M_{y'(ext)} \approx -\gamma M_{x(ext)} = -\gamma M_0 \quad (4.10)$$

$$M_{z'(ext)} \approx \frac{du}{dz} M_{x(ext)} = \frac{du}{dz} M_0 \quad (4.11)$$

The corresponding internal resisting moments are also given in (4.12), (4.13), and (4.14) for each axis.

$$M_{x'(int)} = -EI_x \frac{d^2v}{dz^2} \quad (4.12)$$

$$M_{y'(int)} = EI_y \frac{d^2u}{dz^2} \quad (4.13)$$

$$M_{z'(int)} = GJ \frac{d\gamma}{dz} - EC_w \frac{d^3\gamma}{dz^3} \quad (4.14)$$

The corresponding external and internal moments for an I-beam according to axes are given in (4.15), (4.16), and (4.17), respectively.

$$EI_x \frac{d^2v}{dz^2} + M_0 = 0 \quad (4.15)$$

$$EI_y \frac{d^2u}{dz^2} + \gamma M_0 = 0 \quad (4.16)$$

$$GJ \frac{d\gamma}{dz} - EC_w \frac{d^3\gamma}{dz^3} - \frac{du}{dz} M_0 = 0 \quad (4.17)$$

The first equation is not interested in the calculations because it describes the in-plane behavior of the beam before lateral buckling. Therefore, the lateral-torsional buckling behavior of beam can be gained from the combination of the last two equations. This combining equation is given in (4.18).

$$EC_w \frac{d^4\gamma}{dz^4} - GJ \frac{d^2\gamma}{dz^2} - \frac{M_0^2}{EI_y} \gamma = 0 \quad (4.18)$$

By solving this equation considering the simply supported conditions, the critical moment can be calculated as (4.19) [46].

$$M_{ocr} = \frac{\pi}{L} \sqrt{EI_y GJ} \sqrt{1 + \frac{\pi^2 EC_w}{L^2 GJ}} \quad (4.19)$$

Describing equation (4.19) is supposed that the in-plane deflection has no effect on the lateral torsional buckling behavior of the beam. This can be justified if the major axis flexural rigidity is greater than the minor axis flexural rigidity. However, if flexural rigidities of major and minor axis are of the same of order of magnitude, the effect of bending in the vertical plane direction may be important and should be considered in calculating M_{cr} . This solution is more complicated and an approximate solution was given by Kirby and Nethercot [47] in (4.20).

$$M_{ocr} = \frac{\pi}{L} \sqrt{\frac{EI_y GJ}{1 - (I_y / I_x)}} \sqrt{1 + \frac{\pi^2 EC_w}{L^2 GJ}} \quad (4.20)$$

According to this formula, lateral torsional buckling never happens in circular cross sections or square box sections in which all the component plates have the same thicknesses. This formula also indicates that lateral torsional buckling occurs when the load is applied on the plane of weak axis.

4.5. Design of Members Subjected to Lateral Torsional Buckling Effect

4.5.1. Australian Standard – (AS 4100)

Australian steel design standard AS 4100 [48] gives nominal member moment capacity under lateral torsional buckling with (4.21).

$$M_b = \alpha_m \alpha_s M_s \leq M_s \quad (4.21)$$

α_m and α_s factors are calculated according to (4.22) and (4.23).

$$\alpha_m = \frac{1.7M_m}{\sqrt{M_2^2 + M_3^2 + M_4^2}} \leq 2.5 \quad (4.22)$$

$$\alpha_s = 0.6 \left[\sqrt{\left[\left(\frac{M_s}{M_{oa}} \right)^2 + 3 \right]} - \left(\frac{M_s}{M_{oa}} \right) \right] \quad (4.23)$$

M_s is nominal section capacity, M_{oa} is reference buckling moment which is obtained from elastic analysis of simply supported beams under a uniform bending moment and is given in (4.24).

$$M_{oa} = \sqrt{\left[\left(\frac{\pi^2 EI_y}{l_e^2} \right) \left[GJ + \left(\frac{\pi^2 EI_w}{l_e^2} \right) \right] \right]} \quad (4.24)$$

4.5.2. American Design Specification – (AISC 360-10 / LRFD)

AISC 360-10 [41] specification presents an approach for checking the lateral torsional buckling effects for the steel frame members. This approach is classified into subcategories considering unbraced length limits and the section features such as section type, modulus of elasticity, elastic and plastic section modulus.

For beams of compact sections, there are two possible types of failure: (1) plastic yielding, (2) lateral torsional buckling. The design curve is shown in Figure 4.6.

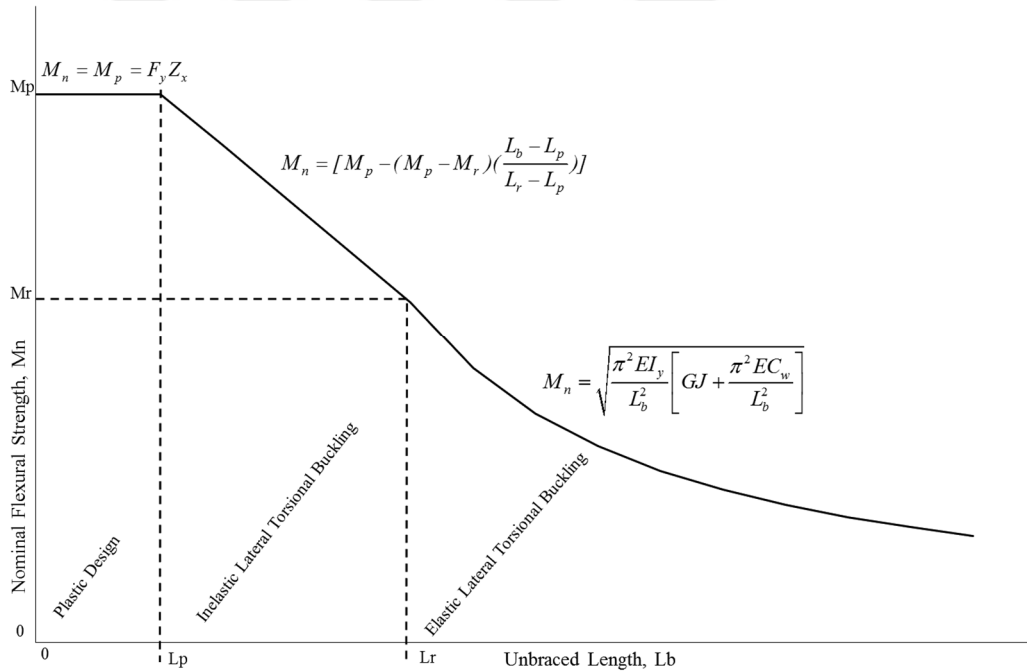


Figure 4.6 : Nominal flexural strength and unbraced length graphic under lateral torsional buckling for I-shaped members.

The unbraced length limits are given in (4.25) and (4.26) according to AISC 360-10 [41] specification :

$$L_p = 1.76 r_y \sqrt{\frac{E}{F_y}} \quad (4.25)$$

$$L_r = 1.95r_{ts} \frac{E}{0.7F_y} \sqrt{\frac{Jc}{S_x h_0}} \sqrt{1 + \sqrt{1 + 6.76 \left(\frac{0.7F_y S_x h_0}{EJc} \right)^2}} \quad (4.26)$$

In which, effective radius of gyration, r_{ts} is determined using (4.27).

$$r_{ts}^2 = \frac{\sqrt{I_y C_w}}{S_x} \quad (4.27)$$

For I-shaped members, which are subjected to bending moment about the strong axis, nominal flexural strength, M_n is determined with respect to length of the unbraced segment of the member L_b . Limits about length of unbraced segment are defined in AISC 360-10 [41]. If $L_b \leq L_p$, full plastic moment is accounted to be developed in the section and the limit state of lateral torsional buckling does not need to be applied. For this situation, (4.28) is directly used for the calculation of M_n . If $L_p \leq L_b \leq L_r$, inelastic lateral torsional buckling may occur and (4.29) is used for calculating M_n . If $L_b > L_r$, elastic lateral torsional buckling may occur and (4.30) is used for calculating M_n .

$$M_n = M_p = F_y Z_x \quad (4.28)$$

$$M_n = C_b \left[M_p - (M_p - 0.7F_y S_x) \left(\frac{L_b - L_p}{L_r - L_p} \right) \right] \leq M_p \quad (4.29)$$

$$M_n = F_{cr} S_x \leq M_p \quad (4.30)$$

F_{cr} , critical stress in (4.30) is calculated using (4.31).

$$F_{cr} = \frac{C_b \pi^2 E}{\left(\frac{L_b}{r_{ts}} \right)^2} \sqrt{1 + 0.078 \frac{Jc}{S_x h_0} \left(\frac{L_b}{r_{ts}} \right)^2} \quad (4.31)$$

Moment modification factor C_b is calculated according to (4.32) in AISC 360-10 [41].

$$C_b = \frac{12.5M_{max}}{2.5M_{max} + 3M_A + 4M_B + 3M_C} \quad (4.32)$$

Moment modification factor is studied in order to improve the capability of representing lateral torsional buckling behavior. Since moment modification factor studies are evaluated in here, these factors are summarized considering the relevant literature.

Moment modification factor is first studied by Salvadory [49] with using (4.33) considering linear moment distribution between the brace points.

$$C_b = 1.75 - 1.05\psi + 0.3\psi^2 \leq 2.3 \quad (4.33)$$

Kirby and Nethercot [47] presented an alternative equation for C_b , which is applicable for any shape of moment diagrams. A slightly modified version is given in (4.34) and is adopted by AISC 360-10 for any moment distribution.

$$C_b = \frac{12.5M_{max}}{2.5M_{max} + 3M_A + 4M_B + 3M_C} \quad (4.34)$$

Serna et al. [32], provide another equation for moment modification factor by curve fitting the numerical analysis results. In the study, numerical analysis results are obtained for equivalent uniform moment factor using the finite difference and finite element methods for a wide range of loading and end support conditions. (4.35) targets to account lateral rotation and warping restraints at the brace points.

$$C_b = \sqrt{\frac{35M_{max}^2}{M_{max}^2 + 9M_A^2 + 16M_B^2 + 9M_C^2}} \quad (4.35)$$

Wong and Driver [50], proposed an equation for C_b factor and it is presented in (4.36).

$$C_b = \frac{4M_{max}}{\sqrt{M_{max}^2 + 4M_A^2 + 7M_B^2 + 4M_C^2}} \leq 2.5 \quad (4.36)$$

4.5.3. British Standard – (BS 5950-1: 2000)

For equal flanged rolled sections, in each length between lateral restraints, the equivalent uniform moment M should not exceed the buckling resistance moment M_b . This can be expressed in (4.37) by BS 5950-1:2000 [51] ;

$$M_x \leq M_b / m_{lt} \quad (4.37)$$

The buckling resistance moment M_b is dependent on the section classification of the member and a bending strength p_b that depends on the slenderness of the beam. M_b is determined in (4.38):

$$M_b = p_b S_x \quad (4.38)$$

For plastic and compact sections S_x is the section plastic modulus, for semi-compact and slender sections Z_x is the section elastic modulus are used instead of S_x .

For I and H sections, the equivalent slenderness λ_{LT} is determined using (4.39), u is a buckling parameter obtained from section property tables.

$$\lambda_{LT} = uv\lambda(\beta_w)^{0.5} \quad (4.39)$$

λ is the slenderness, and this minor axis slenderness are expressed in (4.40)

$$\lambda = \frac{L_e}{r_y} \quad (4.40)$$

British code for steelworks in buildings [51] presents a formulation for determining equivalent uniform moment factor with C_1 as in (4.41) under lateral torsional buckling. C_1 is also equal to I / m_{LT} . All of M values are the absolute moments along L_b .

$$C_1 = \frac{M_{max}}{0.2M_{max} + 0.15M_A + 0.5M_B + 0.15M_C} \leq 2.273 \quad (4.41)$$

4.5.4. European Standard – European Code 3 (EN 1993-1-1)

The design buckling resistance moment of laterally unrestrained beam is defined in EN 1993-1-1 [52] with (4.42);

$$M_{b,Rd} = \chi_{LT} W_y f_y / \gamma_{M1} \quad (4.42)$$

Reduction factor, χ_{LT} is calculated using (4.43).

$$\chi_{LT} = \frac{1}{\phi_{LT} + \sqrt{\phi_{LT}^2 - \bar{\lambda}_{LT}^2}} \quad (4.43)$$

In which, ϕ is calculated as (4.44) and $\bar{\lambda}$ is calculated as (4.45).

$$\phi_{LT} = 0.5 \left[1 + \alpha_{LT} (\bar{\lambda}_{LT} - 0.2) + \bar{\lambda}_{LT}^2 \right] \quad (4.44)$$

$$\bar{\lambda}_{LT} = \sqrt{\frac{W_y f_y}{M_{cr}}} \quad (4.45)$$

Critical elastic lateral torsional buckling moment capacity for the case of beams with doubly symmetric sections and simply supported ends and subjected to a constant

moment over the laterally unbraced length is given with (4.46) in EN 1993-1-1 [52]. In this equation, member is assumed to be loaded from shear center.

$$M_{cr} = C_1 \frac{\pi^2 EI_z}{(kL)^2} \left[\sqrt{\left(\frac{k}{k_w}\right)^2 \frac{I_w}{I_z} + \frac{(kL)^2 GI_t}{\pi^2 EI_z}} \right] \quad (4.46)$$

In which, the effective length factors k and k_w vary from 0.5 for full fixity to 1.0 for no fixity, with 0.7 for one end fixed and one end free.

For a case with k is equal to 1.0, the value of C_1 for any ratio of end moment loading is given with (4.47).

$$C_1 = 1.88 - 1.4\psi + 0.52\psi^2 \leq 2.70, \quad \psi = \frac{M_S}{M_L} \quad (4.47)$$

The end moment ratio, ψ , is taken as positive for moment causing reverse-curvature bending and negative for single-curvature bending.

4.5.5. Turkish Steel Design Code – (TSDC-2016)

TSDC-2016 [43] presents an approach for determining the lateral torsional buckling effects for the steel frame members and it is summarized in this part. This approach is very similar to that of AISC 360-10 [41], and it classifies elastic and inelastic buckling considering unbraced length limits. These unbraced length limits are presented in (4.48) and (4.49).

$$L_p = 1.76i_y \sqrt{\frac{E}{F_y}} \quad (4.48)$$

$$L_r = 1.95i_{ts} \frac{E}{0.7F_y} \sqrt{\frac{Jc}{W_{ex}h_0} + \sqrt{\left(\frac{Jc}{W_{ex}h_0}\right)^2 + 6.76\left(\frac{0.7F_y}{E}\right)^2}} \quad (4.49)$$

In which, effective radius of gyration, i_{ts} is calculated as (4.50).

$$i_{ts}^2 = \frac{\sqrt{I_y C_w}}{W_{ex}} \quad (4.50)$$

For I-shaped members, which are subjected to bending moment about the strong axis, M_n is determined with respect to length of the unbraced segment of the member L_b . This methodology is similar to the AISC 360-10 [41]. When unbraced length exceeds

unbraced length limit, inelastic or elastic lateral torsional buckling may occur. If $L_b \leq L_p$, full plastic moment is accounted to be developed in the section and the limit state of lateral torsional buckling does not need to be applied. For this situation, (4.51) is directly used for the calculation of M_n . If $L_p \leq L_b \leq L_r$, inelastic lateral torsional buckling may occur and (4.52) is used for calculating M_n . If $L_b > L_r$, elastic lateral torsional buckling may occur and (4.53) is used for calculating M_n .

$$M_n = M_p = F_y W_{px} \quad (4.51)$$

$$M_n = C_b [M_p - (M_p - 0,7 F_y W_{ex}) \left(\frac{L_b - L_p}{L_r - L_p} \right)] \quad (4.52)$$

$$M_n = F_{cr} W_{ex} \leq M_p \quad (4.53)$$

The critical stress, F_{cr} is defined in TSDC-2016 [43] as (4.54).

$$F_{cr} = \frac{C_b \pi^2 E}{\left(\frac{L_b}{i_{ts}} \right)^2} \sqrt{1 + 0,078 \frac{Jc}{W_{ex} h_0} \left(\frac{L_b}{i_{ts}} \right)^2} \quad (4.54)$$

4.5.6. Turkish Standard according to plastic theory – (TS 4561)

Design standard TS 4561 [53] is used in structural steel design practice in Turkey up to publication of TSDC-2016 [43]. After the publication of TSDC-2016 [43] in 2016, TS 4561 [53] standard is abolished. Unbraced length limits for TS 4561 are given in (4.55), (4.56), and (4.57) [53].

$$0,625 \leq \frac{M_x}{M_p} \leq 1 \quad \text{for } L_{Kr} = 35 i_y \sqrt{\frac{2400}{\sigma_a}} \quad (4.55)$$

$$-0,625 \leq \frac{M_x}{M_p} \leq 0,625 \quad \text{for } L_{Kr} = \left(60 - 40 \frac{M}{M_p} \right) i_y \sqrt{\frac{2400}{\sigma_a}} \quad (4.56)$$

$$-1 \leq \frac{M_x}{M_p} \leq -0,625 \quad \text{for } L_{Kr} = 85 i_y \sqrt{\frac{2400}{\sigma_a}} \quad (4.57)$$

In case of lateral torsional buckling in steel frame members according to TS 4561 [53], the carrying capacity of this part is calculated by (4.58). In here, (4.59) and (4.60) are used to calculate k_D and M_D values in the calculation of plasticization moment.

$$M_{Kr} = k_D M_p \quad (4.58)$$

$$k_D = \frac{1}{\sqrt[3]{1 + 1,3\left(\frac{M_p}{M_D}\right)^3}} \quad (4.59)$$

$$M_D = C_1 \frac{\pi^2 EI_y (h - t_b)}{2L_D L} \left[\sqrt{1 + (\eta C_2)^2 + \frac{GK_T}{EI_y} \left(\frac{2L}{\pi h}\right)^2} + \eta C_2 \right] \quad (4.60)$$

Member is subjected to moment and axial pressure forces acting around the principal axis giving great moment of inertia when stability loss is caused by lateral torsional buckling. Lateral torsional buckling will result in loss of stability unless it is prevented against the out of plane motion at a sufficient level and the member is not able to reach its plastic moment carrying capacity. In this case, (4.61) is used for section effects.

$$\frac{N}{N_{Kr}} + \frac{C_m M}{M_{Kr} \left(1 - \frac{N}{N_e}\right)} \leq 1 \quad (4.61)$$

4.6. Considering Lateral Torsional Buckling Effects in Nonlinear Analysis Steps

Nonlinear analysis assumes that frame systems are safe against lateral torsional buckling, regardless of lateral support situations. It is clear that this acceptance is far from reflecting the real situation, in many cases, except when composite frames are used, when steel frames are thought to be used more for industrial purposes. In this study, an approach has been proposed to consider the effects of lateral torsional buckling in practical nonlinear analysis steps and to be able to model structure analyzes as accurately as possible in real situations taking into account TSDC-2016 [43] and AISC 360-10 [41] codes.

The strong axes of the steel frame members are generally selected in this direction as the bending stiffness in which the load is applied are large for economical design. For this reason, out-of-plane motion is often determined by considering weak axes. If the out-of-plane displacements and rotational behavior of these elements are not impeded adequately, members will not be able to reach moment-bearing capacities in the plane because of lateral torsional buckling. Consequently, in order to reflect the lateral torsional buckling effects to the nonlinear analysis steps, the axial force and the bending moment interactions are defined by (4.62) and (4.63).

$$\frac{P_r}{P_p} + \frac{8M_r}{9M_n} = 1.0 \quad \text{for} \quad \frac{P_r}{P_p} \geq 0.2 \quad (4.62)$$

$$\frac{P_r}{2P_p} + \frac{M_r}{M_n} = 1.0 \quad \text{for} \quad \frac{P_r}{P_p} < 0.2 \quad (4.63)$$

The inelastic moments are redistributed in the frame systems by incorporating the lateral torsional buckling into the calculations using the defined axial forces and bending moment interactions in nonlinear analysis with (4.62) and (4.63). In the load increment steps, firstly the lateral torsional buckling for each element is controlled on an element basis, and the moment carrying capacity is recalculated for elements exposed to the lateral torsional buckling effect. This applies to parts where the out-of-plane motion of steel frame elements is inhibited. For out-of-plane motion and for elements yielding due to lateral torsional buckling, the contribution of the element to the system is assumed to be zero and the inelastic moment distribution for the element is prevented from being redistributed. This analytical approach proposed in the study contributes to the development of nonlinear analysis methods of steel structures as it aims to determine the overall load carrying capacity of the frame system beyond the elemental lateral torsional buckling behavior. It is also known that many computer software performs nonlinear analysis assuming that the safety against lateral torsional buckling is provided by the designer, and the approach presented here allows the lateral torsional buckling effect to be directly accounted for in the nonlinear analysis steps.

5. NUMERICAL EXAMPLES

Lateral torsional buckling effect on nonlinear analysis of steel frames is investigated using numerical examples. In these examples, different structural parameters are aimed to be focused. In the beginning, a simply supported beam is examined with unequal end moments conditions under the lateral torsional buckling effect. Also, different design specifications are used to compare the results. Following this, a fixed supported beam is analyzed considering lateral torsional buckling. After member based investigations, frames which have different story heights and spans, various loading and support conditions are considered and examined with and without considering lateral torsional buckling effect. Finally, different unbraced length conditions are applied on a simply supported beam and the importance of unbraced lengths is presented. Consequently, frame examples are investigated with different unbraced conditions.

All of the frame examples are selected from the literature and nonlinear behavior of these frames are investigated considering lateral torsional buckling. Moreover, numerical examples are aimed to be performed for determining the effects of different bracing conditions that limit out-of-plane deformations, end-restraint conditions, loading types. Furthermore, different design specifications that account lateral torsional buckling effect is investigated comparatively. Load carrying capacity and joint deflections of steel frame structures are used for evaluating the analysis results. Load increments are performed up to ultimate load parameter value, behavior beyond this limit is not considered in the numerical examples.

5.1. Comparison of Lateral Torsional Buckling Effect According to Design Specifications

Lateral torsional buckling behaviors of I-shaped steel members are examined considering different design approaches using a simply supported steel beam made of IPE 500 section. Loading procedure of simply supported beam is presented in Figure 5.1.

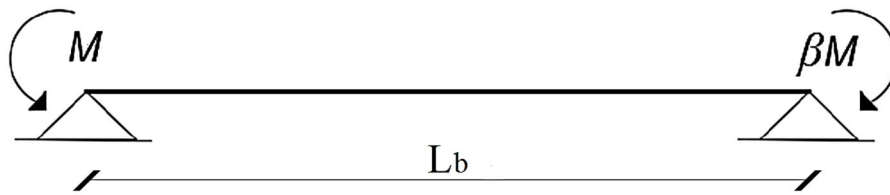


Figure 5.1 : Simply supported I-shaped member under linear moment gradient.

Section properties for IPE500 section are; torsion constant, J is $7.23 \times 10^{-7} \text{ m}^4$, warping constant, C_w is $1.336 \times 10^{-6} \text{ m}^6$, plastic section modulus about the major axis, Z_x is $2.194 \times 10^{-3} \text{ m}^3$.

Lateral torsional buckling analyses are performed considering several standards, codes and also recommended moment gradient factor equations. Beside the analytical approach, LTBeam [54] and finite element based ANSYS [55] are used to validate the analytical analysis results. In Figure 5.2 and Figure 5.3, lateral torsional buckling of I-shaped members are illustrated using LTBeam [54] and ANSYS [55], respectively. According to these figures, when I-shaped member is loaded in its major principle plane, upper flange goes into compression, which means it is trying to get shorter. This flange will therefore tend to buckle out sideways.

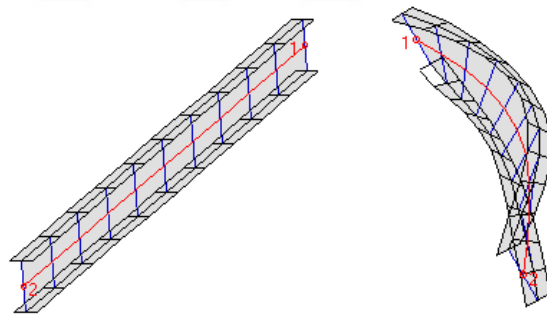


Figure 5.2 : Lateral torsional buckling with LTBeam [54]

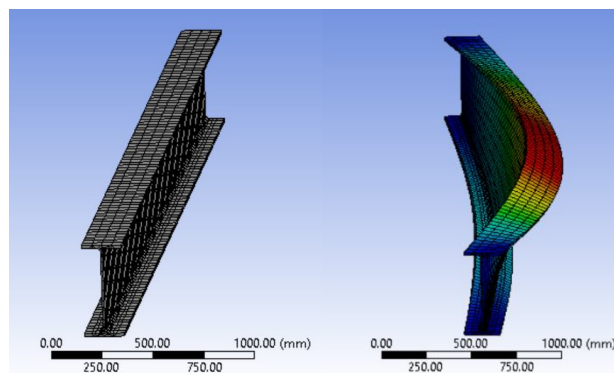


Figure 5.3 : Lateral torsional buckling with FE Analysis [55]

In order to plot the end moment ratio $-1 < \beta < 1$ to elastic lateral torsional buckling moment capacity, different unbraced length conditions are considered in the present study. These unbraced lengths are selected as 8 m, 10 m, 12 m, and 16 m in which lateral torsional buckling occurs in the elastic range.

Lateral torsional buckling behaviors of I-shaped steel members are calculated for simply supported steel IPE 500 beam considering unbraced lengths. In the study, AISC 360-10 [41], AS 4100 [48], BS 5950 [51], EN 1993-1-1 [52], TSDC-2016 [43] and TS 4561 [53] approaches are compared with finite element based LTBeam [54] and ANSYS [55] analysis outcomes. Furthermore, moment gradient factor proposed by researchers [32, 47, 49, 50] are also used and the outcomes are presented for evaluation.

Unbraced member length of 8 m is first used for determining elastic lateral torsional buckling moment capacity considering the changes in the moment ratio values. Outcomes of the analyses are given in Figure 5.4 and Figure 5.5.

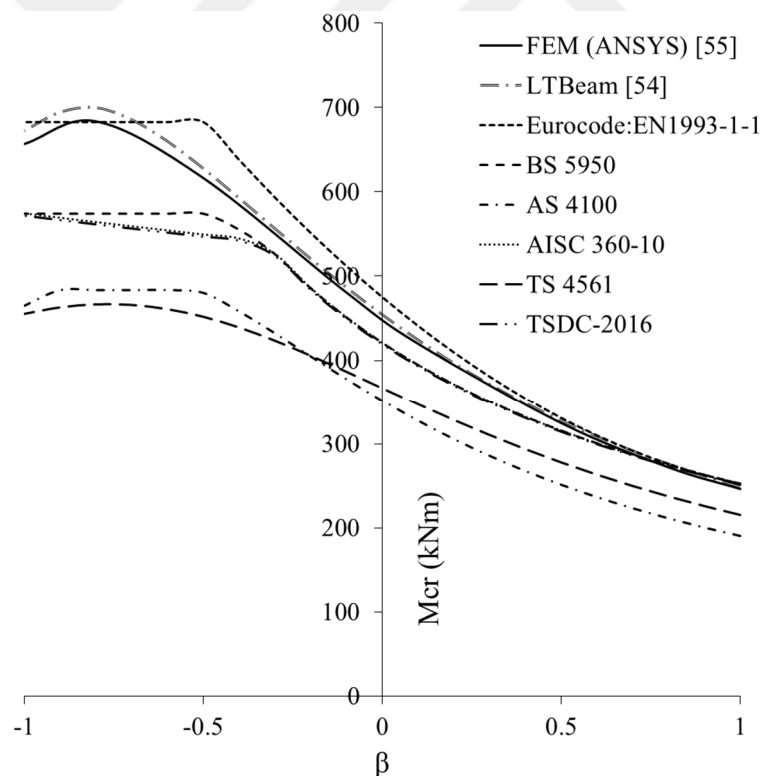


Figure 5.4 : End moment ratio (β) and M_{cr} for doubly symmetric I-beam with $L_b = 8$ m.

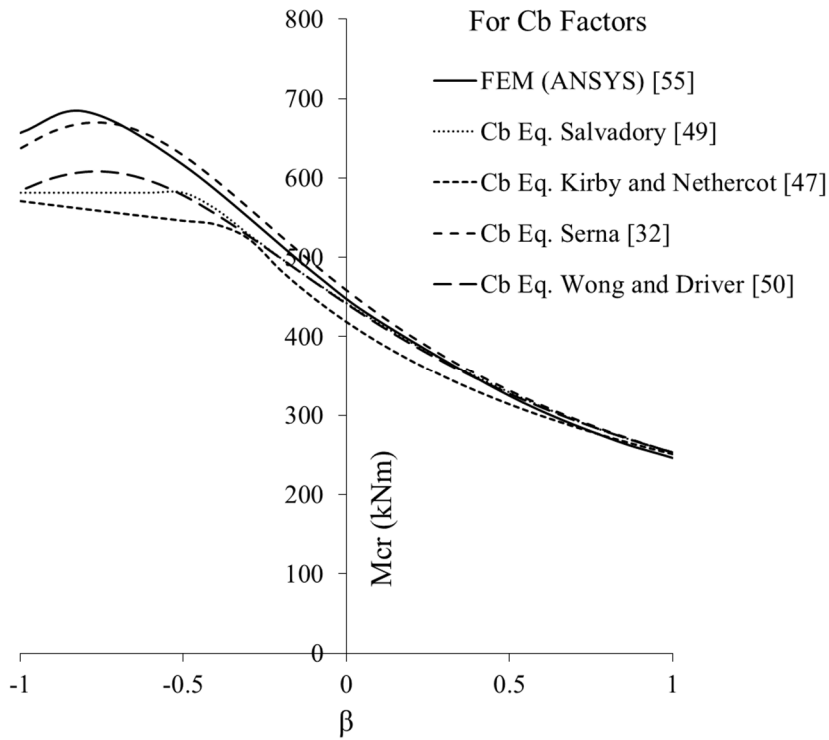


Figure 5.5 : End moment ratio (β) and M_{cr} for doubly symmetric I-beam with $L_b = 8$ m considering C_b factors.

Unbraced member length of 10 m is analyzed and results are presented in Figure 5.6 and Figure 5.7.

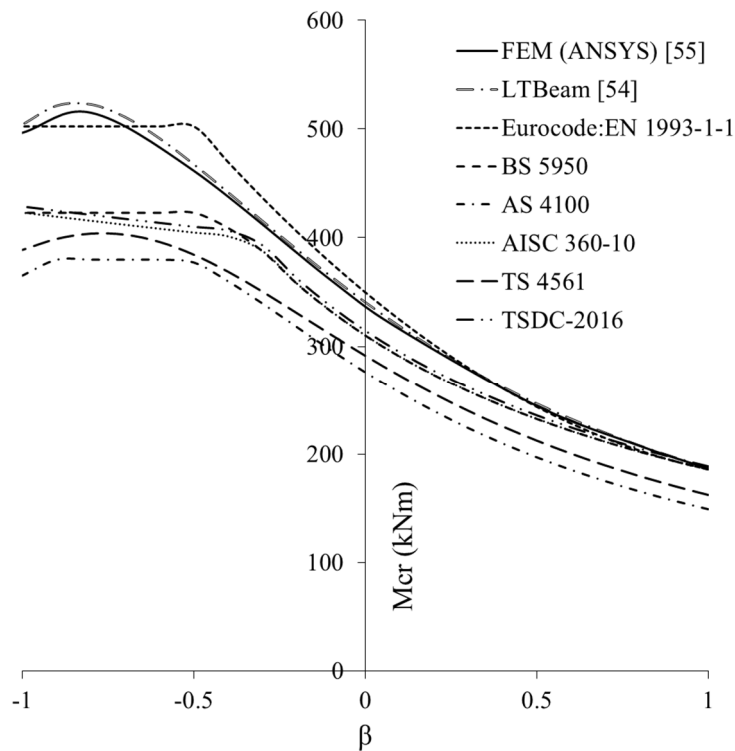


Figure 5.6 : End moment ratio (β) and M_{cr} for doubly symmetric I-beam with $L_b = 10$ m.

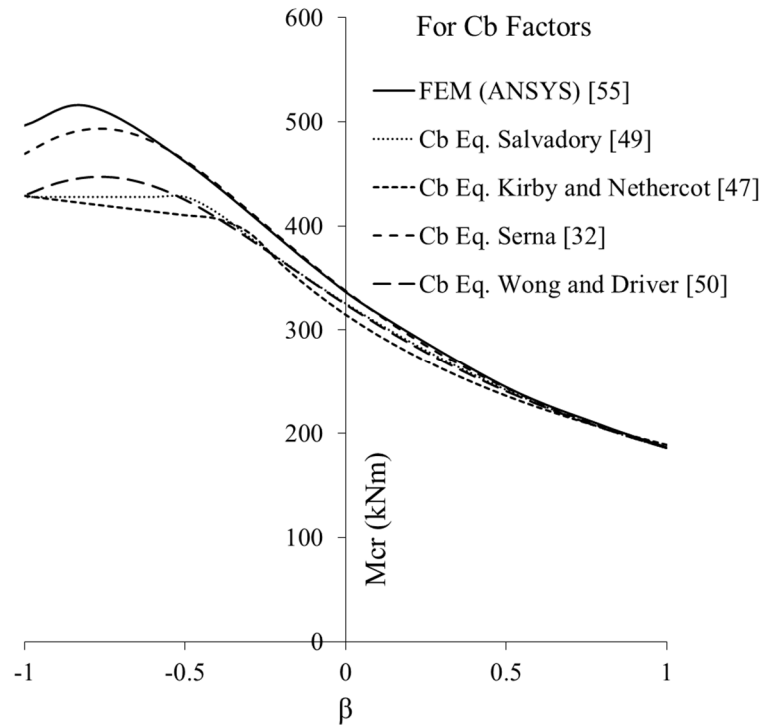


Figure 5.7 : End moment ratio (β) and M_{cr} for doubly symmetric I-beam with $L_b = 10$ m considering C_b factors.

Unbraced member length of 12 m is analyzed and results are presented in Figure 5.8 and Figure 5.9.

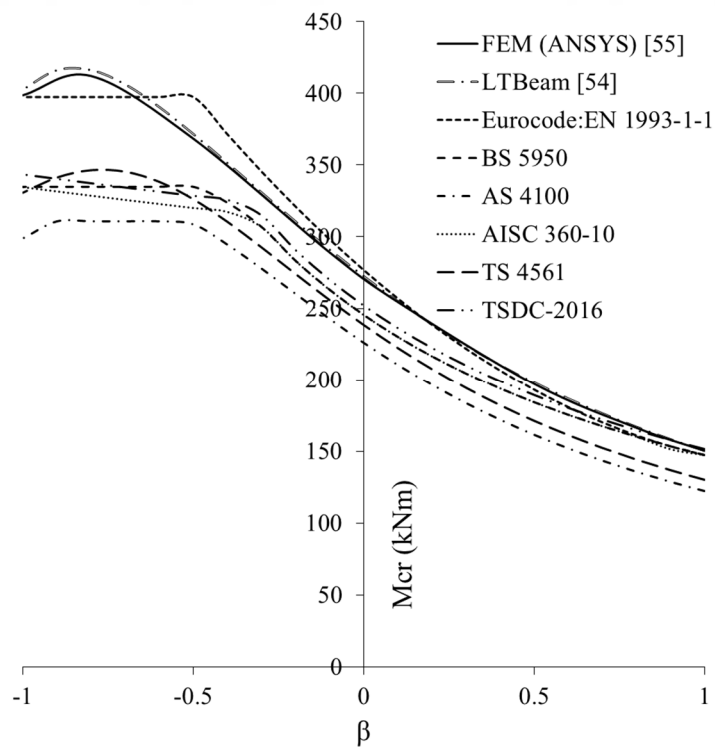


Figure 5.8 : End moment ratio (β) and M_{cr} for doubly symmetric I-beam with $L_b = 12$ m.

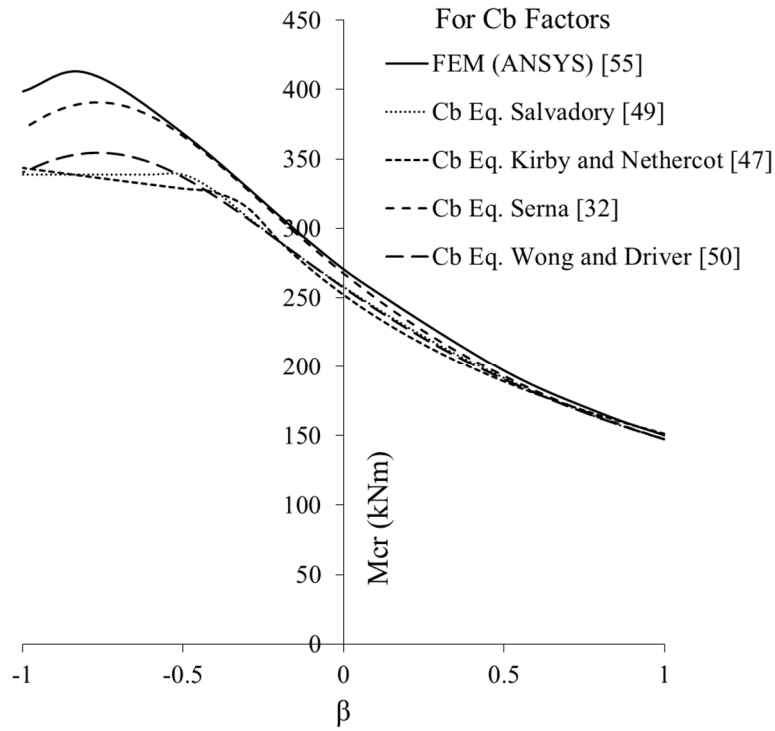


Figure 5.9 : End moment ratio (β) and M_{cr} for doubly symmetric I-beam with $L_b = 12$ m considering C_b factors.

Finally, unbraced member length of 16 m is analyzed and results are presented in Figure 5.10 and Figure 5.11.

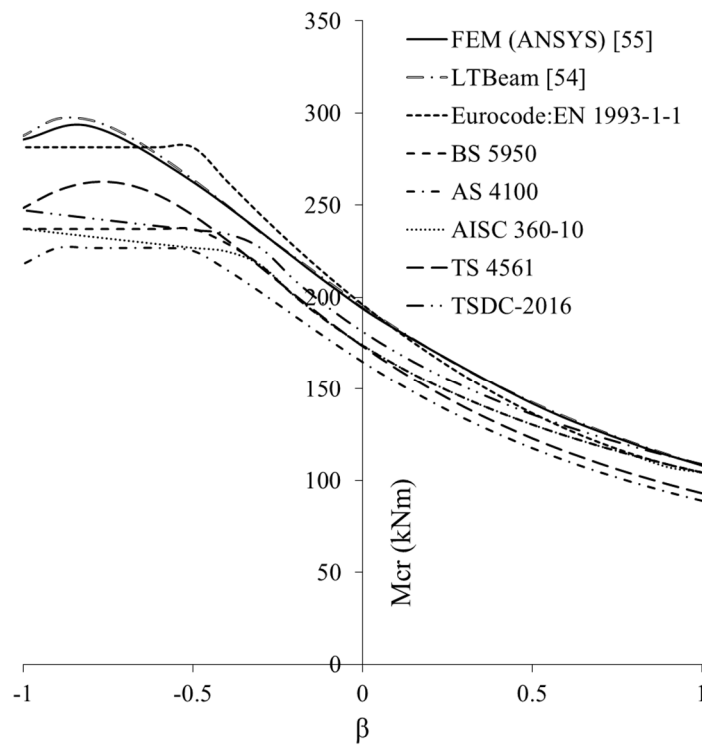


Figure 5.10 : End moment ratio (β) and M_{cr} for doubly symmetric I-beam with $L_b = 16$ m.

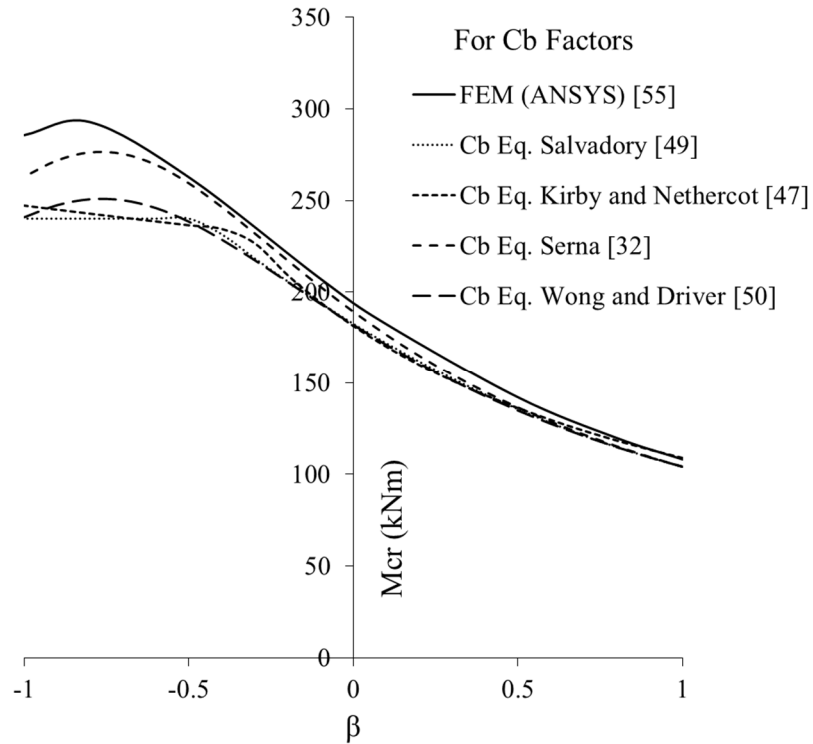


Figure 5.11 : End moment ratio (β) and M_{cr} for doubly symmetric I-beam with $L_b = 16$ m considering C_b factors.

According to the numerical example of the study, TS 4561 [53] and AS 4100 [48] give more conservative results than the other approaches. AISC 360-10 [41], TSDC-2016 [43] and BS 5950 [51] give close results to each other. Results of EN 1993-1-1 [52] are generally close to FEM [55] and LTBeam [54] results. Unbraced member length increases cause significant decrease in elastic moment capacity under lateral torsional buckling. In addition, differences in between analysis approaches decrease with the increase of unbraced member length. In order to improve the accuracy of determining the elastic critical moment capacity, moment gradient factors from the literature are also investigated. Results of the numerical example of this study show that C_b equation provided by Serna et al. [32] are more close to FEM [55] results than other approaches considered in the study.

5.2. Nonlinear Analysis of Fix Supported Beam under Uniformly Distributed Load

In order to investigate lateral torsional buckling effects on structural steel members, a beam which has fixed supports at both ends, is selected and structural behavior is determined [56]. Beam member has 12 m length and W 24x55 steel section. Section

properties for W 24x55 section is defined as torsion constant, J is $491 \times 10^3 \text{ mm}^4$, warping constant, C_w is $1040 \times 10^9 \text{ mm}^6$, plastic section modulus about the major axis, Z_x is $2200 \times 10^3 \text{ mm}^4$. Distributed load is applied as 20 kN/m and steel beam is shown in Figure 5.12.

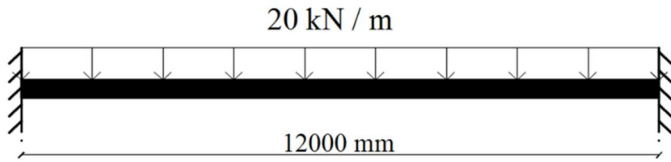


Figure 5.12 : Fixed end beam.

For monitoring the lateral torsional buckling effects and evaluating the structural behavior, nonlinear analysis results without and with considering lateral torsional buckling are given in Figure 5.13. Degradation due to lateral torsional buckling is represented and load parameter - midpoint vertical displacement relationships are plotted. Also, plastic hinge formations are also given in Figure 5.13.

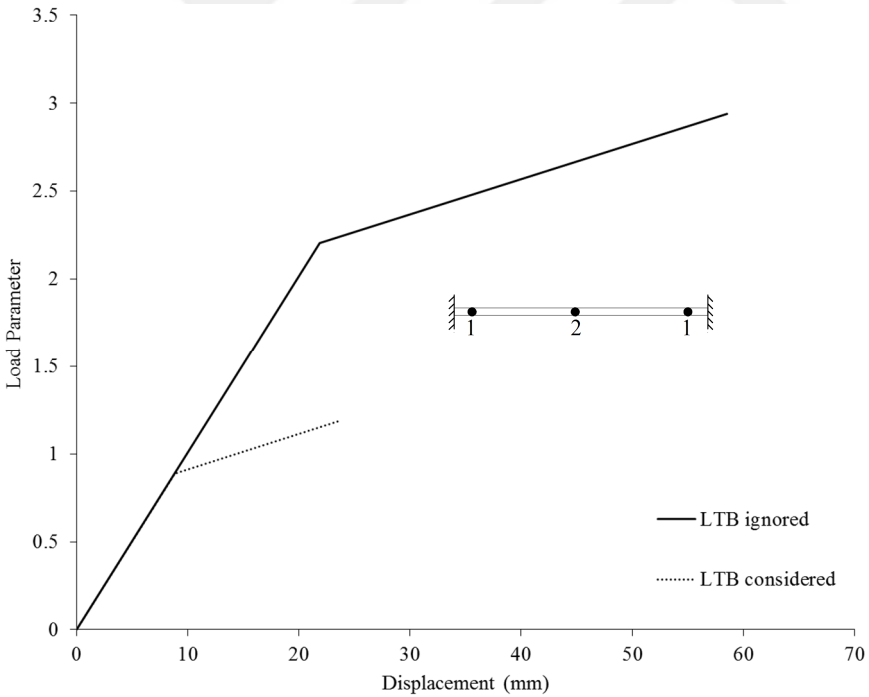


Figure 5.13 : Fixed end beam analysis results.

Analysis results for beam member show that load carrying capacity decreased 65.2% when lateral torsional buckling is considered. It is observed that lateral torsional buckling has decreased the load carrying capacity of the beam significantly.

5.3. First-Order Elastic-Plastic Analysis of One Story Side-Sway Prevented Frames

Single-story steel frames in which side-sway is prevented are selected from literature and shown in Figure 5.14. In the literature, plastic zone analysis was used and lateral torsional buckling effect was not considered [57].

In order to analyze these frames, geometric and section properties, loading details are presented. These single-story frames have different restraint conditions fix supports and pinned support, respectively. Out-of-plane motion is limited using braces at the joints of the member ends and bracing points are also presented in Figure 5.14. Beams and columns in these frames are rigidly connected about their strong-axis bending direction and same section is used in both frames. Cross section of the beam is W 16x50 ($J= 63300 \text{ mm}^4$, $C_w= 610 \times 10^9 \text{ mm}^6$, $Z_x= 1510 \times 10^3 \text{ mm}^4$). Cross section of the columns is W 8x31 ($J= 223 \times 10^3 \text{ mm}^4$, $C_w= 142 \times 10^9 \text{ mm}^6$, $Z_x= 498 \times 10^3 \text{ mm}^4$). These frames are both subjected to uniformly distributed load W_b along the beam and point loads P_c at the end joints of the beam members. Relationship about loads are given as; $P_b = W_b L_b$ and $\beta = P_b / (2P_c + P_b)$ where β is the ratio of the load. In this study, β is accounted as 0.34 to evaluate these examples as given in the literature [57].

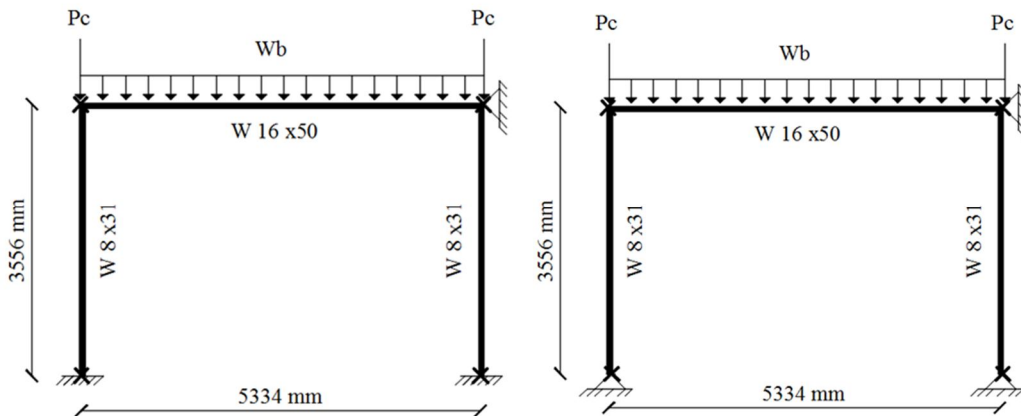


Figure 5.14 : Single-story frame with fix support and pin support.

Nonlinear analysis is applied on the single-story frames and lateral torsional buckling effect is considered for determining the realistic behavior [58]. Load carrying capacities - midpoint vertical displacements of the beams are calculated and the graphics are plotted. Load parameter – vertical displacement graphic for fix support and pin support conditions is presented in Figure. 5.15. Also, plastic hinge formations for fix supported and pin supported conditions are given in Figure 5.16, respectively.

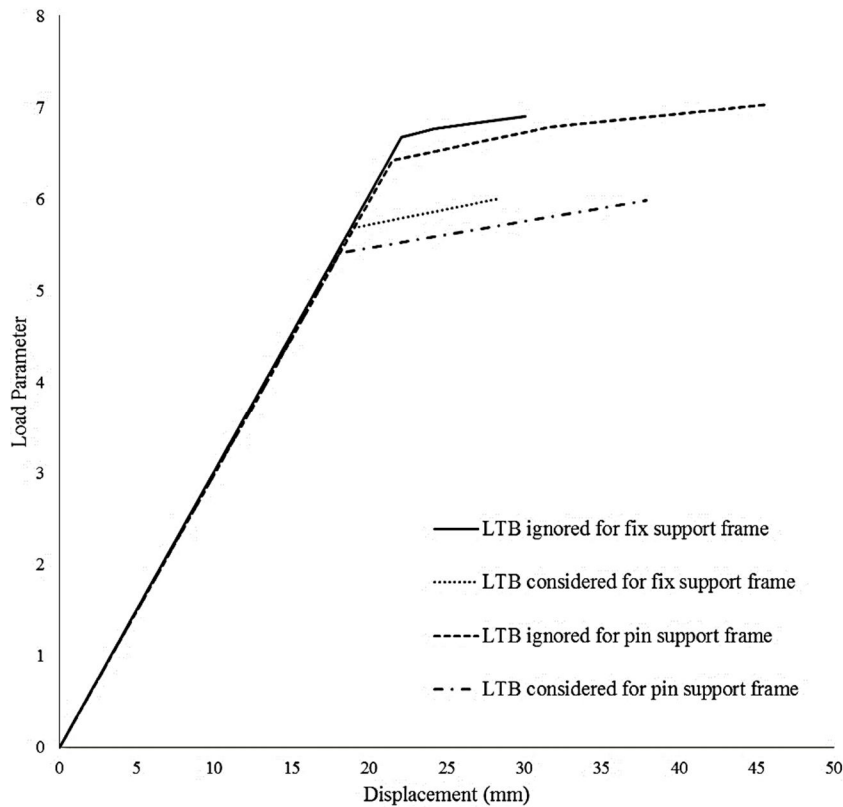


Figure 5.15 : Load parameter – beam midpoint vertical displacement of single-story frame with fix supports.

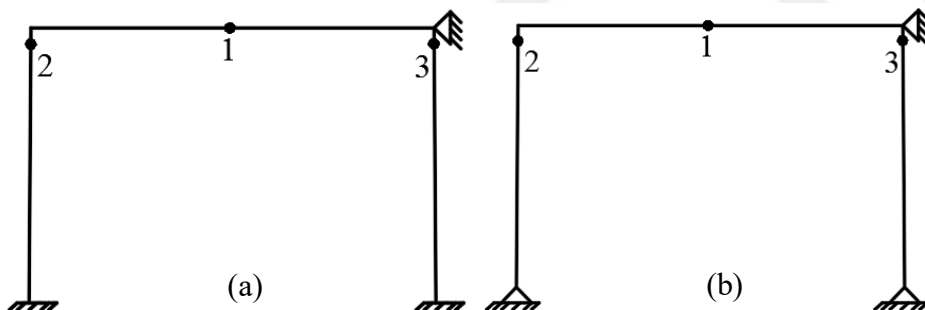


Figure 5.16 : Order of plastic hinge formations (a) for fix support frame (b) for pin support frame.

Nonlinear analysis results show that considering lateral torsional buckling decreased the load carrying capacity by 9.9% and 10.2% for fix and pin support conditions. For this example, lateral torsional buckling have no vital influence on the vertical midpoint displacements of the beams. Vertical midpoint displacement values for the pin supported frame is greater than the fix supported frame. In this example, considering lateral torsional buckling in the nonlinear analysis decreased the load carrying capacity but the displacement values are not significantly affected. On the other hand, support conditions have changed slightly the midpoint displacements.

5.4. First-Order Elastic-Plastic Analysis of Ziemann Frame

A benchmark frame that exists in the literature [59] is used for determining the load carrying capacity due to lateral torsional buckling. This frame has two spans and two stories. Cross section of the beams are W 27x84 ($J= 1170 \times 10^3 \text{ mm}^4$, $C_w= 4810 \times 10^9 \text{ mm}^6$, $Z_x= 4000 \times 10^3 \text{ mm}^4$), W 36x170 ($J= 6290 \times 10^3 \text{ mm}^4$, $C_w= 26500 \times 10^9 \text{ mm}^6$, $Z_x= 10900 \times 10^3 \text{ mm}^4$), W 21x44 ($J= 320 \times 10^3 \text{ mm}^4$, $C_w= 567 \times 10^9 \text{ mm}^6$, $Z_x= 1560 \times 10^3 \text{ mm}^4$) and W 27x102 ($J= 2200 \times 10^3 \text{ mm}^4$, $C_w= 6440 \times 10^9 \text{ mm}^6$, $Z_x= 5000 \times 10^3 \text{ mm}^4$). Cross section of the columns are W 8x15 ($J= 57 \times 10^3 \text{ mm}^4$, $C_w= 13.9 \times 10^9 \text{ mm}^6$, $Z_x= 223 \times 10^3 \text{ mm}^4$), W 14x132 ($J= 5120 \times 10^3 \text{ mm}^4$, $C_w= 6850 \times 10^9 \text{ mm}^6$, $Z_x= 3830 \times 10^3 \text{ mm}^4$), W 14x120 ($J= 3900 \times 10^3 \text{ mm}^4$, $C_w= 6100 \times 10^9 \text{ mm}^6$, $Z_x= 3470 \times 10^3 \text{ mm}^4$), W 8x13 ($J= 36.3 \times 10^3 \text{ mm}^4$, $C_w= 11 \times 10^9 \text{ mm}^6$, $Z_x= 187 \times 10^3 \text{ mm}^4$) and W 14x109 ($J= 2960 \times 10^3 \text{ mm}^4$, $C_w= 5420 \times 10^9 \text{ mm}^6$, $Z_x= 3150 \times 10^3 \text{ mm}^4$). Beams and columns are rigidly connected about their strong axis bending direction and out-of-plane motion is prevented at the joints of the member. Dimensions, structural sections and applied load values of the steel frame are also given in Figure 5.17. Horizontal displacement is monitored for the joint A and positive direction for displacement is accounted.

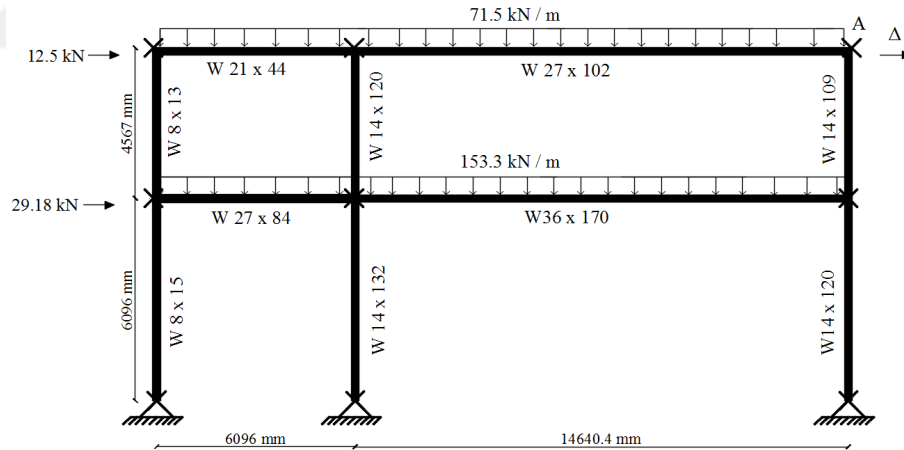


Figure 5.17 : Ziemann Frame [59].

Ziemann frame is analyzed for considering lateral torsional buckling effect and the structural behavior is investigated [56]. Load carrying capacity – lateral displacements of joint A are calculated and the graphic is plotted in Figure 5. 18. Also, order of plastic hinge formations are given in Figure 5.19 for lateral torsional buckling considered and ignored cases, respectively.

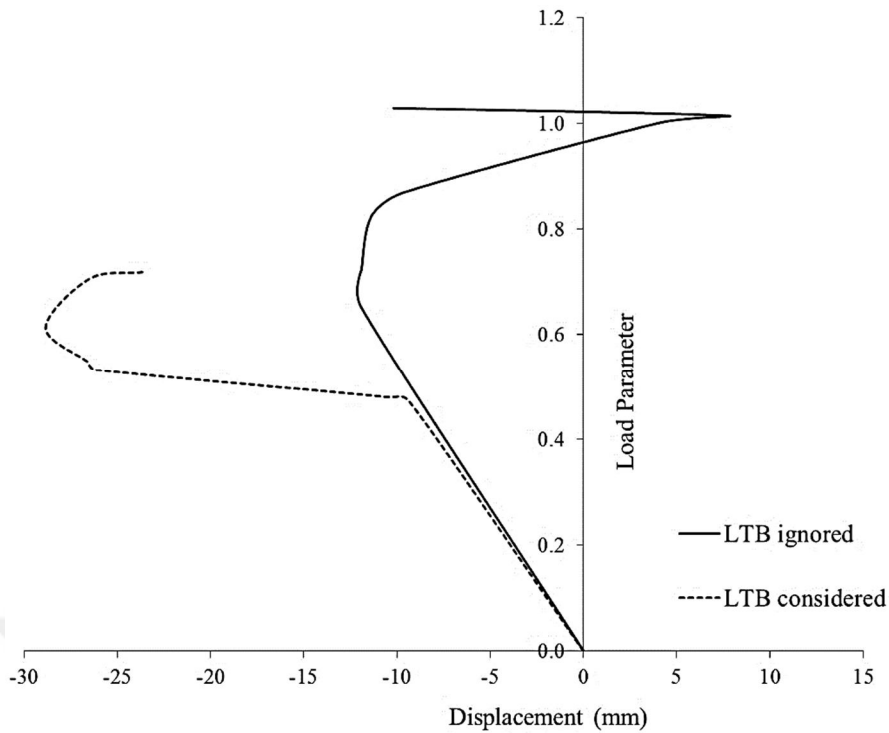


Figure 5.18 : Peak point lateral displacements and load parameters of Ziemann frame.

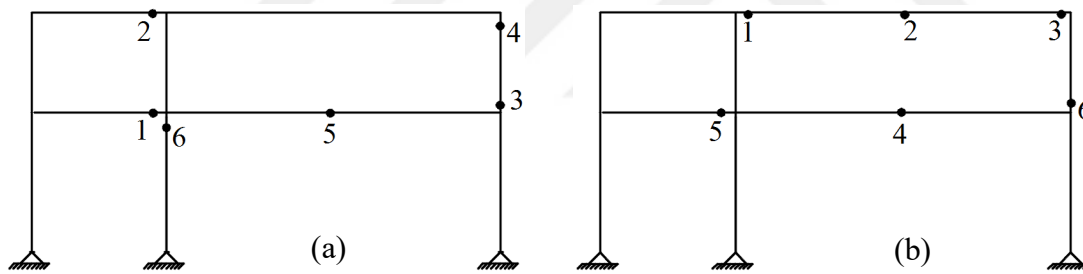


Figure 5.19 : Order of plastic hinge formations (a) lateral torsional buckling ignored (b) lateral torsional buckling considered.

Nonlinear analyses are performed for the Ziemann frame with and without considering lateral torsional buckling. In literature, ultimate load parameter has been found as approximately 1.00 and in this study, ultimate load parameter is calculated as 1.03 for lateral torsional buckling ignored case. Load parameter decrease when the lateral torsional buckling is considered in the nonlinear analysis steps Moreover, horizontal displacements are affected from lateral torsional buckling effect and direction changes have been observed. This is due to change in the order of plastic hinge formations. If lateral torsional buckling behavior is considered, load carrying capacity decreases as 32.0 %. It is determined that lateral torsional buckling is considerable for nonlinear analysis of steel frames in order to decide the structural behavior.

5.5. Second-Order Elastic-Plastic Analysis of Two Stories and Two Spans Frame

Steel frame selected from the literature [60] is investigated with and without considering lateral torsional buckling. This frame have two stories and two spans. Cross section of the beams are W 24x84 ($J= 1540 \times 10^3 \text{ mm}^4$, $C_w= 3440 \times 10^9 \text{ mm}^6$, $Z_x= 3670 \times 10^3 \text{ mm}^4$), W 21x62 ($J= 762 \times 10^3 \text{ mm}^4$, $C_w= 1600 \times 10^9 \text{ mm}^6$, $Z_x= 2360 \times 10^3 \text{ mm}^4$). Cross section of the columns are W 8x28 ($J= 224 \times 10^3 \text{ mm}^4$, $C_w= 83.8 \times 10^9 \text{ mm}^6$, $Z_x= 446 \times 10^3 \text{ mm}^4$), W 8x35 ($J= 320 \times 10^3 \text{ mm}^4$, $C_w= 166 \times 10^9 \text{ mm}^6$, $Z_x= 569 \times 10^3 \text{ mm}^4$), W 8x18 ($J= 71.6 \times 10^3 \text{ mm}^4$, $C_w= 32.8 \times 10^9 \text{ mm}^6$, $Z_x= 279 \times 10^3 \text{ mm}^4$). Section types, dimensions and applied loads are also shown in Figure 5.20. Out-of-plane motion is prevented at the joints of the member. Lateral displacement (Δ) is monitored at the top point of the frame and shown in Figure 5.20.

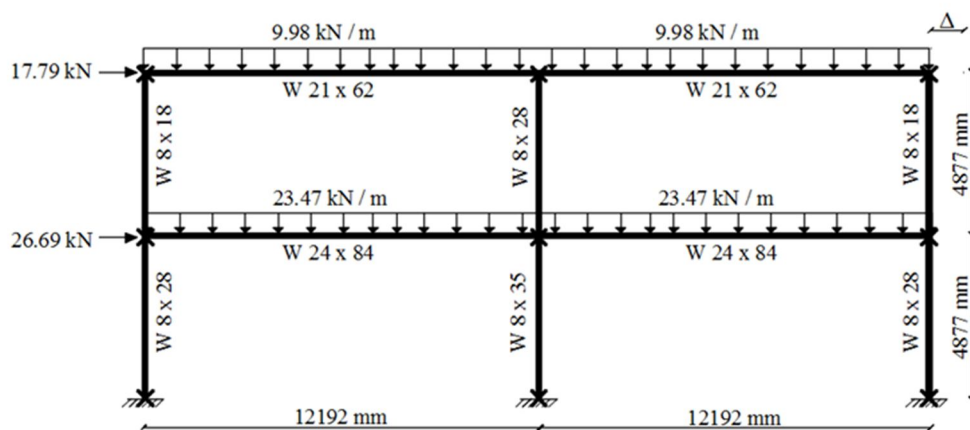


Figure 5.20 : Two story and two span frame.

Steel frame is analyzed under the lateral torsional buckling effect and second-order elastic-plastic analysis method is used in the analyses. According to the analysis results, structural behavior is examined. In this frame, moment modification factor ($C_b = 1$) case is also examined because AISC 360-10 [41] and TSDC-2016 [43] specifications recommend to use $C_b = 1$ in order to be on the safe side in the calculations of lateral torsional buckling and results are compared other analysis results. Load carrying capacity – lateral displacements of top point of the frame (Δ) are calculated and the graphics are plotted in Figure 5.21. Also, order of plastic hinge formations are given in Figure 5.22 for lateral torsional buckling considered and ignored cases, respectively.

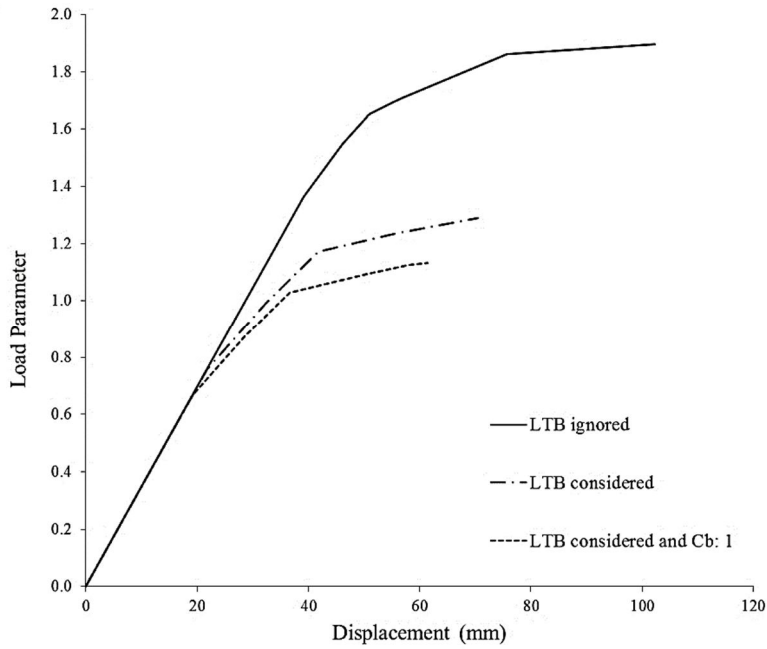


Figure 5.21 : Peak point lateral displacements and load parameters of two stories and two spans frame.

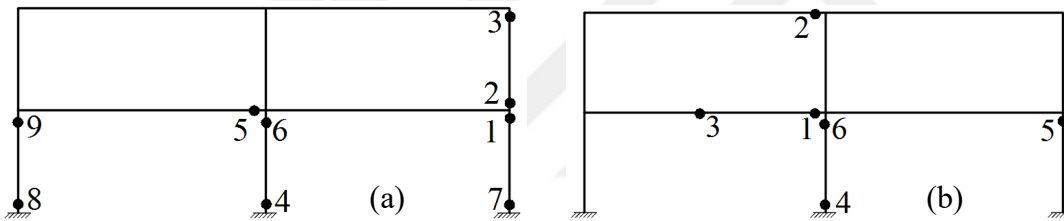


Figure 5.22 : Order of plastic hinge formations (a) lateral torsional buckling ignored (b) lateral torsional buckling considered.

In Table 5.1, ultimate load parameters and decreasing in load carrying capacities of the examined steel frame structure under different conditions are given.

Table 5.1 : Ultimate load parameter and decreasing in load carrying capacity for two stories and two spans frame.

Lateral torsional buckling (LTB) effect	Ultimate load parameter	% decrease in load carrying capacity
From the literature ignoring LTB [60]	1.91	-
LTB ignored	1.90	-
LTB considered	1.29	32.11
LTB considered and $C_b = 1$	1.13	40.53

For calibrating the results, steel frame is firstly analyzed with not considering lateral torsional buckling effect and result are approximately same the literature result with

% 0.8 difference. Lateral torsional buckling effect in all of the approximations decrease the load carrying and displacement capacity of the frame. Especially, $C_b = 1$ case, load carrying capacity is far from the real solutions and very conservative in the design. Moreover, order of plastic formations are changed in this analyses when lateral torsional buckling is considered in the nonlinear analysis steps.

5.6. Second-Order Elastic-Plastic Analysis of Three Stories and Two Spans Frame

Steel frame selected from the literature [60] is investigated considered and ignored lateral torsional buckling. This frame have three stories and three spans. Cross section of the beams are W 18x40 ($J = 337 \times 10^3 \text{ mm}^4$, $C_w = 387 \times 10^9 \text{ mm}^6$, $Z_x = 1280 \times 10^3 \text{ mm}^4$). Cross section of the columns are W 8x31 ($J = 223 \times 10^3 \text{ mm}^4$, $C_w = 142 \times 10^9 \text{ mm}^6$, $Z_x = 498 \times 10^3 \text{ mm}^4$), W 10x45 ($J = 629 \times 10^3 \text{ mm}^4$, $C_w = 322 \times 10^9 \text{ mm}^6$, $Z_x = 900 \times 10^3 \text{ mm}^4$), W 6x25 ($J = 192 \times 10^3 \text{ mm}^4$, $C_w = 40.3 \times 10^9 \text{ mm}^6$, $Z_x = 310 \times 10^3 \text{ mm}^4$), W 8x35 ($J = 320 \times 10^3 \text{ mm}^4$, $C_w = 166 \times 10^9 \text{ mm}^6$, $Z_x = 569 \times 10^3 \text{ mm}^4$), W 5x16 ($J = 79.9 \times 10^3 \text{ mm}^4$, $C_w = 10.9 \times 10^9 \text{ mm}^6$, $Z_x = 158 \times 10^3 \text{ mm}^4$), W 6x20 ($J = 99.9 \times 10^3 \text{ mm}^4$, $C_w = 30.3 \times 10^9 \text{ mm}^6$, $Z_x = 246 \times 10^3 \text{ mm}^4$). Section types, dimensions and applied loads are shown in Figure 5.23. Out-of-plane motion is prevented at the joints of the member. Lateral displacement (Δ) is monitored at the top point of the frame and it is also shown in Figure 5.23.

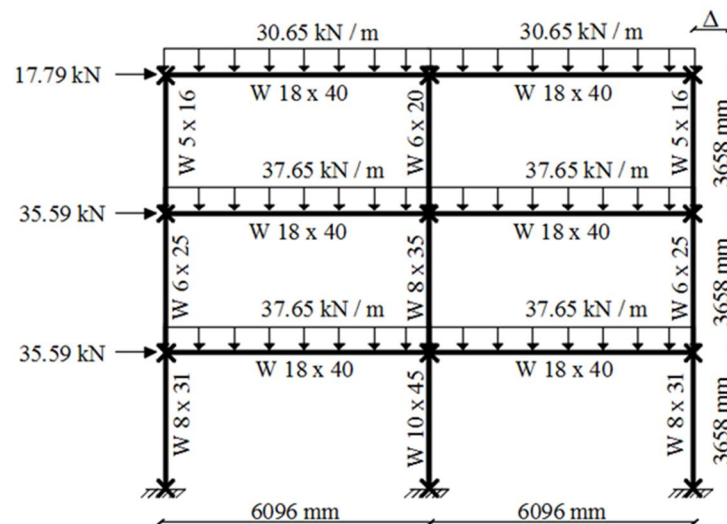


Figure 5.23 : Three stories and two spans frame.

Steel frame is analyzed under the lateral torsional buckling effect and second-order elastic plastic analysis method is used in the analyses. According to the analysis

results, structural behavior is examined. In this frame, moment modification factor ($C_b = 1$) case is examined as in the previous example and compared with other analysis results. Load carrying capacity – lateral displacements of top point of the frame (Δ) are calculated and the graphics are plotted in Figure 5.24. Also, order of plastic hinge formations are given in Figure 5.25 for lateral torsional buckling considered and ignored cases, respectively.

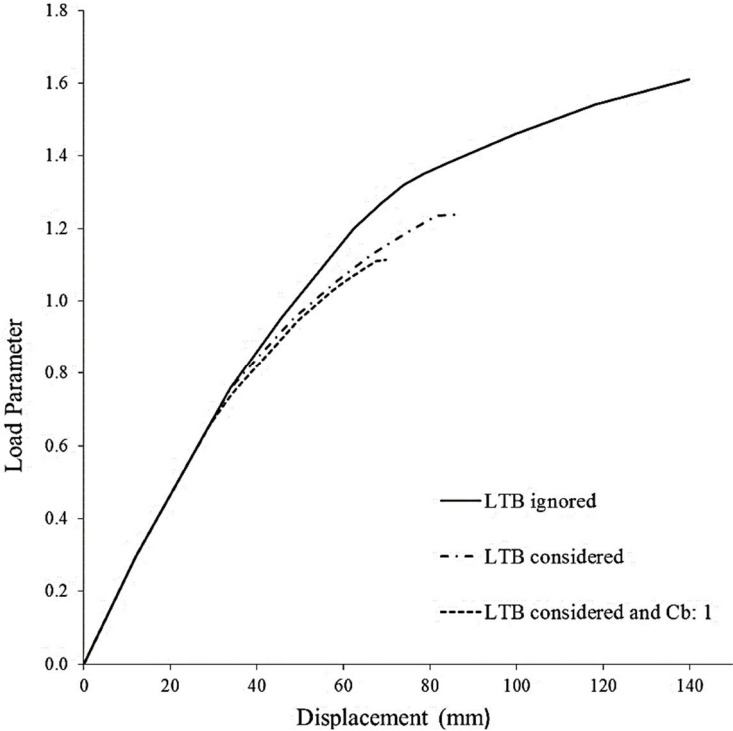


Figure 5.24 : Peak point lateral displacements and load parameters of three stories and two spans frame.

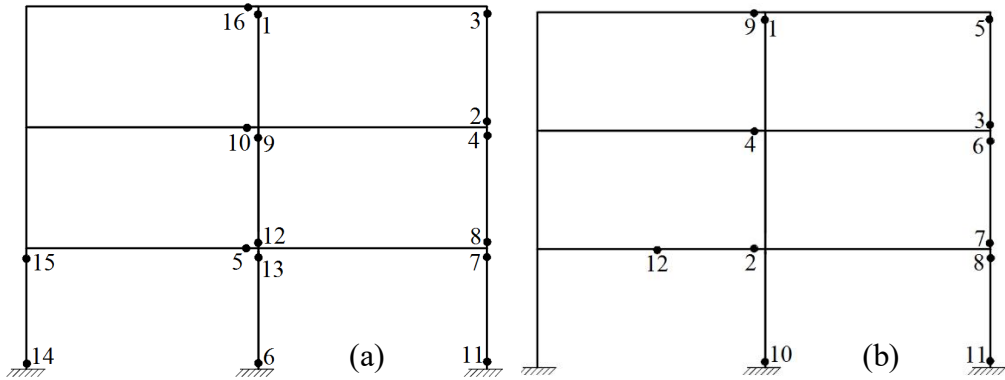


Figure 5.25 : Order of plastic hinge formations (a) lateral torsional buckling ignored (b) lateral torsional buckling considered.

In Table 5.2, ultimate load parameters and decreasing in the load carrying capacities of the examined steel frame structure under different conditions are given.

Table 5.2 : Ultimate load parameter and decreasing in load carrying capacity for three stories and three spans frame.

Lateral torsional buckling (LTB) effect	Ultimate load parameter	% decrease in load carrying capacity
From the literature ignoring LTB [60]	1.63	-
LTB ignored	1.61	-
LTB considered	1.24	22.98
LTB considered and $C_b=1$	1.11	31.06

For calibrating the results, steel frame is firstly analyzed with not considering lateral torsional buckling effect and result are seen that approximately same the literature result with % 1.2 difference. These analysis results show the analogy with previous example results and order of plastic formations are also changed in this analyses when lateral torsional buckling is considered in nonlinear analysis steps. Load carrying and displacements capacities of frame under the lateral torsional buckling effect have decreased considerably.

5.7. Analysis of Simply Supported Beam with Different Unbraced Length Conditions

In order to examine lateral torsional buckling behavior, a simply supported beam is selected with different unbraced length conditions. Simply supported beam is loaded with uniformly distributed load and the total length of the beam is selected as 12.00 m. Out-of-plane motion is prevented using fictitious braces. These bracing points, that are also used to determine the unbraced length of the segments, are applied on different points on the beam and presented in Figure 5.26. Unbraced segment lengths are selected as 12 m, 6 m, 4 m, 3 m, 2.4 m, and 2 m. Cross section of beams is also chosen as W 16x40 ($J= 330 \times 10^3 \text{ mm}^4$, $C_w= 465 \times 10^9 \text{ mm}^6$, $Z_x= 1200 \times 10^3 \text{ mm}^4$).

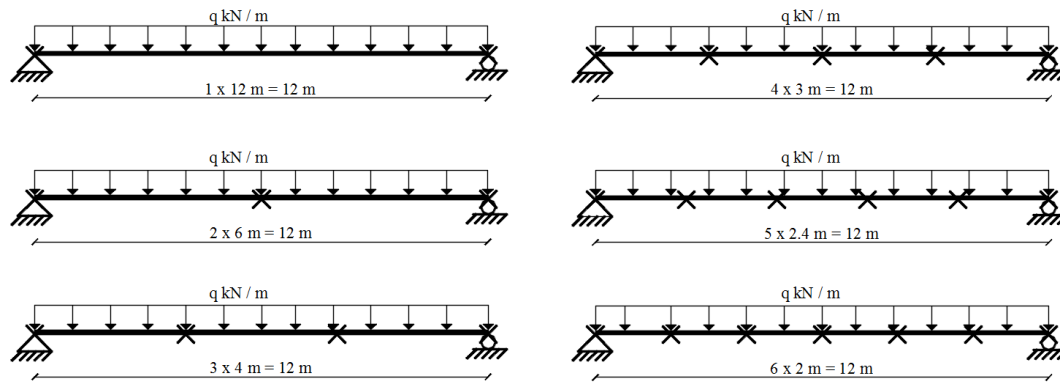


Figure 5.26 : Simply supported beams with different unbraced conditions.

In these analysis, TSDC-2016 [43] and TS 4561 [53] are compared according to load carrying capacity of the beam under the lateral torsional buckling effect. Unlike other analysis, different unbraced conditions are examined in order to determine importance of unbraced length of the beam under the lateral torsional buckling effect. Analysis results are given in Table 5.3, comparatively.

Table 5.3 : Load carrying capacity of simply supported beam.

Unbraced length of beam, L_b (m)	Load carrying capacity, q (kN/m)		% decreasing in load carrying capacity	
	According to TSDC-2016	According to TS 4561	According to TSDC-2016	According to TS 4561
12.00	4.57	5.65	72.61	66.11
6.00	13.20	13.62	20.79	18.28
4.00	13.62	16.67	18.27	0
3.00	15.97	16.67	4.17	0
2.40	16.08	16.67	3.51	0
2.00	16.67	16.67	0	0

The load carrying capacity of the simply supported beam is calculated separately for the different unbraced conditions, and as the unsupported element length increased, the load carrying capacity of the beam element decreased due to lateral torsional buckling. It has been found here that considerable reduction in the load carrying capacity of the element occurs due to the lateral torsional buckling effect. This basic numerical example is to be considered in order to attain the predicted structural performance. As a result of examining the lateral torsional buckling behavior considering the unbraced element lengths, it has been found that the load carrying

capacities can be calculated more practically by the TSDC-2016 [43] when compared to TS 4561 [53] standard.

5.8. First-Order Elastic-Plastic Analysis of Multi-Story Frame

A multi-story frame is selected from literature [61] and nonlinear analysis is performed accounting lateral torsional buckling. Cross sections of the columns are W 12x79 ($J=1600 \times 10^3 \text{ mm}^4$, $C_w=1970 \times 10^9 \text{ mm}^6$, $Z_x=1950 \times 10^3 \text{ mm}^4$) and W 10x60 ($J=1030 \times 10^3 \text{ mm}^4$, $C_w=709 \times 10^9 \text{ mm}^6$, $Z_x=1220 \times 10^3 \text{ mm}^4$). Cross sections of the beams are W 16x40 ($J=330 \times 10^3 \text{ mm}^4$, $C_w=465 \times 10^9 \text{ mm}^6$, $Z_x=1200 \times 10^3 \text{ mm}^4$). Out-of-plane motion is prevented by using midpoint bracing where point loads are applied. Braces are first applied from the joints at the member ends as shown in Figure 5.27 (a). Similarly, braces are applied from both the joints at the member ends and from midpoints of the members as illustrated in Figure 5.27 (b). Section types, dimensions and applied loads are also shown in Figure 5.27 (a) (b). In both frames, beams and columns are rigidly connected about their strong axis bending direction and same section is used for both frames. In this analysis, r factor is selected 0.24 as in the literature [61].

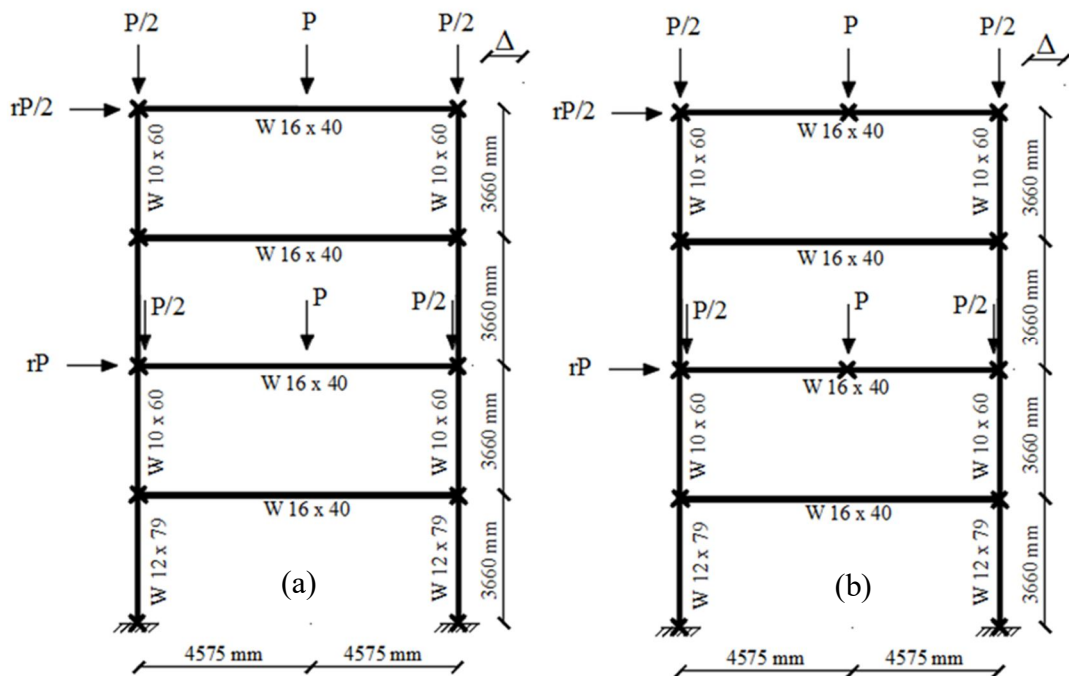


Figure 5.27 : Multi-story frame (a) braced from joints (b) braced from joints and midpoints of the beams.

Multi-story frame is analyzed accounting lateral torsional buckling for different unbraced length segments [58]. Nonlinear analysis results with and without considering lateral torsional buckling are shown in Figure 5.28. Moreover, effects of different unbraced segment lengths are investigated by limiting out-of-plane motions. Also, order of plastic hinge formations are given in Figure 5.29 for lateral torsional buckling considered and ignored cases, respectively.

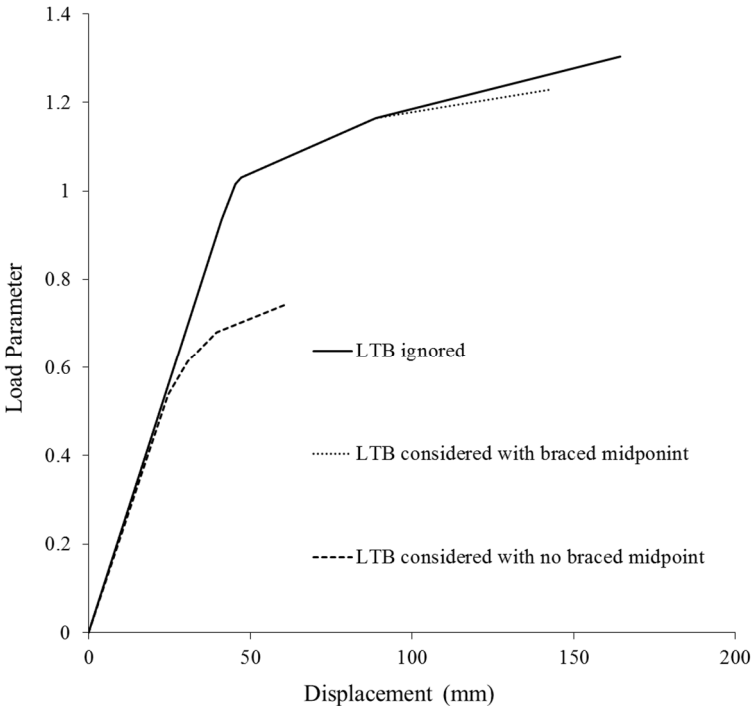


Figure 5.28 : Multi-story frame analysis results.

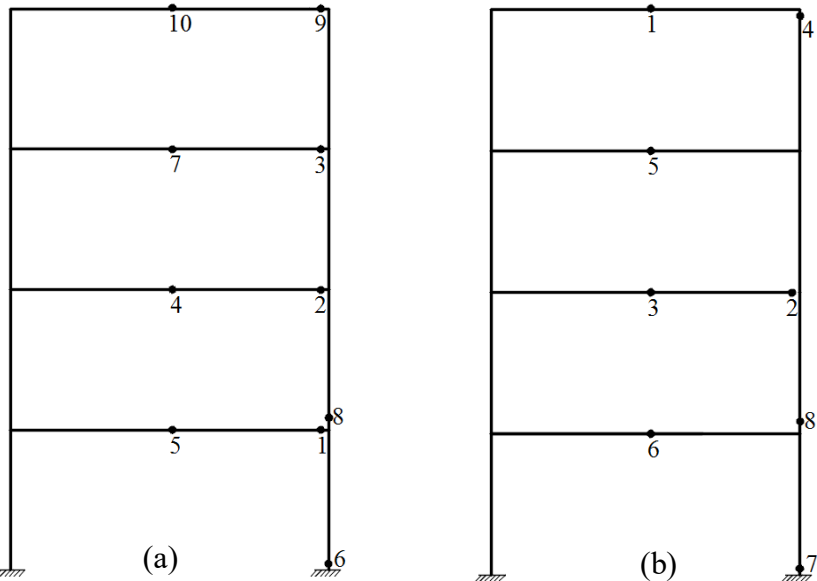


Figure 5.29 : Order of plastic hinge formations (a) lateral torsional buckling ignored (b) lateral torsional buckling considered.

In Table 5.4, ultimate load parameters and decreasing in load carrying capacities of the examined steel frame structure under different conditions are given comparatively.

Table 5.4 : Ultimate load parameter and decreasing in load carrying capacity for three stories and three spans frame.

Lateral torsional buckling (LTB) effect	Ultimate load parameter	% decreasing in load carrying capacity
LTB ignored	1.30	-
LTB considered with only joints braces	1.23	5.38
LTB considered with midpoint braces	0.71	45.38

Multi-story frame that is braced from both member end joints and beam mid-points show that structural behavior is almost the same for first four plastic hinges when compared to conventional nonlinear analysis behavior in which lateral torsional buckling is ignored. After this loading point, lateral torsional buckling governs the behavior and load carrying capacity decreases.

5.9. Solution Details for Second-Order Elastic-Plastic Analysis of One Story and One Span Frame

A steel frame is selected from the literature [54] and is investigated considering lateral torsional buckling. This frame have one story and one span. Section types, dimensions and applied loads are shown in Figure 5.30. Cross section properties of the columns and beam are given in Table 5.5. Out-of-plane motion is prevented from joints in this example. Lateral displacement (Δ) is observed at the top point of the frame and shown in Figure 5.30.

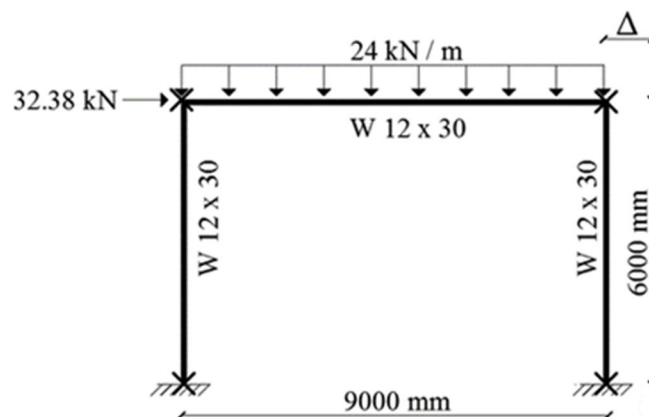


Figure 5.30 : One story and one span frame.

Material properties for W 12x30 section are given in Table 5.5;

Table 5.5 : W12x30 section properties.

Section Properties		
W12x30		
A	5670.0	mm ²
E	200000	N/mm ²
F _y	250	N/mm ²
J	190000.0	mm ⁴
C _w	1.93E+11	mm ⁶
S _x	633000.0	mm ³
S _y	102000.0	mm ³
h _o	302	mm
r _{ts}	45	mm
r _y	38.6	mm
Z _x	706000.0	mm ³
Z _y	157000.0	mm ³

Plastic moment and normal force capacity of the W 12x30 section are $M_p = 176.5 \text{ kNm}$ and $P_p = 1417.5 \text{ kN}$, respectively.

Lateral torsional buckling effect is calculated for beam member of the frame structure according to criteria of design specifications. In here, AISC 360-10 [41] are preferred in order to calculate lateral torsional buckling effect. As mentioned before, TSDC-2016 [43] and AISC 360-10 [41] specifications rules show similarity when calculating lateral torsional buckling.

For sections of examined frame structure, it is also shown in Figure 5.31, unbraced length limits of beam member are $L_p = 1921.5 \text{ mm}$, $L_r = 5913.1 \text{ mm}$, and $L_b = 9000 \text{ mm}$. According to length limit values, elastic lateral torsional buckling occur because $L_b > L_r$. In the analysis, lateral torsional buckling effect is calculated step by step accounting the moment modification factor C_b after every hinge formation.

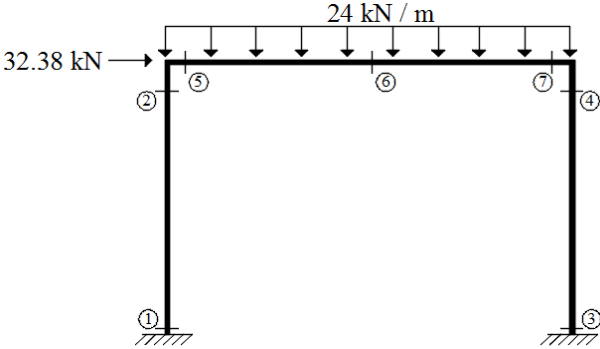


Figure 5.31 : Sections of one story and one span frame.

Procedure in order to examine frame structure given in Figure 4.32 is given step by step;

1. The existing loads applied to the structure are called reference loads. Under the applied reference loads, the structure is analyzed. Current loads are smaller than maximum carrying load capacities. In the opposite case, the building cannot carry these loads.
2. The load parameter at each crossing examined is obtained by dividing the plastic moment capacity by the moment value which is formed by the reference loads at that point.
3. The location of the smallest load parameter in the sections examined is the location of the first plastic joint and the load parameter at that crossing becomes the first load parameter.
4. The displacements, internal forces and reference forces in the structure is multiplied by previously founded load parameter and behavior of the structure under the load parameter is calculated.
5. In the investigated structure, a hinge is put where the first plastic joint is formed. This is after it has reached the plastic moment capacity of that section, it cannot carry more moment.
6. Structure is solved again in order to calculate moment and normal forces after the plastic hinge formation.
7. Displacements and internal forces are multiplied with founded new load parameter.
8. Cumulative load parameter, displacements and internal forces are found for every examining section.
9. After other plastic hinge is found, structure is solved again. This process next until the mechanism has lost its behavior or stability.

When lateral torsional buckling effect is considered, beam members are investigated step by step after the each plastic hinge formation occur. Therefore, changing of plastic moment capacity of member is calculated and added in procedure at Step 6. According to this, structure is solved and place of hinge formation is decided.

Selected and previously examined frame from the literature [57] is solved considering with and without lateral torsional buckling. Detailed information about the solution steps are presented in this part for clarification.

5.9.1. Nonlinear analysis of one story and one span frame ignoring lateral torsional buckling effect

Second-order elastic-plastic analysis is carried out in this part. Lateral torsional buckling effect is ignored in the nonlinear analysis steps. After the frame is linear elastically analyzed, required parameters under the applied load is given in Table 5.6.

According to (3.15), B_1 coefficient can be calculated;

$$B_1 = \frac{C_m}{1 - \frac{P_r}{P_{el}}} \geq 1$$

For beam-columns subject to transverse loading between supports, the value of C_m shall be taken conservatively as 1.0 for all cases [43] or determined by using formulation.

$$C_m = 0.6 - 0.4(M_1 / M_2)$$

where M_1 and M_2 calculated from a first-order analysis, are the smaller and larger moments, respectively, at the ends of that portion of the member unbraced in the plane of bending under consideration.

$$C_{m,1} = 0.603$$

$$C_{m,2} = 0.897$$

P_{el} (N) is the elastic critical buckling strength of the member in the plane of bending.

$$P_{el} = 9630346 \text{ N}$$

It is permitted to use first-order estimate of P_r ($P_r = P_m + P_t$) in B_1 formulation [43].

$$P_{r,1} = 108540 \text{ N}$$

$$P_{r,2} = 125730 \text{ N}$$

$$B_{1,1} = 0.6$$

$$B_{1,2} = 0.9$$

B_1 should be taken as 1.0 because it have to be greater than 1.0 according to (3.15).

According to (3.16), B_2 coefficient can be calculated;

$$B_2 = \frac{1}{1 - \frac{P_{story}}{P_{e,story}}} \geq 1$$

$$P_{story} = 215910 \text{ N}$$

$$P_{e,story} = R_M \frac{HL}{\Delta_H}$$

$$R_M = 1 - 0.15(P_{mf} / P_{story})$$

P_{mf} is total vertical load in columns in the story that are part of moment frames in N.

$$P_{mf} = 215910 \text{ N}$$

$$R_M = 0.85$$

H is the story shear produced by the lateral forces used to compute Δ_H in N.

$$H_1 = 32050 \text{ N}$$

L is the height of story in mm.

$$L = 6000 \text{ mm}$$

$$P_{e,story} = 6776741 \text{ N}$$

Δ_H is the first-order interstory drift in mm.

$$\Delta_{H,1} = 24.12 \text{ mm}$$

$$B_2 = 1.0329$$

Table 5.6 : First load parameter and control values.

Section	Mp	Pp	B1	B2	Mnt	Mlt	Pnt	Plt	ΔM1	ΔP1	P/Pp	0.2	Δp1
1	176.5	-1417.5	1	1.033	-58.37	56.67	-112.46	3.93	0.17	-108.41	0.076	<	25.516
2	176.5	-1417.5	1	1.033	122.13	-36.05	-109.84	6.55	84.89	-103.08	0.073	<	1.933
3	176.5	-1417.5	1	1.033	59.56	59.04	-112.64	-13.09	120.55	-126.16	0.089	<	1.375
4	-176.5	-1417.5	1	1.033	-122.92	-40.53	-110.02	-10.47	-164.79	-120.84	0.085	<	1.024
5	-176.5	-1417.5	1	1	-122.13	36.05	-62.47	15.45	-86.08	-47.01	0.033	<	1.983
6	176.5	-1417.5	1	1	124.82	2.18	-62.47	15.45	127.00	-47.01	0.033	<	1.358
7	-176.5	-1417.5	1	1	-122.92	-40.53	-62.47	15.45	-163.45	-47.01	0.033	<	1.061

$$\delta_{1,1} = \Delta p_{1,1} \times \delta_{x,1}$$

$$\delta_{1,1} = 1.024 \times 0.02412 = 0.0247$$

First hinge occurs when load parameter $p_1 = 1.024$ and maximum top point displacement of frame is 0.0247 m.

After the first plastic hinge occurs, frame structure is solved again. Required parameters are given in Table 5.7.

According to (3.15), B_1 coefficient can be calculated;

$$B_1 = \frac{C_m}{1 - \frac{P_r}{P_{el}}} \geq 1$$

$$C_m = 0.6 - 0.4(M_1 / M_2)$$

$$C_{m,1} = 0.33$$

$$C_{m,2} = 0.60$$

$$P_{el} = 9630346 \text{ N}$$

$$P_{r,1} = 124715 \text{ N}$$

$$P_{r,2} = 109549 \text{ N}$$

$$B_{1,1} = 0.3$$

$$B_{1,2} = 0.6$$

B_1 should be taken as 1.0 because it have to be greater than 1.0 according to (3.15).

According to (3.16), B_2 coefficient can be calculated;

$$B_2 = \frac{1}{1 - \frac{P_{story}}{P_{e,story}}} \geq 1$$

$$P_{story} = 215910 \text{ N}$$

$$P_{e,story} = R_M \frac{HL}{\Delta_H}$$

$$R_M = 1 - 0.15(P_{mf} / P_{story})$$

P_{mf} is total vertical load in columns in the story that are part of moment frames in N.

$$P_{mf} = 215910 \text{ N}$$

$$R_M = 0.85$$

H is the story shear produced by the lateral forces used to compute Δ_H in N.

$$H_2 = 72310 \text{ N}$$

L is the height of story in mm.

$$L = 6000 \text{ mm}$$

$$P_{e,story} = 4080339 \text{ N}$$

Δ_H is the first-order interstory drift in mm.

$$\Delta_{H,2} = 90.38 \text{ mm}$$

$$B_2 = 1.0558$$

Table 5.7 : Second load parameter and control values.

Section	M _p	P _p	B ₁	B ₂	M _{nt}	M _{lt}	P _{nt}	P _{lt}	M ₁	P ₁	ΔM ₂	ΔP ₂	P/P _p	0.2	Δp ₂
1	176.5	-1417.5	1	1.056	-77.57	192.46	-130.55	5.84	0.17	-111.04	125.64	-124.39	0.088	<	1.270
2	176.5	-1417.5	1	1.056	162.01	-93.76	-127.93	8.45	86.96	-105.59	63.01	-119.00	0.084	<	1.178
3	176.5	-1417.5	1	1.056	0.00	147.64	-94.55	-15.00	123.48	-129.23	155.89	-110.39	0.078	<	0.276
4	-	-	-	-	-	-	-	-	-	-	-	-	-	-	-
5	-176.5	-1417.5	1	1	-162.01	93.76	-72.31	47.70	-88.17	-48.16	-68.25	-24.61	0.017	<	1.223
6	176.5	-1417.5	1	1	166.34	51.30	-72.31	47.70	130.09	-48.16	217.64	-24.61	0.017	<	0.198
7	-176.5	-1417.5	1	1	0.00	0.00	-72.31	47.70	-167.43	-48.16	0.00	-24.61	0.017	<	3.965

Second load parameter can be calculated;

$$p_2 = p_1 + \Delta p_2$$

$$p_2 = 1.024 + 0.198 = 1.222$$

Displacement value is calculated when loads are increased $p_2 = 1.222$ times.

$$\delta_{1,2} = \delta_{1,1} + \Delta p_{1,2} \times \delta_{x,2}$$

$$\delta_{1,2} = 0.0247 + 0.198 \times 0.09038 = 0.04261$$

After the first and second plastic hinges occur, frame structure is solved again.

Required parameters are given in Table 5.8.

B_1 and B_2 coefficients can be calculated using previously expressed calculation methods.

Table 5.8 : Third load parameter and control values.

Section	M _p	P _p	B ₁	B ₂	M _{nt}	M _{lt}	P _{nt}	P _{lt}	M ₁	P ₁	ΔM ₂	ΔP ₂	P/P _p	0.2	Δp ₃
1	176.5	-1417.5	1	1.086	-237.70	465.14	-167.5	-5.57	25.061	-135.68	267.29	-173.6	0.122	<	0.514
2	176.5	-1417.5	1	1.086	494.69	8.8393	-164.9	-2.95	99.439	-129.16	504.28	-168.1	0.119	<	0.134
3	176.5	-1417.5	1	1.086	0.00	470.4	-57.6	-3.6	154.36	-151.10	510.71	-61.5	0.043	<	0.025
4	-	-	-	-	-	-	-	-	-	-	-	-	-	-	-
5	-176.5	-1417.5	1	1	-494.69	-8.8	-154.4	76.05	-101.69	-53.03	-503.5	-78.4	0.055	<	0.141
6	-	-	-	-	-	-	-	-	-	-	-	-	-	-	-
7	-176.5	-1417.5	1	1	0.00	0.00	-154.45	76.05	-167.43	-53.03	0.00	-78.40	0.055	<	1.182

Third load parameter can be calculated;

$$p_3 = p_2 + \Delta p_3$$

$$p_3 = 1.222 + 0.025 = 1.247$$

Displacement value is calculated when loads are increased $p_3 = 1.247$ times.

$$\delta_{1,3} = \delta_{1,2} + \Delta p_{1,3} \times \delta_{x,3}$$

$$\delta_{1,3} = 0.04261 + 0.025 \times 0.2879 = 0.04973$$

After all of the occurred plastic hinges are considered, frame structure is solved again.

Required parameters are given in Table 5.9.

Table 5.9 : Fourth load parameter and control values.

Section	M _p	P _p	B1	B2	M _{nt}	M _{lt}	P _{nt}	P _{lt}	M ₁	P ₁	ΔM ₂	ΔP ₂	P/P _p	0.2	Δp ⁴
1	176.5	-1417.5	1	1.188	-237.70	935.54	-167.5	-5.57	31.675	-139.98	873.43	-174.1	0.123	<	0.154
2	176.5	-1417.5	1	1.188	494.69	8.8393	-164.9	-2.95	111.92	-133.32	505.18	-168.4	0.119	<	0.109
3	-	-	-	-	-	-	-	-	-	-	-	-	-	-	-
4	-	-	-	-	-	-	-	-	-	-	-	-	-	-	-
5	-176.5	1417.5	1	1	-494.69	-8.8	-154.4	154.5	-114.15	-54.97	-503.5	0.0	0.000	<	0.131
6	-	-	-	-	-	-	-	-	-	-	-	-	-	-	-
7	-	-	-	-	-	-	-	-	-	-	-	-	-	-	-

Fourth load parameter can be calculated;

$$p_4 = p_3 + \Delta p_4$$

$$p_4 = 1.247 + 0.109 = 1.356$$

Displacement value is calculated when loads are increased $p_3 = 1.356$ times.

$$\delta_{1,4} = \delta_{1,3} + \Delta p_{1,4} \times \delta_{x,4}$$

$$\delta_{1,3} = 0.05973 + 0.109 \times 0.5765 = 0.1126$$

Frame structure have failed after the fourth plastic hinge occur. Analysis is catted at this point because frame structure reach the maximum load carrying capacity.

5.9.2. Nonlinear analysis of one story and one span frame considering lateral torsional buckling effect

Before analyzed frame structure, it have to be decided that lateral torsional buckling affect or doesn't affect beam member. For this, frame is firstly solved under the reference loads and required parameters are obtained.

For beam member;

$C_{b,1}$ and M_n are calculated using (4.32) and (4.30), respectively.

$$C_{b,1} = 1.584$$

$$M_p = M_n = 100.2 \text{ kNm and } P_p = P_n = 804.7 \text{ kN}$$

For beam member, calculated nominal moment capacity is used in the frame structure nonlinear analysis and this is given in Table 5.10.

Table 5.10 : First load parameter and control values.

Section	M _p	P _p	B ₁	B ₂	M _{nt}	M _{lt}	P _{nt}	P _{lt}	ΔM ₁	ΔP ₁	P/P _p	0.2	Δp ₁
1	-176.5	-1417.5	1	1.033	-58.83	56.67	-112.46	3.93	-0.29	-108.41	0.076	<	25.068
2	176.5	-1417.5	1	1.033	122.31	-36.05	-109.84	6.55	85.07	-103.08	0.073	<	1.929
3	176.5	-1417.5	1	1.033	60.03	59.04	-112.64	-13.09	121.02	-126.16	0.089	<	1.370
4	-176.5	-1417.5	1	1.033	-123.11	-40.53	-110.02	-10.47	-164.97	-120.84	0.085	<	1.023
5	-100.2	-804.7	1	1	-122.31	36.05	-62.57	15.45	-86.26	-47.12	0.059	<	1.123
6	100.2	-804.7	1	1	124.63	2.18	-62.57	15.45	126.81	-47.12	0.059	<	0.772
7	-100.2	-804.7	1	1	-128.11	-46.73	-64.57	15.45	-174.84	-49.12	0.061	<	0.563

$$\delta_{1,1} = \Delta p_{1,1} \times \delta_{x,1}$$

$$\delta_{1,1} = 0.563 \times 0.02412 = 0.013585$$

First hinge occur when load parameter $p_1 = 0.563$ and maximum top point displacement of frame is 0.013585 m.

After the first plastic hinge occur, beam member is investigated again and moment modification factor $C_{b,2}$ is calculated according to moment distribution of the member. In Table 5.11, nonlinear analyzed results under lateral torsional buckling effect are given.

$$C_{b,2} = 1.163$$

$$M_p = M_n = 73.6 \text{ kNm and } P_p = P_n = 590.8 \text{ kN}$$

Table 5.11 : Second load parameter and control values.

Section	M _p	P _p	B ₁	B ₂	M _{nt}	M _{lt}	P _{nt}	P _{lt}	M ₁	P ₁	ΔM ₂	ΔP ₂	P/P _p	0.2	Δp ₂
1	176.5	-1417.5	1	1.056	-78.26	191.77	-130.60	5.80	-0.18	-65.21	124.22	-124.48	0.088	<	1.308
2	176.5	-1417.5	1	1.056	162.43	-93.42	-127.98	8.42	51.18	-62.01	63.80	-119.09	0.084	<	1.706
3	176.5	-1417.5	1	1.056	0.00	147.12	-94.50	-14.96	72.80	-75.89	155.34	-110.30	0.078	<	0.610
4	176.5	-1417.5	1	1.056	0.00	0.00	-91.88	-12.34	-99.24	-72.69	0.00	-104.92	0.074	<	41.522
5	-73.6	-590.8	1	1	-162.43	93.42	-72.50	47.53	-48.59	-26.54	-69.02	-24.97	0.042	<	0.331
6	73.6	-590.8	1	1	186.13	58.13	-76.90	52.53	71.43	-26.54	244.25	-24.37	0.041	<	0.002
7	-	-	-	-	-	-	-	-	-	-	-	-	-	-	-

Second load parameter can be calculated;

$$p_2 = p_1 + \Delta p_2$$

$$p_2 = 0.563 + 0.002 = 0.565$$

Displacement value is calculated when loads are increased $p_2 = 0.565$ times.

$$\delta_{1,2} = \delta_{1,1} + \Delta p_{1,2} \times \delta_{x,2}$$

$$\delta_{1,2} = 0.013585 + 0.002 \times 0.09006 = 0.015386$$

After the second plastic hinge occur, beam member is investigated again and moment modification factor $C_{b,3}$ is calculated according to moment distribution of the member.

$$C_{b,3} = 1.938$$

M_n are calculated using (3.52). because unbraced length of the member change. Hence, lateral torsional buckling effect can be neglected since nominal flexural strength equal to plastic moment capacity of the section. After frame structure is analyzed, results are given in Table 5.12.

$$M_n = M_p \text{ and } P_n = P_p$$

Table 5.12 : Third load parameter and control values.

Section	Mp	Pp	B1	B2	Mnt	Mlt	Pnt	Plt	M1	P1	ΔM2	ΔP2	P/Pp	0.2	Δp3
1	176.5	-1417.5	1	1.086	-239.61	466.09	-167.51	-5.57	0.08	-61.31	266.42	-173.56	0.122	<	0.623
2	176.5	-1417.5	1	1.086	494.69	8.84	-164.90	-2.95	48.05	-58.30	504.28	-168.09	0.119	<	0.242
3	176.5	-1417.5	1	1.086	0.00	496.37	-67.58	-4.60	68.47	-71.28	538.90	-72.58	0.051	<	0.191
4	176.5	-1417.5	1	1.086	0.00	0.00	-54.97	-0.98	-92.92	-68.27	0.00	-56.03	0.040	<	76.016
5	-176.5	-1417.5	1	1	-494.69	-8.84	-154.77	76.21	-48.72	-26.59	-503.52	-78.56	0.055	<	0.248
6	-	-	-	-	-	-	-	-	-	-	-	-	-	-	-
7	-	-	-	-	-	-	-	-	-	-	-	-	-	-	-

Third load parameter can be calculated;

$$p_3 = p_2 + \Delta p_3$$

$$p_3 = 0.565 + 0.191 = 0.756$$

Displacement value is calculated when loads are increased $p_3 = 0.756$ times.

$$\delta_{1,3} = \delta_{1,2} + \Delta p_{1,3} \times \delta_{x,3}$$

$$\delta_{1,3} = 0.015386 + 0.191 \times 0.28854 = 0.068768$$

Beam member is failed because it reaches capability of plastic deformation under the lateral torsional buckling. There is no connection between column members for frame structure after this occur.

After the third plastic hinge, beam member is investigated and moment modification factor $C_{b,4}$ equal to $C_{b,3}$ value. Nonlinear analysis results are given in Table 5.13.

$$C_{b,4} = 1.938$$

$$M_n = M_p \text{ and } P_n = P_p$$

Table 5.13 : Fourth load parameter and control values.

Section	M _p	P _p	B1	B2	M _{nt}	M _{lt}	P _{nt}	P _{lt}	M1	P1	ΔM2	ΔP2	P/P _p	0.2	Δp ₄
1	176.5	-1417.5	1	1.084	-235.32	583.81	-161.95	-161.95	50.87	-94.39	397.76	-337.57	0.238	<	0.286
2	176.5	-1417.5	1	1.084	485.85	485.85	-161.95	-161.95	144.17	-90.34	1012.70	-337.57	0.238	<	0.026
3	-	-	-	-	-	-	-	-	-	-	-	-	-	-	-
4	176.5	-1417.5	1	1.084	0.00	0.00	0.00	-53.98	-92.92	-78.95	0.00	-58.54	0.041	<	72.577
5	-176.5	-1417.5	1	1	-485.85	-485.85	-152.58	-136.24	-144.71	-41.56	-971.69	-288.82	0.204	<	0.030
6	-	-	-	-	-	-	-	-	-	-	-	-	-	-	-
7	-	-	-	-	-	-	-	-	-	-	-	-	-	-	-

Fourth load parameter can be calculated;

$$p_4 = p_3 + \Delta p_4$$

$$p_4 = 0.756 + 0.026 = 0.7817$$

Displacement value is calculated when loads are increased $p_4 = 0.782$ times.

$$\delta_{1,4} = \delta_{1,3} + \Delta p_{1,4} \times \delta_{x,4}$$

$$\delta_{1,3} = 0.068768 + 0.026 \times 0.5 = 0.081683$$

Frame structure have failed until the fourth plastic hinge occur because of the lateral torsional buckling effect. Beam member fails without reaching its full capacity. As a result of this, places of plastic hinge formations and behavior of the frame structure change. Results are plotted as a graphic in Figure 5.32 in order to compare the results. Also, plastic hinge formations for lateral torsional buckling ignored and considered cases are given as (a) and (b) in Figure 5.32.

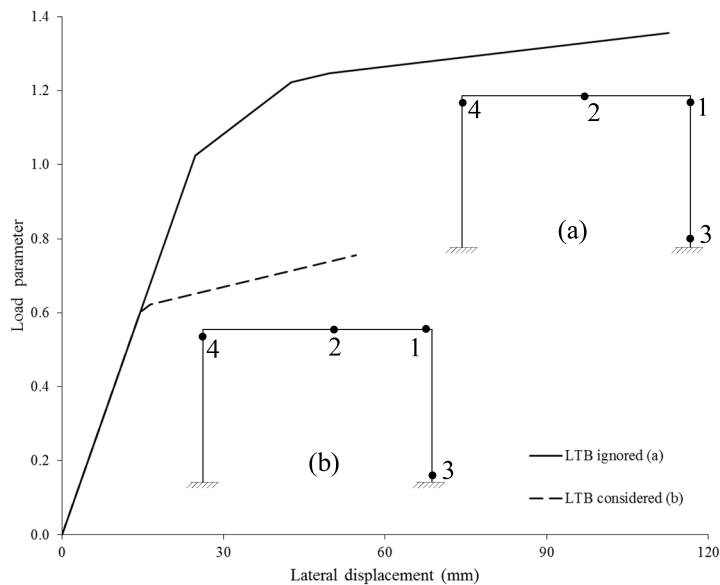


Figure 5.32 : One story and one span frame analysis results.

5.9.3. Second-Order Elastic-Plastic Analysis of One Story and One Span Frame Considering Braces in Out-of-Plane Directions

A steel frame is selected from the literature [57] and is investigated considering lateral torsional buckling. This frame have one story and one span. Cross sections of the columns and beam are W 12x30 ($J= 190 \times 10^3 \text{ mm}^4$, $C_w= 193 \times 10^9 \text{ mm}^6$, $Z_x= 706 \times 10^3 \text{ mm}^4$). Section types, dimensions and applied loads are also shown in Figure 5.33. Out-of-plane motion is prevented at only joints, mid-point and three points of the beam member. Lateral displacement (Δ) is observed at the top point of the frame and shown in Figure 5.33.

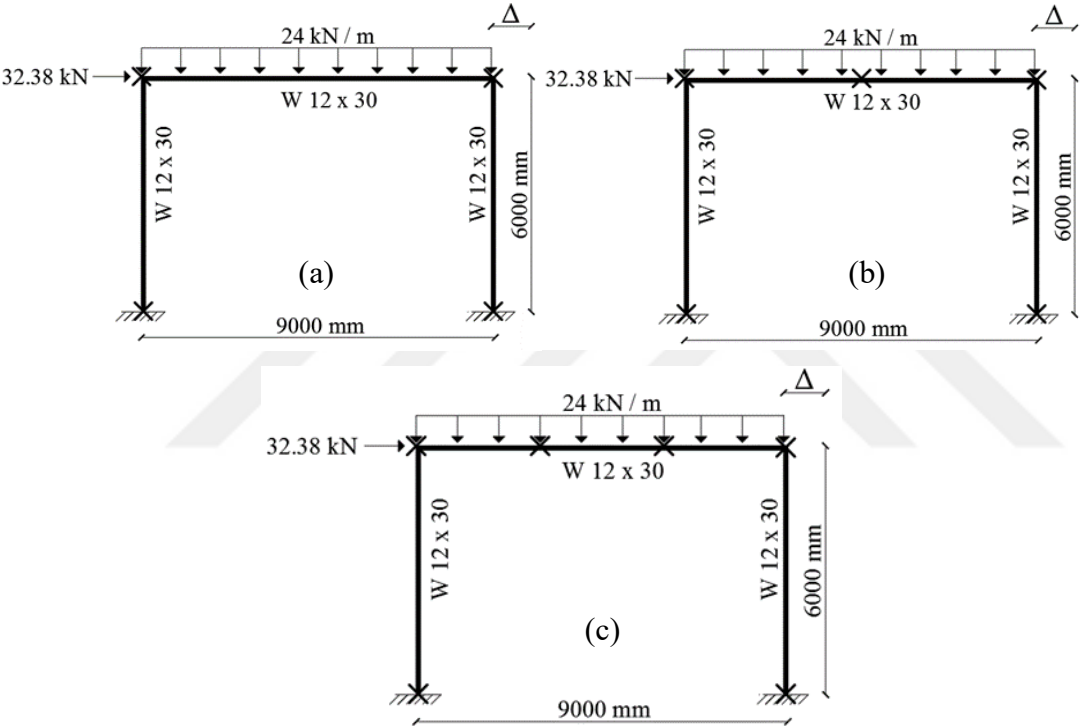


Figure 5.33 : Out of plane motion prevented from (a) only joints (b) mid-point of the beam (c) three points of the beam for one story frame.

One story and one span frame is analyzed under the lateral torsional buckling effect and second-order elastic plastic analysis method is used in the analyses. In this frame analyses, lateral torsional buckling calculations are carried out with using TSDC-2016 [43] and TS 4561 [53]. Moment modification factor ($C_b = 1$) case is examined and compared with other analysis results. Moreover, different unbraced length conditions are investigated. Load carrying capacity – lateral displacements of top point of the frame (Δ) are calculated and the graphics are plotted in Figure 5.34.

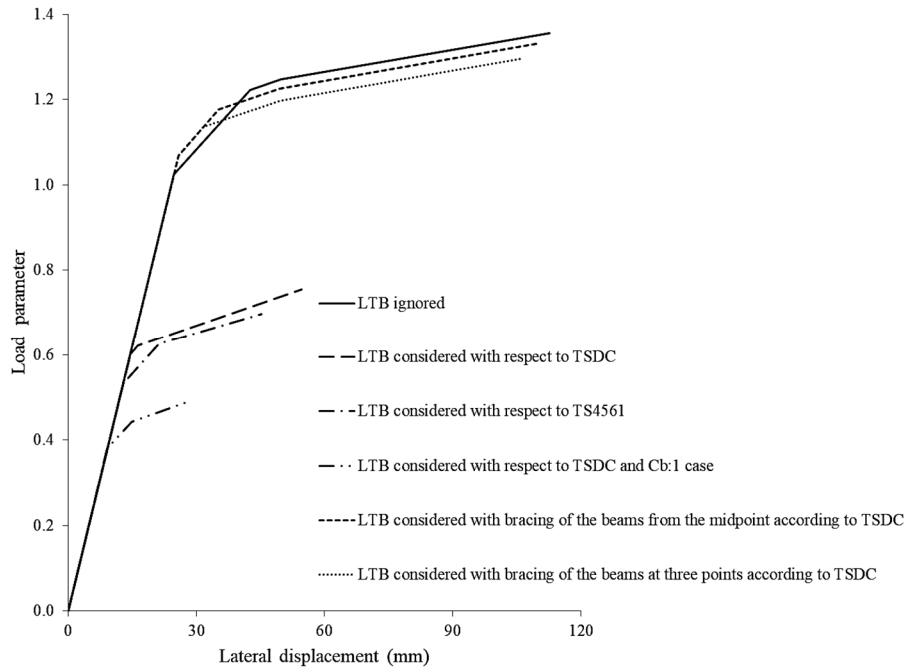


Figure 5.34 : Peak point lateral displacements and load parameters of one story and one span frame.

In Table 5.14, ultimate load parameter capacities of the examined steel frame structure under different conditions are given. In order to determine importance of unbraced length conditions and approximations of design codes on the lateral torsional buckling effect, results are given comparatively.

Table 5.14 : Ultimate load parameter and decreasing in load carrying capacity for one story and one span frame.

Lateral torsional buckling (LTB) effect	Ultimate load parameter	% decrease in load carrying capacity
LTB ignored	1.36	-
LTB considered with respect to TSDC	0.75	44.8
LTB considered with respect to TS 4561	0.70	48.6
LTB considered with respect to TSDC and $C_b=1$	0.49	63.6
LTB considered with bracing of beams from the midpoint according to TSDC	1.33	1.8
LTB considered with bracing of beams at three midpoint according to TSDC	1.30	4.4

Nonlinear analysis results show that considering lateral torsional buckling decreased the load carrying capacity for all of conditions. In this example, considering lateral torsional buckling effect according to TSDC-2016 [43] and TS 4561 [53] standards give the very closer results under the lateral torsional buckling. However, accounting $C_b=1$ case in lateral torsional buckling calculations decrease the load carrying capacity

more than enough. On the other hand, changing unbraced length conditions on the beam elements increase the load carrying capacity and eliminate lateral torsional buckling effect.

5.10. Second-Order Elastic-Plastic Analysis of Two Stories and One Span Frame

A steel frame is selected from the literature [57] and is investigated considering lateral torsional buckling. This frame have two stories and one span. Cross sections of the columns are W 10x33 ($J= 243 \times 10^3 \text{ mm}^4$, $C_w= 212 \times 10^9 \text{ mm}^6$, $Z_x= 636 \times 10^3 \text{ mm}^4$). Cross sections of the beams are W 21x44 ($J= 320 \times 10^3 \text{ mm}^4$, $C_w= 567 \times 10^9 \text{ mm}^6$, $Z_x= 1560 \times 10^3 \text{ mm}^4$) and W 16x31 ($J= 192 \times 10^3 \text{ mm}^4$, $C_w= 198 \times 10^9 \text{ mm}^6$, $Z_x= 885 \times 10^3 \text{ mm}^4$). Section types, dimensions and applied loads are also shown in Figure 5.35. Out-of-plane motion is prevented at only joints, mid-point and three points of the beam member. Lateral displacement (Δ) is observed at the top point of the frame and shown in Figure 5.35.

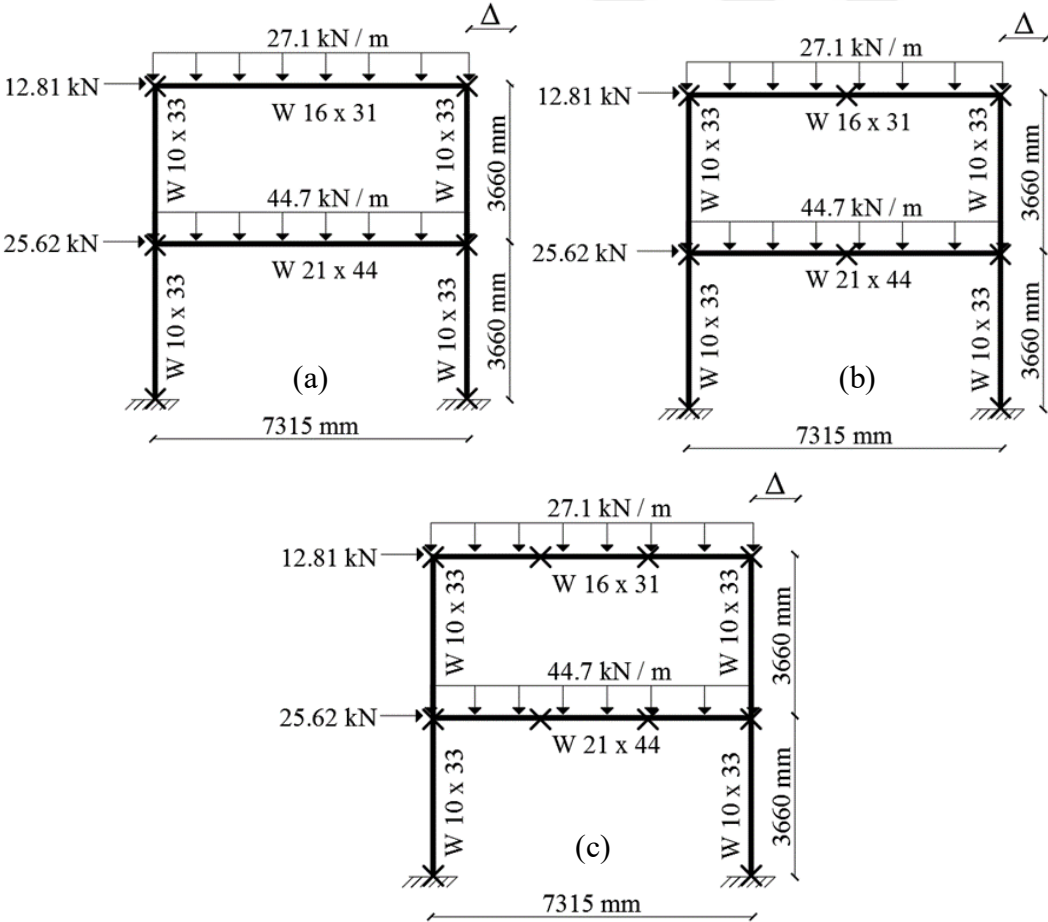


Figure 5.35 : Out of plane motion prevented from (a) only joints (b) mid-point of the beam (c) three points of the beam for one story frame.

Two stories and one span frame is analyzed under the lateral torsional buckling effect and second-order elastic plastic analysis method is used in the analyses. In this frame analyses, lateral torsional buckling calculations are carried out with using TSDC-2016 [43] and TS 4561 [53]. Moment modification factor ($C_b = 1$) case is examined and compared other analysis results. Moreover, different unbraced length conditions are investigated. Load carrying capacity – lateral displacements of top point of the frame (Δ) are calculated and the graphics are plotted in Figure 5.36. Also, order of plastic hinge formations are given in Figure 5.37 for lateral torsional buckling considered and ignored cases, respectively.

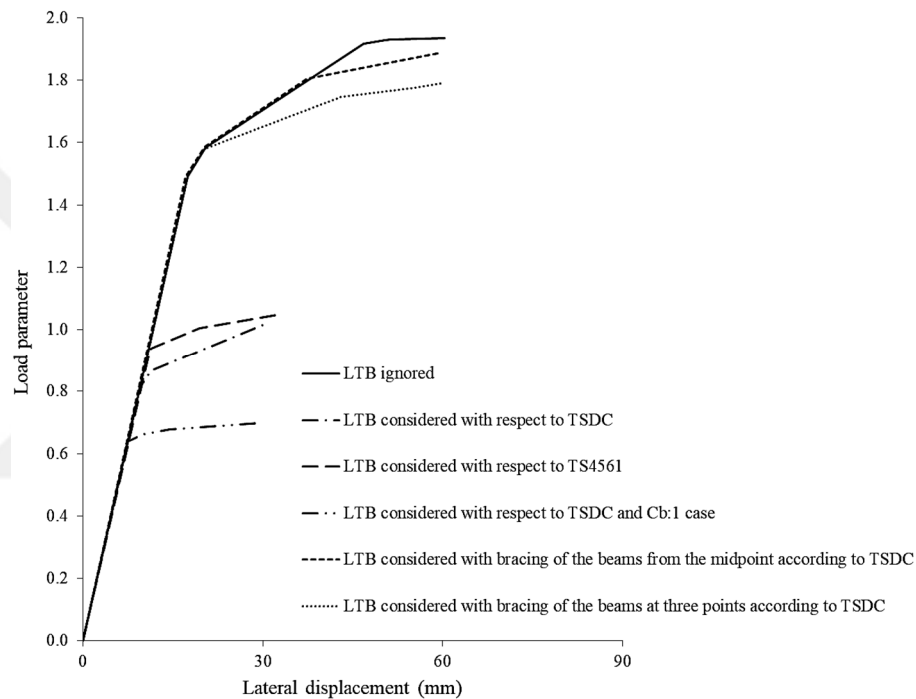


Figure 5.36 : Peak point lateral displacements and load parameters of two stories and one span frame.

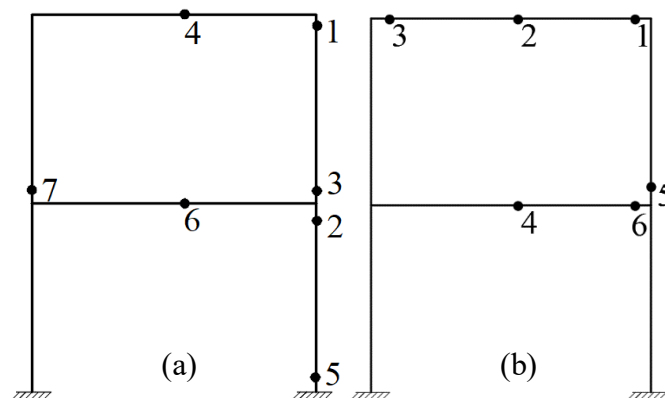


Figure 5.37 : Order of plastic hinge formations (a) lateral torsional buckling ignored (b) lateral torsional buckling considered.

In Table 5.15, ultimate load parameter capacities of the examined steel frame structure under different conditions are given. In order to determine importance of unbraced length conditions and approximations of design codes on the lateral torsional buckling effect, results are given comparatively.

Table 5.15 : Ultimate load parameter and decreasing in load carrying capacity for two stories and one span frame.

Lateral torsional buckling (LTB) effect	Ultimate load parameter	% decrease in load carrying capacity
LTB ignored	1.93	-
LTB considered with respect to TSDC	1.02	47.4
LTB considered with respect to TS 4561	1.00	47.6
LTB considered with respect to TSDC and $C_b=1$	0.70	63.9
LTB considered with bracing of beams from the midpoint according to TSDC	1.89	2.5
LTB considered with bracing of beams at three midpoint according to TSDC	1.79	7.5

According to the analysis results, lateral torsional buckling effect decrease the load carrying capacity significantly. TSDC and TS4561 standards give approximately same results under the lateral torsional buckling effect. However, accounting $C_b=1$ case in lateral torsional buckling calculations decrease the load carrying capacity more than enough. On the other hand, changing unbraced length conditions on the beam elements increase the load carrying capacity and eliminate lateral torsional buckling effect.

5.11. Second-Order Elastic-Plastic Analysis of Three Stories and One Span

Frame

A steel frame is selected from the literature [57, 60] and is investigated considering lateral torsional buckling. This frame have two stories and one span. Cross sections of the columns are W 8x48 ($J= 816 \times 10^3 \text{ mm}^4$, $C_w= 250 \times 10^9 \text{ mm}^6$, $Z_x= 803 \times 10^3 \text{ mm}^4$) and W 8x35 ($J= 320 \times 10^3 \text{ mm}^4$, $C_w= 166 \times 10^9 \text{ mm}^6$, $Z_x= 569 \times 10^3 \text{ mm}^4$). Cross sections of the beams are W 21x44 ($J= 320 \times 10^3 \text{ mm}^4$, $C_w= 567 \times 10^9 \text{ mm}^6$, $Z_x= 1560 \times 10^3 \text{ mm}^4$) and W 14x30 ($J= 158 \times 10^3 \text{ mm}^4$, $C_w= 238 \times 10^9 \text{ mm}^6$, $Z_x= 775 \times 10^3 \text{ mm}^4$). Section types, dimensions and applied loads are shown in Figure 5.38. Out-of-plane motion is prevented at only joints, mid-point and three points of the beam member. Lateral displacement (Δ) is observed at the top point of the frame and shown in Figure 5.38.

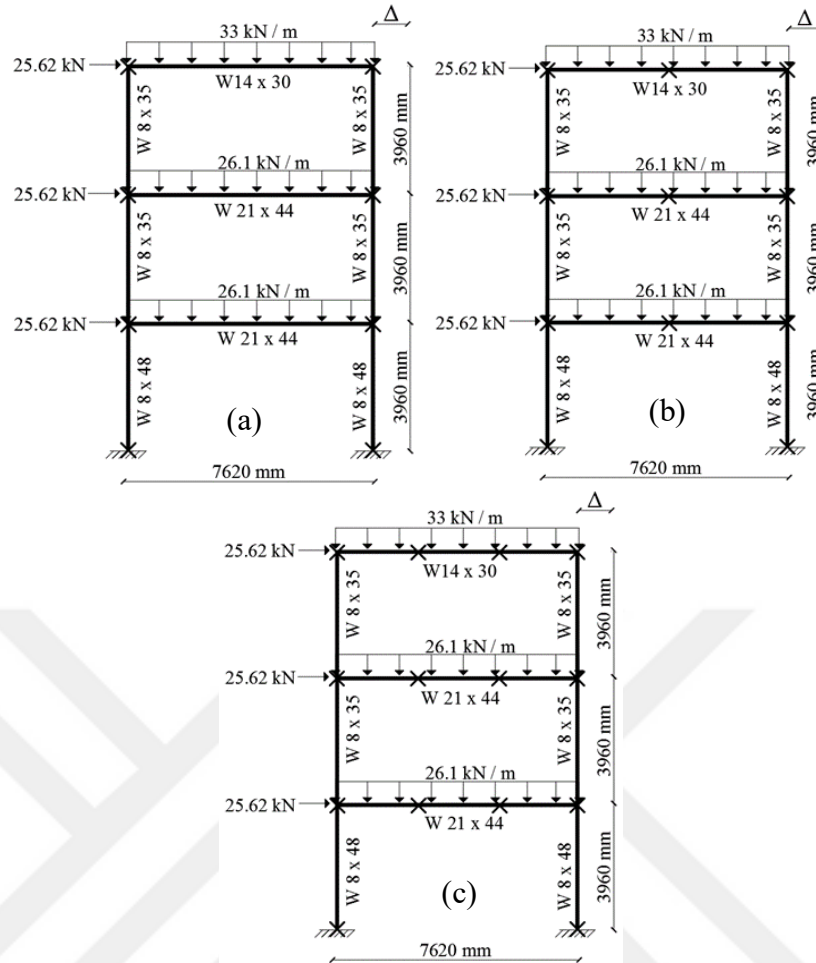


Figure 5.38 : Out of plane motion prevented from (a) only joints (b) mid-point of the beam (c) three points of the beam for one story frame.

Three stories and one span frame is analyzed under the lateral torsional buckling effect and second-order elastic plastic analysis method is used in the analyses. In this frame analyses, lateral torsional buckling calculations are carried out with using TSDC [43] and TS 4561 [53]. Moment modification factor ($C_b = 1$) case is examined and compared other analysis results. Moreover, different unbraced length conditions are investigated. Load carrying capacity – lateral displacements of top point of the frame (Δ) are calculated and the graphics are plotted in Figure 5.39. Also, order of plastic hinge formations are given in Figure 5.40 for lateral torsional buckling considered and ignored cases, respectively.

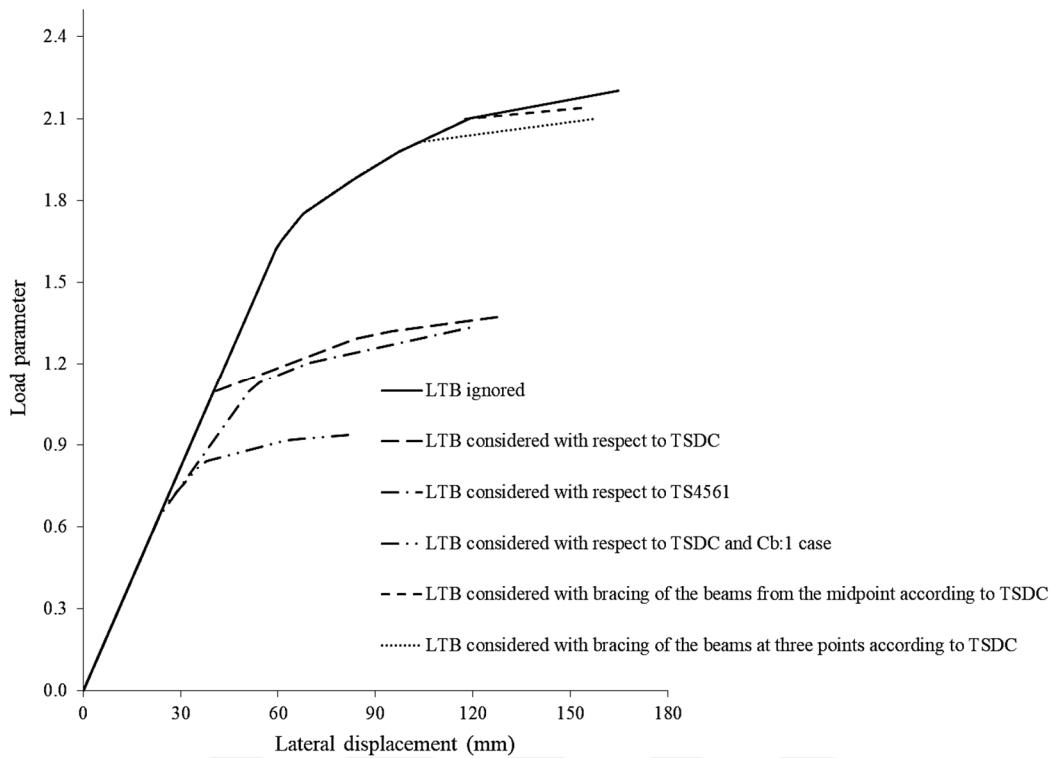


Figure 5.39 : Peak point lateral displacements and load parameters of three stories and one span frame.

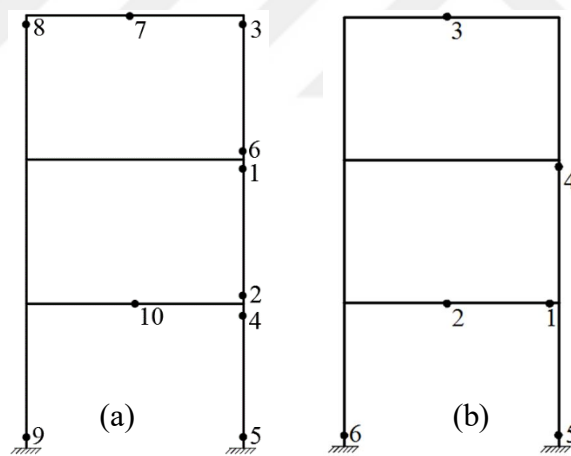


Figure 5.40 : Order of plastic hinge formations (a) lateral torsional buckling ignored (b) lateral torsional buckling considered.

In Table 5.16, ultimate load parameter capacities of the examined steel frame structure under different conditions are given. In order to determine importance of unbraced length conditions and approximations of design codes on the lateral torsional buckling effect, results are given comparatively.

Table 5.16 : Ultimate load parameter and decreasing in load carrying capacity for three stories and one span frame.

Lateral torsional buckling (LTB) effect	Ultimate load parameter	% decrease in load carrying capacity
From the literature ignoring LTB [60]	2.19	-
LTB ignored	2.20	-
LTB considered with respect to TSDC	1.38	33.5
LTB considered with respect to TS 4561	1.34	39.1
LTB considered with respect to TSDC and $C_b=1$	0.94	57.4
LTB considered with bracing of beams from the midpoint according to TSDC	2.14	2.7
LTB considered with bracing of beams at three midpoint according to TSDC	2.10	4.7

These analysis results show the analogy with previously examined frame structures. Load carrying and displacement capacities of frame under the lateral torsional buckling effect have decreased considerably. Bracing of the beams from the different points increase load carrying capacity and eliminate lateral torsional buckling effect.

6. CONCLUSION

Within scope of this thesis, lateral torsional buckling effect is examined in nonlinear analysis steps. Member base analyses are performed to show decreasing of the load carrying capacity of the member. For this purpose, lateral torsional buckling of I-shaped steel members are investigated considering finite element program outcomes and several design standard and code approaches using different unbraced member lengths and linear moment gradient. On the other hand, nonlinear analysis of steel frames is investigated with and without considering lateral torsional buckling. In order to apply the lateral torsional buckling behavior in the nonlinear analysis steps, it is seen that the proposed approach can be practically applied considering TSDC-2016 [43] or AISC 360-10 [41], and in the case of neglecting the lateral torsional buckling behavior, the results in the literature can be obtained with nonlinear analysis. In this analyses, different unbraced length conditions are also taken in to consideration. The following is a summary of the most significant findings from these studies.

1. In the case of the simple beam examples investigated for the first time in the study, the lateral torsional buckling effect is examined with considering different out-of-plane supports and the variations in the load carrying capacity of the member are given in details. When the out-of-plane motion is not prevented from any point of the beam, the load carrying capacity of the beam member decrease considerably. It is concluded that required quantity of out-of-plane support has to be selected in order to prevent lateral torsional buckling effect. If out-of-plane motion is neglected, the beams may not reach its potential load carrying capacities due to lateral torsional buckling, which will result in uneconomical designs.
2. Nonlinear analysis results show that load carrying capacity of the structure and the displacements of the selected joints are overestimated when lateral torsional buckling is neglected. This may cause inadequate structural design since the structural performance is evaluated using load – displacement capacities in modern performance based design codes.

3. Out of plane bracings of frame members become substantial since unbraced length conditions have direct influence on lateral torsional buckling of members of the frames. Likewise, member lengths become crucial for steel structures. It has been found that the load carrying capacity of frame systems increases in case of a decrease in the length of the lateral unsupported element. However, higher load carrying capacity has been achieved for the case of dividing the two equal parts, while the beam members are divided into three equal parts, so that the load carrying capacity of the beam members is expected to increase more than the single point part by dividing the beam members into two equal parts. The reason for this is that the moment modification factor C_b in TSDC-2016 [43] and AISC 360-10 [41] caused by the loads on the beam head parallel to the beam axis cannot accurately reflect the sudden changes in the moment diagram for the elements to which the load is applied.
4. Loading type of the member is also an influencing parameter for the lateral torsional buckling for frame members since shape of bending moment diagrams affects member capacity directly.
5. The nonlinear analysis of the systems examined in the study using the TS 4561 [53] standard, which has been abolished from the activation date of the TSDC-2016 [43] code on September 1, 2016. The results obtained by using this standard and the results obtained by using TSDC-2016 [43] are presented comparatively. Although the results of some of the examined examples are close to the results of TS 4561 [53] and TSDC-2016 [43], the formulas used in TS 4561 [53] are very complicated and far from practical. The formulas related to the lateral torsional buckling in the TSDC-2016 [43] have significant advantages because they are contemporary and practical in terms of their application to nonlinear analysis steps.
6. In TSDC-2016 [43] and AISC 360-10 [41] codes, it is stated that the moment modification factor, $C_b= 1$ may be taken in order to shorten the calculation steps and to remain safe at the same time. This is also taken into consideration in various frame samples examined in the study and it has been seen that the load carrying capacity is limited to a considerable extent according to the results of the calculations obtained and this will cause the use of the building elements below the existing capacities. This leads to economical disadvantages, so that in analyzes the moment modification factor, C_b , has to

be calculated so that the performance of the building elements can be fully utilized.

7. In nonlinear analysis steps, lateral torsional buckling effect is considered and ignored for all of the selected steel frames. According to analysis results, it is seen that order of plastic hinge formations in most examined steel frames changes for lateral torsional buckling effect considered and ignored cases. This also changes the frame behavior and decreases the load carrying and displacement capacities of the frames.

As a conclusion, lateral torsional buckling which is a global stability problem and has significant effect on the nonlinear analysis of steel frame structures. For this reason, lateral torsional buckling is very crucial especially for beam members and it should be considered in nonlinear analysis steps.

For the future studies, lateral torsional buckling effect should be implemented in commercial structural engineering programs. Also, C_b , moment modification factor which affect directly lateral torsional buckling should be studied in detail.

REFERENCE

1. **Li, G.-Q. and J.-J. Li** (2007). Advanced analysis and design of steel frames, John Wiley & Sons.
2. **Chen, W.-F. and S. Toma** (1994). Advanced analysis of steel frames: theory, software, and applications, CRC press.
3. **Giberson, M.F.** (1969). Two nonlinear beams with definitions of ductility. Journal of the Structural Division.
4. **El-Zanaty, M., D. Murray, and R. Bjorhovde** (1980). Inelastic behavior of multistory steel frames, Structural Engineering Report No. 83, University of Alberta, Canada.
5. **Banerjee, P. and S. Raveendra** (1987). New boundary element formulation for 2-D elastoplastic analysis. Journal of engineering mechanics, **113**(2): p. 252-265.
6. **Shi, G. and S. Atluri** (1988). Elasto plastic large deformation analysis of space frames: A plastic hinge and stress based explicit derivation of tangent stiffnesses. International Journal for Numerical Methods in Engineering, **26**(3): p. 589-615.
7. **Gharpuray, V. and J.D. Aristizabal-Ochoa** (1989). Simplified second-order elastic-plastic analysis of frames. Journal of computing in civil engineering, **3**(1): p. 47-59.
8. **Haldar, A. and N. Ker-Ming** (1989). Elasto-plastic large deformation analysis of PR steel frames for LRFD. Computers & Structures, **31**(5): p. 811-823.
9. **Clarke, M., et al.** (1992). Advanced analysis of steel building frames. Journal of Constructional Steel Research, **23**(1): p. 1-29.
10. **Kim, S.-E. and W.-F. Chen** (1996). Practical advanced analysis for braced steel frame design. Journal of Structural Engineering, **122**(11): p. 1266-1274.
11. **Liew, J.R., et al.** (2000). Improved nonlinear plastic hinge analysis of space frame structures. Engineering Structures, **22**(10): p. 1324-1338.
12. **Chan, S.** (2001). Non-linear behavior and design of steel structures. Journal of Constructional Steel Research, **57**(12): p. 1217-1231.
13. **Choi, S.-H. and S.-E. Kim** (2002). Optimal design of steel frame using practical nonlinear inelastic analysis. Engineering structures, **24**(9): p. 1189-1201.
14. **Ziemian, R.D. and W. McGuire** (2002). Modified tangent modulus approach, a contribution to plastic hinge analysis. Journal of Structural Engineering, **128**(10): p. 1301-1307.
15. **Zhou, Z.-H. and S.-L. Chan** (2004). Elastoplastic and large deflection analysis of steel frames by one element per member. I: One hinge along member. Journal of Structural Engineering, **130**(4): p. 538-544.
16. **Chan, S.-L. and Z.-H. Zhou** (2004). Elastoplastic and large deflection analysis of steel frames by one element per member. II: Three hinges along member. Journal of Structural Engineering, **130**(4): p. 545-553.

17. **Kim, S.-E., et al.** (2004). Automatic design of space steel frame using practical nonlinear analysis. *Thin-walled structures*, **42**(9): p. 1273-1291.
18. **Yoo, H. and D.-H. Choi** (2008). New method of inelastic buckling analysis for steel frames. *Journal of Constructional Steel Research*, **64**(10): p. 1152-1164.
19. **Thai, H.-T. and S.-E. Kim** (2009). Practical advanced analysis software for nonlinear inelastic analysis of space steel structures. *Advances in Engineering Software*, **40**(9): p. 786-797.
20. **Saffari, H., et al.** (2012). Elasto–plastic analysis of steel plane frames using Homotopy Perturbation Method. *Journal of Constructional Steel Research*, **70**: p. 350-357.
21. **Doan-Ngoc, T.-N., et al.** (2016). Second-order plastic-hinge analysis of planar steel frames using corotational beam-column element. *Journal of Constructional Steel Research*, **121**: p. 413-426.
22. **Dux, P.F. and S. Kitipornchai** (1983). Inelastic beam buckling experiments. *Journal of Constructional Steel Research*, **3**(1): p. 3-9.
23. **Pandey, M.D. and A.N. Sherbourne** (1990). Elastic, lateral-torsional stability of beams: general considerations. *Journal of structural engineering*, **116**(2): p. 317-335.
24. **Kemp, A.R.** (1996). Inelastic local and lateral buckling in design codes. *Journal of structural engineering*, **122**(4): p. 374-382.
25. **Helwig, T.A., K.H. Frank, and J.A. Yura** (1997). Lateral-torsional buckling of singly symmetric I-beams. *Journal of Structural Engineering*, **123**(9): p. 1172-1179.
26. **Trahair, N. and Y.-L. Pi** (1997). Torsion, bending and buckling of steel beams. *Engineering Structures*, **19**(5): p. 372-377.
27. **Papangelis, J., N. Trahair, and G. Hancock** (1998). Elastic flexural–torsional buckling of structures by computer. *Computers & Structures*, **68**(1): p. 125-137.
28. **Suryoatmono, B. and D. Ho** (2002). The moment–gradient factor in lateral–torsional buckling on wide flange steel sections. *Journal of Constructional Steel Research*, **58**(9): p. 1247-1264.
29. **AISC** (1994). *Manual of steel construction, load and resistance factor design*. Chicago: American Institute of Steel Construction, Chicago-Illinois.
30. **AISC** (1986). *Load and resistance factor design specification for structural steel buildings*. Chicago: American Institute of Steel Construction, Chicago-Illinois.
31. **Lim, N.-H., et al.** (2003). Elastic buckling of I-beams under linear moment gradient. *International journal of solids and structures*, **40**(21): p. 5635-5647.
32. **Serna, M.A., et al.** (2006). Equivalent uniform moment factors for lateral–torsional buckling of steel members. *Journal of Constructional Steel Research*, **62**(6): p. 566-580.
33. **Aydin, M.R.** (2010). Elastic flexural and lateral torsional buckling analysis of frames using finite elements. *KSCE Journal of Civil Engineering*, **14**(1): p. 25-31.
34. **Taras, A. and R. Greiner** (2010). New design curves for lateral–torsional buckling—Proposal based on a consistent derivation. *Journal of Constructional Steel Research*, **66**(5): p. 648-663.

35. **Bradford, M.A. and Y.-L. Pi** (2012). A new analytical solution for lateral-torsional buckling of arches under axial uniform compression. *Engineering Structures*, **41**: p. 14-23.
36. **Wu, L. and M. Mohareb** (2012). Finite-element formulation for the lateral torsional buckling of plane frames. *Journal of Engineering Mechanics*, **139**(4): p. 512-524.
37. **Kucukler, M., L. Gardner, and L. Macorini** (2015). Lateral-torsional buckling assessment of steel beams through a stiffness reduction method. *Journal of Constructional Steel Research*, **109**: p. 87-100.
38. **Ozbasaran, H., R. Aydin, and M. Dogan** (2015). An alternative design procedure for lateral-torsional buckling of cantilever I-beams. *Thin-Walled Structures*, **90**: p. 235-242.
39. **Chen, W.-F. and E.M. Lui** (1991). *Stability design of steel frames*. CRC press.
40. **Chen, W.F. and I. Sohal** (2013). *Plastic design and second-order analysis of steel frames*, Springer.
41. **ANSI/AISC360-10** (2010). *Specification for Structural Steel Buildings*. American Institute of Steel Construction, Chicago-Illinois.
42. **Seçer, M.** (2003). Çelik yapılarda non-lineer çözüm yöntemleri, *M.Sc. Thesis*, Dokuz Eylül Üniversitesi: İzmir.
43. **TSDC** (2016). *Turkish Steel Design Code*. Ministry of Environment and Urbanization, Ankara, Turkey.
44. **Al-Mashary, F. and W.F. Chen** (1990). Elastic second-order analysis for frame design. *Journal of Constructional Steel Research*, **15**(4): p. 303-322.
45. **Chen, W.F. and E.M. Lui** (1987). *Structural stability: theory and implementation*, Elsevier.
46. **Timoshenko, S.** (1940). *Strength of materials*, Van Nostrand, New York.
47. **Kirby, P. and D.A. Nethercot** (1979). *Design for structural stability*, Halsted Press.
48. **AS4100** (1998). *Steel structures*. Standards Australia, NSW, Australia.
49. **Salvadori, M.G.** (1955). Lateral buckling of I-beams. *Transactions of the American Society of Civil Engineers*, **120**(1): p. 1165-1177.
50. **Wong, E. and R.G. Driver** (2010). Critical evaluation of equivalent moment factor procedures for laterally unsupported beams. *Engineering Journal*, **47**(1): p. 1.
51. **BS5950-1** (2000). *Structural use of steelwork in building*, London, UK.
52. **EN1993-1-1** (2005). *Design of steel structures-Part 1-1: General rules and rules for buildings*. European Committee for Standardization, Brussels, Belgium.
53. **TS4561** (1985). *Calculation Rules According to Plastic Theory of Steel Structures*. TSE, Ankara, Turkey.
54. **Galéa, Y.** (2012). *LTBeam Version 1.0*. 11. CTICM. France.
55. **Ansys, H.** (2013). *version 15.0*, Ansys. Inc., Canonsburg, PA USA.
56. **Secer, M. and E.T. Uzun** (2017). Corrosion Damage Analysis of Steel Frames Considering Lateral Torsional Buckling. *Procedia Engineering*, **171**: p. 1234-1241.
57. **Liew, J.R., D. White, and W. Chen** (1993). Second-order refined plastic-hinge analysis for frame design. Part II. *Journal of Structural Engineering*, **119**(11): p. 3217-3236.

58. **Secer, M. and E.T. Uzun** (2016). Nonlinear analysis of steel frames accounting lateral torsional buckling. 21st International Scientific Conference: Mechanika 2016, Kaunas University of Technology.
59. **Ziemian, R.D., W. McGuire, and G.G. Deierlein** (1992). Inelastic limit states design. Part I: Planar frame studies. *Journal of Structural Engineering*, **118**(9): p. 2532-2549.
60. **Foley, C.M. and S. Vinnakota** (1997). Inelastic analysis of partially restrained unbraced steel frames. *Engineering structures*, **19**(11): p. 891-902.
61. **Kassimali, A.** (1983). Large deformation analysis of elasticplastic frames. *Journal of Structural Engineering*, **109**(8): p. 1869-1886.



CURRICULUM VITAE



Name Surname: Ertuğrul Türker UZUN
Place and Date of Birth: Altındağ, 04.02.1991
Address: İzmir Katip Celebi University, Faculty of Engineering and Architecture, Department of Civil Engineering
E-Mail: ertugrulturker.uzun@ikc.edu.tr
B.Sc.: Anadolu University / Civil Engineering, 2014

Professional Experience and Rewards:

- Turna Yapı Denetim (Eskişehir), Civil Engineer, June 2014 – February 2015
- Izmir Katip Celebi University Civil Engineering Department, Research Assistant, February 2015 - ...

List of Publications:

- Secer, M. and Uzun, E.T. Nonlinear analysis of steel frames accounting lateral torsional buckling, Proceedings of 21th International Conference “MECHANIKA 2016”, Lithuania, 12-13 May 2016.
- Secer, M. and Uzun, E.T. 2017. Corrosion damage analysis of steel frames considering lateral torsional buckling, Procedia Engineering, 17: 1231-1241
- Uzun, E.T. and Secer, M. 2017. Evaluation of building retrofitting alternatives from sustainability perspective, Procedia Engineering, 17: 1137-1146.

- Secer, M. and Uzun, E.T. Elastic lateral torsional buckling of simply supported beams under concentrated load and linear moment gradient, WMCAUS 2017, Czech Republic, 12-16 June 2017.
- Uzun, E.T. and Secer, M. Investigation of lateral torsional buckling behavior of I-shaped steel members, Sixth National Symposium on Steel, Timber and Composite Structures, Bulgaria, 1-3 November 2017. (Abstract accepted-under review).

